Effect of nanoparticles on B- and T- lymphocyte activation: *in vitro* and *in vivo* studies

Thesis submitted for the degree of

Doctor of Philosophy

By

D. Mallaiah

(08LBPH13)

Department of Biochemistry

School of Life Sciences

University of Hyderabad

Hyderabad-500046

India

Enrolment No: 08LBPH13

October 2016

University of Hyderabad

School of Life Sciences

Department of Biochemistry

Hyderabad-500046, India

CERTIFICATE

This is to certify that this thesis entitled **"Effect of nanoparticles on B- and T-lymphocyte activation: *in vitro* and *in vivo* studies"** submitted to University of Hyderabad by **Mr. D. Mallaiah**, for the degree of Doctor of Philosophy, is based on studies carried out by him under my supervision. I declare that, to the best of my knowledge, this work has not been submitted earlier for award of any degree or diploma from any other University/Institution.

Prof. M. Ramanadham
(Research Supervisor)

Head

Department of Biochemistry

Dean

School of Life sciences

University of Hyderabad

School of Life Sciences

Department of Biochemistry

Hyderabad- 500046, India

DECLARATION

I hereby declare that, the work presented in my thesis is entirely original and was carried out by me in the Department of Biochemistry, University of Hyderabad, under the supervision of **Prof. M. Ramanadham**. I further declare that, this work has not been submitted earlier for the award of any degree or diploma from any other University or Institution.

D. Mallaiah

Date: (Regd.No:08LBPH13)

Prof. M. Ramanadham
(Research Supervisor)

Acknowledgements

I am grateful to my research supervisor, **Prof. M. Ramanadham**, for readily accepting me as his research student and providing an opportunity to work under his invaluable guidance, constant support and encouragement during entire course of my research work.

I thank my Doctoral committee members Prof. N. Siva Kumar and Dr. Krishnaveni Mishra for assessing my research work.

I am thankful to former Deans Prof. A. S. Rahavendra, Prof. M. Ramanadham, Prof. R.P.Sharma and present I/c Dean, School of Life Sciences, Prof. P. Reddanna, former Heads of the department, Prof. M. Ramanadham, Prof. K. V. A. Ramaiah, Prof. O. H. Setty and present Head, Department of Biochemistry, Prof. N. Siva Kumar, for allowing me to utilize facilities at the School and department level.

I thank all the faculty members and research scholars of School of Life Sciences for their support for the completion of the work.

I express my sincere thanks to my lab postdoctoral student Dr. S.A.A. Latheef for his valuable suggestions and help in time of need.

I sincerely acknowledge Dr. A. Venugopal, Dr. Kishore, Dr. B. Kishore Kumar, Dr. S. Thirupati Reddy, Dr. N. Pavan Kumar Reddy, Mr. Rohit Sai Reddy, Kavya and Mr. Shashi, Dr. Maruti Mulaka, Dr. S.L.Balakrishna for their assistance to carry out my research work.

I wish to thank my friends Dr. Satish Kumar, Dr.R.Seshagiri Rao, Dr.M.Ramakrishna, Dr.M.Chandayya, Dr.Sriram Gopi, Mr.T.Sampath Babu, Mr.Vasanth Kumar for their support and encouragement during my interactions with them.

I wish to thank my parents Sri.D.Kashanna and Late Smt.D.Rangamma, wife Smt.D.Sheba, Father-in-law Sri.T.Abraham and Mother-in-law Smt.T.Prema, for their support, co-operation and encouragement.

I would like to thank my lab attendant Late Mr. Kistappa and all the non-teaching staff of the Department of Biochemistry.

I am very much thankful to TEM facility of Center for Nanotechnology and DST which provided funds under the Nanotechnology mission grant.

I heartfully acknowledge the financial support from UGC, New Delhi, India.

D. Mallaiah

Contents

ABBREVIATIONS

AFM	Atomic force microscopy
ALP	Alkaline phosphatase
ALT	Alanine aminotransferase
ANOVA	Analysis of variance
AST	Aspartate aminotransferase
BSA-NP	Bovine serum albumin nanoparticles
CD	Cluster of differentiation
Con A	Concanavalin A
cpm	Counts per minute
CuNP	Copper nanoparticles
DAG	Diacyl glycerol
DLS	Dynamic light scattering
ELISA	Enzyme linked immunosorbent assay
FBS	Fetal bovine serum
FCS	Fetal calf serum
GC	Germinal centers
GNP	Gold nanoparticles
HEPES	4-(2-Hydroxyethyl) piperazine-1-ethanesulfonic acid
IFN	Interferon
IL	Interleukin
IP3	Inositol 1,4,5 trisphosphate
LPS	Lipopolysaccharide
MDA	Malondialdehyde
MHC	Major histocompatibility complex
MTT	3-[4, 5-Dimethylthiazole-2-yl]-2,5 diphenyl tetrazolium bromide
NC	Nanoconjugates

nm	Nanometer
NP	Nanoparticle(s)
NTA	Nanoparticles tracking analysis
PAMPs	Pathogen associated-molecular patterns
PBL	Peripheral blood lymphocytes
PBS	Phosphate buffered saline
PEG	Poly ethylene glycol
PHA	Phytohaemagglutinin
PKC	Protein kinase C
POPOP	1, 4-bis (5-phenyl-2-yl-) benzene
PPO	2, 5 Diphenyloxazole
PRRs	Pattern recognition receptors
PWM	Pokeweed mitogen
Rho	Rhodamine
RITC	Rhodamine isothiocyanate
RPMI-1640	Roswell park memorial institute-1640
S-HRP	Streptavidin-Horse radish peroxidase
SI	Stimulation index
SNP	Silver nanoparticles
SPR	Surface plasmon resonance
TBA	Thiobarbituric acid
TBS	Tris-buffered saline
TCR	T-cell antigen receptor complex
TEM	Transmission electron microscopy
TLRs	Toll-like receptors
TMB	Tetramethyl benzidine
TPP	Tripolyphosphate
WBC	White blood cell

Chapter 1

Introduction

Nanoparticles (NP): Definition and properties

NP are defined as particles of matter with diameter of less than 100 nm and show different physico-chemical properties compared to bulk materials with the same chemical composition. In terms of size, NP form bridge between bulk materials and atomic or molecular structures. Percentage of surface atoms in relation to total number of atoms in bulk material is less, whereas at nanoscale, percentage of atoms at the surface is significantly high. NP are thermodynamically unstable and have high surface free energy. With a decrease in size of NP, surface area per unit mass or volume, dissolution in terms of release of ions from surface and chemical reactivity increases (Auffan et al., 2009). Some metallic NP exhibit unusual optical properties as they are small enough to confine their electrons yielding quantum effect and surface plasmon resonance (Roduner, 2006). NP are not restricted to man-made materials, but also exist in nature. Biomolecules such as proteins, polysaccharides and organisms such as viruses and, bacteria are well known natural nanostructures (Buzea et al., 2007).

Classification of NP

NP can be classified based on their chemical composition, size, shape and surface charge. In terms of chemical composition, NP are classified as organic or inorganic. Polymeric and carbon based are considered as organic NP. Inorganic NP comprise metals (e.g., Au, Ag, Cu etc.), metal oxides (e.g., ZnO, $TiO_{2\ etc.,}$), magnetic metallic oxides (e.g., iron oxides) and semiconductors (e.g., CdSe and CdTe) (Sekhon and Kamboj, 2010). Carbon based NP comprise of fullerenes, carbon nanotubes, and graphene (Wen et al., 2015). Polymeric NP are prepared from natural polymers like albumin, chitosan, gelatin and also from synthetic polymers like poly lactide, polylactide-glycolides and poly ethylene glycol (PEG). Based on their structural features, polymeric NP are further classified into nanospheres and nanocapsules (Vauthier and Bouchemal, 2009).

Preparation and characterization of NP

NP can be prepared by different types of physical, chemical and biological methods. Two major strategies are employed for the preparation of NP– "top-down" and "bottom-up". In top-down approach, the bulk material is broken down gradually to nano sized materials by physical and chemical means. Wet ball milling, high pressure

homogenization and chemical etching are some examples of top-down methods. The major drawback of top-down approach is imperfect formation of NP surface structure. In bottom-up approach, atoms or molecules are assembled into molecular clusters / structures of nano size. Bottom-up approach is commonly used in different chemical and biological methods. Chemical reduction methods are commonly used for preparation of NP due to ease of synthesis and low cost. However, drawbacks are contamination by precursor chemicals and production of hazardous by-products. A few methods have involved use of microbes and plants for preparation of NP (Thakkar et al., 2010). Polymeric NP have been prepared using one of the following approaches- 1. By dispersion of preformed polymers 2. Polymerization of monomers and 3. Ionic gelation or coacervation of hydrophilic polymers (Mohanraj and Chen, 2006).

Robust techniques are needed to characterize NP. The most commonly used techniques are listed in Table 1.

Table 1: Techniques for the characterization of NP

S.No.	Technique
1	Dynamic light scattering (DLS)
2	Scanning electron microscopy (SEM)
3	Transmission electron microscopy (TEM)
4	Atomic force microscopy (AFM)
5	UV-visible spectroscopy
6	Nanoparticles tracking analysis (NTA)

(Compiled from Lin et al., 2014; Lopez-Serrano et al., 2014).

Distinct absorption profile of NP obtained using UV-visible spectroscopy provides information about empirical size, concentration, state of aggregation and bio-conjugation (Sapsford et al., 2011). SEM and TEM allow characterization of NP in terms of their physical properties such as size, shape and degree of aggregation. EM techniques use accelerated beam of electrons and electromagnetic lenses to produce high resolution images. However, disadvantage of all EM measurements is that they are done in non-

physiological conditions and sample is disintegrated under the influence of electron beam (Lin et al., 2014). Nanoparticles tracking analysis (NTA) measures size distribution and concentration of particles in liquid suspension. This novel technology utilizes the properties of both light scattering and Brownian motion of NP (Filipe et al., 2010).

Functional role of NP

NP can penetrate into animal tissues and some cell types due to their small size. This property has been exploited in passive and active targeting of NP for disease diagnosis and treatment. Passive targeting is based on the phenomenon of enhanced permeability and retention. NP of finite size accumulates more in the leaky blood vessels of tumour than normal tissue and therefore is useful in cancer therapy. However, passive targeting potential may be limited, as all tumours do not exhibit enhanced permeability and retention effect. Active targeting is achieved through the intentional enrichment of NP surface with specific ligands such as antibodies, peptides and aptamers. Active targeting exploits the principle of specific recognition between the receptor on the tumour cell and the targeting ligand on NP surface. Functionalized NP have been developed for safe and reliable targeted drug delivery of hydrophilic, hydrophobic drugs and other biological macromolecules. In addition, NP functionalized with suitable imaging agents have been used to detect tumour cells and infection loci by optical imaging of whole animals (Barreto et al., 2011).

Three approaches have been used for the preparation of functionalized NP or nanoconjugates (NC); 1) adsorption, 2) non-specific covalent conjugation and 3) selective and orientation-controlled conjugation. Adsorption of protein molecules to NP surface is mediated mainly by non-covalent interactions. Impact of NP-protein interactions on the structure of adsorbed protein depends on hydrophobic or hydrophilic surfaces, surface curvature and morphology of NP. In non-specific covalent conjugation, functional groups of protein are linked to NP. It ensures a permanent association between NP and protein and also probably limits denaturing interactions. Disadvantages of covalent conjugation are lack of control over protein orientation and effect of chemical modification on biological activity. Selective, orientation-controlled conjugation falls into two main categories; 1. Non-covalent, based on specific high affinity interaction, e.g., streptavidin - biotin, polyhistidine - Ni-nitrilotriacetic acid etc., 2. Covalent, employing

specific chemical reactions, e.g., thiol chemistry, enzyme mediated ligation, etc., (Avvakumova et al., 2014).

Specificity and targeting efficacy of NC depend on their size, shape, surface curvature and ligand density. Conjugation of multiple recognition molecules to NP creates a multivalent NC with enhanced specificity and efficacy (Josan et al., 2011). NC have been demonstrated to have a short half-life in circulation, following *in vivo* administration. Non-specific adsorption of proteins and uptake by phagocytes has been shown to be probable factors responsible for their short half-life. Recognition and sequestration of NC by cells of reticuloendothelial and immune system has been found to be prevented by coating them with biocompatible PEG (Walkey et al., 2012). However, formation of PEG-specific antibodies and their role in clearance of PEG-coated NC from blood has been demonstrated (Ishida and Kiwada, 2008).

Toxicity of NP

Exposure of humans to NP is on the rise due to their growing use in several biomedical applications and commercial products. Therefore, there is an urgent need to assess the adverse effects of NP on living organisms. It has been proposed that novel physico-chemical properties of NP may present new health risks to the biological system which is being evaluated by scientific and regulatory communities. NP can enter human body through various routes and may pass through biological barriers of cells and accumulate within. Several studies have demonstrated that NP have toxic effects at cellular, sub-cellular and molecular level (Elsaesser et al., 2012). Internalization of NP by cells is influenced by their size, shape, surface coating and cell cycle phase (Kim et al., 2012a). Mechanism by which NP influence cellular function can be either chemical and /or physical. Dissolution and release of toxic ions, induction of oxidative stress, lipid peroxidation, generation of reactive oxygen species, disturbance of electron or ion transport across cell membrane transport etc., have been reported (Kittler et al., 2010; Kim et al., 2009; Wang et al., 2014; Fu et al., 2014; Vardanyan et al., 2015). Physical mechanisms may include disruption of cell membrane, changes in protein conformation and protein aggregation/fibrillation (Leroueil et al., 2008; Linse et al., 2007; Zaman et al., 2014). At sub-cellular level, NP have been shown to affect mitochondrial function leading to apoptosis (Mallick et al., 2016). NP sequester to lysosomes and rough endoplasmic reticulum and may alter intracellular transport (Greulich et al., 2011). It has also been

reported that NP diffuse and are transported to the nucleus through nuclear membrane pores (Pante and Kann, 2002). At molecular level, NP interacts with proteins either by chaperone like activity or inducing protein configuration (Takahashi et al., 2011; Wagner et al., 2010). Genotoxic potential of NP has not been evaluated in detail, but, reactive oxygen species has been proposed to play a key role in DNA damage (Bhabra et al., 2009).

Inhalation, absorption through skin and oral ingestion are the main routes by which NP gain entry into biological tissues. Inhaled particles are endocytosed by alveolar epithelial cells and then translocate to liver, spleen, heart, etc., via blood circulation (Yacobi et al., 2010). NP administered orally are absorbed in the gastro-intestinal tract and also translocate to other tissues via circulation. Small size of NP plays a role in the absorption in the gut (Powell et al., 2010). In biological environment, proteins bind to the surface of bare NP and form complexes known as protein corona. Inner hard protein corona is long-lived, consisting of one or two protein layers which exchange slowly with their environment. Outer protein corona is bound weakly and rapidly exchanges with surrounding proteins. It has been shown that protein corona adsorbed onto surface of transferrin conjugated NP prevent their binding to target cellular receptors and soluble transferrin receptors (Salvati et al., 2013). Adsorbed proteins also contribute to biological effect of NP through activation or inactivation of receptor-dependent signaling. In the formation of bio-corona, not only proteins but lipids can also be adsorbed on to NP surface. Combined protein-lipid corona may play a role in the interaction of NP with cells (Kapralove et al., 2012). Adsorption of plasma proteins to NP *in vitro* depends mainly on their physico-chemical properties and composition of culture medium. Analysis of proteins bound to NP revealed that the most abundant ones are albumin, apo-lipoprotein, immunoglobulins, complement and fibrinogen. When same proteins bind to different types of NP, then the biological outcome should be same. But, different NP have been shown to exhibit differential biological effect (Deng et al., 2012). Protein adsorption may equalize surface charge of different NP. However, stripping of protein in the lysosomes may expose intrinsic surface charge of NP (Wang et al., 2013).

In some organs, NP extravasation may be restricted by the existence of natural barriers formed by tight junctions between endothelial cells. However, NP penetration of blood–brain and placental barrier has been demonstrated (Yamashita et al., 2011). NP

localized in liver may affect activity of enzymes involved in metabolic transformations, for e.g., cytochrome P450. Finally, NP can be excreted from the body via urine and /or feces. But, in some cases, NP have been shown to be retained in the body for long time period (Lee et al., 2013). To minimize the possible health risks due to clinical use of NP, their potential toxicity has to be evaluated in detail. Describing the physico-chemical properties that are driving the nanoparticles toxicities remains a challenge (Fadeel et al., 2013). It has been argued that the final common pathways for pathological effects, that is oxidative stress, inflammation and genotoxicity are entirely shared by both nanoparticles and conventional particles and no novel pathways are anticipated (Donaldson and Poland, 2013). Yet, it remains possible that the pathological effects may be nonetheless related to the physicochemical properties of NP which resemble the complexity of natural nano-scale machineries rather than apparent simplicity of chemicals (Maynard et al., 2011).

Immunotoxicity of NP

Immunotoxicity is defined as adverse effects on functioning of immune system upon exposure to foreign agents. Although, general toxicity of NP has been reported, studies on immunotoxicity are limited (Di Gioacchino et al., 2011). Therefore, there is a need to evaluate the interaction of NP with cellular and soluble components of immune system.

Two types of immunity are manifested in higher animals – innate (constitutive) and adaptive (acquired). Host immune cells recognize molecules that are considered as "non-self" (foreign) and display an immune response towards them. Outcome of such response can either be stimulation or suppression. Immune stimulation is desirable in conditions like control of cancer, efficacy of vaccines etc. But, excessive immune stimulation is undesirable and can cause severe adverse reactions, e.g., hypersensitivity. On the other hand, immune suppression is useful in the treatments of allergies, autoimmune diseases and organ transplantation. But, immune suppression is detrimental to the host in conditions like pathogenic infections and cancer.

In vivo, four possible modes of interaction of NP with immune cells can be envisaged:- 1) Elicitation of immune response to NP *per se* 2) Immune stimulation or immune suppression by NP 3) Induction of cytotoxicity in immune cells by NP and 4) No effect – immune compatibility.

Effect of NP on innate immunity

Innate immune system is considered as the first line of defense and consists of distinct cell types and soluble mediators. The major cell types participating in innate immune system are neutrophils, eosinophils, monocytes, macrophages, dendritic cells and natural killer cells. Complement, acute phase reactants, lysozyme etc., are the important soluble mediators. Innate immune response is manifested rapidly (within hours) and in a non-specific manner. Innate immune cells mainly recognize conserved pathogen associated-molecular patterns (PAMPs) through pattern recognition receptors (PRRs) called Toll-like receptors (TLRs) present on their cell surface (Kawai and Akira, 2010). A few studies have demonstrated interaction of NP with TLRs (Kim et al., 2012b; Tsai et al., 2012). Formation of a complex between TLR 4 and NP has been shown to activate TLR signaling pathway (Mano et al., 2013). Computational studies have proposed that internal hydrophobic pockets of TLRs may be capable of direct binding with carbon NP (Turabekova et al., 2014).

NP are endocytosed by the phagocytic cells (Kuhn et al., 2014). Internalized NP can activate 'inflammasomes' which are cytoplasmic multiprotein complexes involved in caspase-1 activation. Maturation and secretion of inflammatory cytokines, pro-IL-1β and pro-IL-18 is mediated by activated caspase-1. Silver nanoparticles (SNP) have been shown to induce inflammasome formation and subsequent release of IL-1β by human blood monocytes (Yang et al., 2012).

When NP enters blood stream, they can interact with serum proteins which include complement or acute phase proteins. Complement is made up of about 20 proteins present in plasma in varying concentrations. Depending on the recognition, complement is known to get activated via three distinct pathways- classical, alternative and lectin-mediated. In classical pathway, complement gets activated upon recognition of antigen-antibody complex and involves formation of multi-protein complexes acquiring enzyme activity. Direct lysis of the target is achieved by the formation of membrane attack complex or indirectly by opsonization (coating with C3b) of target resulting in phagocytosis by macrophages. It has been shown that opsonin-coated NP are recognized and taken up by macrophages and other phagocytic cells (Nie, 2010). When the target is too large to engulf, it can result in frustrated phagocytosis. Capture and engulfment of NP may occur

at tissue level due to the action of reticuloendothelial system (RES) that includes tissue macrophages, leukocytes, dendritic cells, epithelial and endothelial cells. Phagocytosis is a receptor-mediated endocytosis (mannose, complement, Fc_γ and scavenger receptors) and can be influenced by the properties of NP. Phagocytes also use other routes to engulf foreign materials, which are receptor independent that include different forms of pinocytosis: macro, clathrin-dependent, caveolin-dependent and clathrin/caveolin independent. Large particles are taken up by classical phagocytosis and the fluids and solutes by pinocytosis (Shang et al., 2014). Production of inflammatory cytokines has been demonstrated following phagocytosis of NP through mannose or complement or Fc_γ receptors (Kim et al., 2006; Cuna et al., 2006; Vonarbourg et al., 2006). However, GNP internalized via scavenger receptor did not induce production of inflammatory cytokines (Shukla et al., 2005).

In addition to phagocytic mechanism, innate immune cells also form extra cellular traps, which act as major physical barriers for nanoparticles (Bartneck et al., 2010). Inflammatory leukocytes produce enzymes such as myeloperoxidases to degrade NP like carbon nanotubes. Macrophages have been shown to degrade carbon nanotubes through superoxide / peroxynitrite driven oxidative pathway (Kagan et al., 2014).

NP are more likely to interact with red blood cells than immune cells as they constitute the major cell components of blood. Induction of hemolysis by NP has been reported (Aseichev etal., 2014; Choi et al., 2011). SNP have been shown to cause erythrocyte hemolysis in a size-dependent manner (Chen et al., 2015). Extended presence of NP in blood circulation may increase their interaction with platelets, cells involved in coagulation cascade and blood clotting. Carbon NP induced platelet aggregation in *vitro* and vascular thrombosis *in vivo* has been reported (Radomski et al., 2005).

Effect of NP on adaptive immunity

Adaptive immunity is subdivided into humoral (B lymphocyte mediated) and cell mediated (T lymphocyte mediated) responses. In adaptive immune response, recognition of “non-self” (foreign) antigen is highly specific and involves clonal proliferation and differentiation. Effector response is manifested either as production of antibody (humoral) or secretion of cytokines (cell-mediated) from relevant activated and differentiated B and T cells respectively.

Antigen-presenting cells such as dendritic cells, macrophages constitute the bridge between innate and adaptive immunity. Effect of NP on dendritic cell function may influence B and /or T cell function. NP interaction with innate immune system can influence the adaptive immune reaction through production of cytokines and chemokines. Target specific interaction of the NP with lymphocyte membrane ligands could lead to modulation of immune function called immunomodulation: immunostimulation or immunosuppression.

Immunostimulation

Immunostimulatory properties of NP include their immunogenicity, adjuvanticity, ability to induce inflammatory response and trigger hypersensitivity reactions. Direct induction of T and/or B cell mediated specific immune reaction has not been reported. In addition, IgE mediated allergic response to NP have not been documented. However, generation of antibodies to "buckeyball" C60-fullerene of 1 nm diameter has been reported (Braden et al., 2000). Fullerene derivative was made use of as a hapten by conjugation to a protein carrier. Thus, NP may behave as hapten, acquire antigenicity when bound to a protein carrier possibly as a result of their small size. Proteins adsorbed on NP may undergo conformational changes resulting in exposure of cryptic epitopes. It has been suggested that immune response may be induced towards these epitopes upon recognition (Fadeel, 2012). Adjuvants are compounds that augment immune response when they are administered along with an antigen. Adjuvant properties of NP have been investigated. When animals were immunized with a protein conjugated to the surface of GNP, higher levels of specific antibodies were produced than using classical adjuvant, alum (Dykman et al., 2004).

NP may induce hypersensitivity reactions in individuals upon exposure / treatment. The reactions may include allergy (type I hypersensitivity) or contact dermatitis and delayed type hypersensitivity (type IV). B and T lymphocytes may recognize NP as 'foreign' and undergo activation and differentiation. This results in production of specific IgE which mediates allergic reactions. On the other hand, activated T lymphocytes produce a variety of lymphokines that mediate delayed type of hypersensitivity reactions. Both type I and IV hypersensitivity reactions lead to a profound inflammatory response. A

few studies have reported that NP induces inflammatory reactions (Gojova et al., 2007; Nemmar et al., 2016; Braakhuis et al., 2014).

Immunosuppression

Immunosuppression is manifested as a reduction in activation or efficacy of immune system. Direct effects of NP in mediating immunosuppression have been reported (Tkach et al., 2011). Fullerenes, when incubated with mast cells and peripheral blood basophils decreased IgE receptor-mediated signaling, production of reactive oxygen species and degranulation (Ryan et al., 2007). Immunosuppressive properties of fullerenes mentioned above have been suggested to be due to elevation of regulatory T cell number and inhibition of Th17 cells. Multi-walled carbon nanotubes have been shown to be immunosuppressive following *in vivo* inhalation and the effect mediated via activation of cyclooxygenase pathway (Mitchell et al., 2009). Iron oxide NP treatment to mice prior to an antigen challenge decreased production of antigen specific antibodies and cytokines (Shen et al., 2011).

Size, shape, charge and hydrophobic properties of NP have been found to influence their effects on immune system. Small difference in the size of NP has been shown to cause significant change in inflammatory response (Hussain et al., 2009). Uptake of rod shaped nanoparticles has been shown to be faster than nanospheres by primary immune cells (Bartneck et al., 2010). Anionic NP did not stimulate secretion of cytokines while cationic NP did (Tan et al., 1999). Splenic lymphocyte responses have been shown to be increased in a linear manner by gold nanoparticles (GNP) with graded increase in surface hydrophobicity (Moyano et al., 2012).

Assessment of adverse immune effects during preclinical evaluation will help in identifying potential concerns before a NP based product enters in to clinical trials. Immunologically screened NP improves the quality of diagnostic and therapeutic interventions. As no single test can predict the immune effects of NP, combinations of *in vitro* and *in vivo* studies are recommended for evaluation (Vatsan et al., 2013)

Lymphocyte proliferation, cytokine secretion, viability etc., have been used to assess the effects of NP on immune cells *in vitro* and *in vivo* (Oostingh et al., 2011). NP which are being tested are added to lymphocyte population from lymphoid tissues like

spleen and lymph node in the presence and absence of B-and T-lymphocyte specific mitogens.

Applications of NP

NP have been mainly evaluated in cancer diagnostics and treatment. However, they have been tried for a number of other conditions such as cardiovascular, neurological, gastrointestinal, autoimmune, inflammatory, infectious and reproductive diseases (Barkalina et al., 2014). Delivery of NP (for eg., gold nanorods) to tumors followed by irradiation with near infra-red light, resulting in local heating and extravascular coagulation is also one strategy for cancer therapy (Tong and Kohane, 2012). GNP have been used in the delivery of drugs, nucleic acids and antigens (Dykman et al., 2012). The antibacterial properties of NP are also exploited largely. SNP are widely used in industrial and health care products (Rizzello et al., 2014). Copper nanoparticles (CuNP) are also used in many applications such as food packaging, treatment of drinking water, treatment of industrial effluent etc., due to their anti-bacterial, anti-viral and anti-fungal properties (Drelich et al., 2011).

Due to biocompatibility, non-toxicity and low-immunogenicity biological NP have many applications in clinical medicine. Bovine serum albumin nanoparticles (BSA- NP) have been used in the delivery of anti- cancer drugs (Zhao et al., 2010). Chitosan NP have been shown to increase membrane permeability and are used in delivery of various drugs (Wang et al., 2011). Apo-transferrin NP have been used successfully in the delivery of anti-cancer drugs in experimental animal models (Golla et al., 2013).

Engineered NP hold promise for the development of new generations of vaccines, adjuvants and immunomodulatory agents. Designed NP can be used for tuning or taming of the immune system. The unique properties of NP also can be exploited in the modulation of immune response (Smith et al., 2013). Highly complex, adaptable and programmable NP can revolutionize treatment of numerous disorders. NP can be engineered to specifically target cells of mononuclear phagocyte system to restore peripheral immune tolerance and to regulate monocyte activities in several inflammatory conditions by mopping up circulating inflammatory mediators (Getts et al., 2015).

Aim and scope of the work

The major objective of the present thesis work has been to investigate the effects of metallic and biological NP on lymphocyte activation *in vitro* and *in vivo* using primary lymphocytes from mouse, rat and humans. Representative malignant B and T cell lines were used to study the effect of the above mentioned NP on proliferative response and cytotoxicity. Mitogen induced B and T lymphocyte activation has been studied in presence of metallic (Gold, Silver and Copper) and biological (Apo-transferrin, BSA and Chitosan) NP *in vitro*. Primary splenic lymphocytes from mouse, rat and human peripheral blood lymphocytes (PBL) were used. Human myeloma cell line, U266B1 and human T cell line, SUPT-1, (lymphoblastic lymphoma) were used for *in vitro* studies. Effect of oral administration of metallic NP (*in vivo*) on lymphocyte activation has been studied using a rat model.

Following experiments were carried out in order to achieve the above mentioned objectives:

- Preparation and characterization of metallic and biological NP
- Effect of metallic and biological NP on proliferative response and viability of splenic lymphocytes from mouse, rat and from human peripheral blood *in vitro*
- Effect of metallic NP on proliferative response and cytotoxicity of representative malignant human B-and T- cell lines
- Tissue localization of metallic NP following oral administration using *ex-vivo* imaging
- Effect of metallic NP on proliferative response and cytokine secretion by splenic and thymic lymphocytes following oral administration to rats.

  and
- Assessment of liver and kidney function markers in plasma of rats administered orally with metallic NP

Chapter 2

Materials and Methods

A. Materials

1. Animals

Female C57BL/6J mice, 8-12 weeks of age and female wistar rats, 6-8 weeks of age, were purchased from National Center for Laboratory Animal Sciences, National Institute of Nutrition, Hyderabad. The animals were maintained under hygienic conditions in the animal facility of University of Hyderabad until use. The use of the above animals for experimental studies was approved by the Institutional Animal Ethics Committee.

2. Cell lines

SUP-T1 and U266B1 cell lines were procured from National Center for Cell Science, Pune, India.

3. Chemicals

RPMI-1640 medium (with 2mM L-glutamine and 25mM HEPES buffer), Phytohaemagglutinin (PHA), Pokeweed mitogen (PWM), Concanavalin A (Con A), Lipopolysaccharide (LPS) from *E.coli*, Heparin, Histopaque (d=1.077), 3-[4,5-Dimethylthiazole-2-yl]-2,5 diphenyl tetrazolium bromide (MTT), Bovine serum albumin, Apo-transferrin, Low molecular weight Chitosan, Tripolyphosphate (TPP), Copper nanoparticles, Rhodamine isothiocyanate (RITC), 2,5 Diphenyloxazole (PPO), 1,4-Bis(5-phenyl-2-oxazolyl-)benzene (POPOP), tissue culture grade Sodium bicarbonate, Penicillin G (Sodium salt) and, Streptomycin sulfate were purchased from Sigma – Aldrich, India. ^{3}H-Thymidine, (Low specific activity, 185-200 GBq / mmole) was purchased from BRIT, INDIA. Fetal calf serum (FCS) was purchased from Biological Industries, Israel and Fetal bovine serum (FBS) from GIBCO- Life technologies, India. Sterile tissue culture plastic ware - microtiter plates (96 well, flat bottom), tissue culture flasks (25 cm^2), petriplates (25 and 100 mm), 15 ml and 50 ml centrifuge tubes were procured from Corning, USA. Rat IL-4, IL-2, TNF-alpha and IFN-gamma cytokine ELISA kits were procured from Bender MedSystems, USA. Biochemical assay kits for urea, creatinine, alanine aminotransferase (ALT) and aspartate aminotransferase (AST) were purchased from Transasia Bio-medicals Ltd, India. All other chemicals used were of analytical grade and obtained from SRL chemicals, Glaxo and E. Merk, India.

B. Methods

1. Preparation of RPMI-1640 medium

Powdered RPMI-1640 medium was dissolved in double distilled water and 2.2 g of sodium bicarbonate (tissue culture grade) was added. pH was adjusted to 7.2 and the volume was made up to 1 litre with double distilled water. Medium was then sterile filtered using a sartorius filtration unit fitted with a 0.22 µm membrane filter and was stored at 4º C until use. The medium was supplemented with penicillin – 100 units/ml and streptomycin-100 µg / ml just before use. Sterile stock solutions of the above mentioned antibiotics were prepared and kept frozen in desired aliquots at -20°C.

2. Isolation of mouse and rat splenic lymphocytes

Principle

Single cell suspensions of splenic lymphocytes were prepared essentially as described earlier (Zimmerman and Kern, 1973). Tissue was teased mechanically to get a single cell suspension. Enriched lymphocyte population was obtained by density gradient centrifugation using histopaque to remove erythrocytes.

Reagents

1. RPMI 1640 medium containing 5 % FBS
2. Histopaque: d = 1.077

Procedure

The mouse or rat was sacrificed using mild ether anesthesia. Spleen was quickly dissected out and was placed in sterile medium. Adhering connective tissue and fat were removed.Then it was transferred onto a sterile stainless steel wire mesh of 100 micron pore size, which kept on sterile petridish. Spleen was minced thoroughly and single cell suspension was prepared by teasing the pieces of tissue using stainless steel brushes mounted on arterial forceps. Cell suspension that percolated through the mesh was transferred to a centrifuge tube and was allowed to stand for 5 min on ice. The cell suspension was collected into a centrifuge tube and large clumps of tissue settled at the bottom of the tube were discarded. Then it was centrifuged at 400 x g for 10 min using a Remi table top centrifuge. The cell pellet was resuspended in 6 ml of RPMI-1640 medium and centrifugation step was repeated as above. Then the pellet was suspended in RPMI-1640 and 6.0 ml cell suspension was layered over 3 ml of Histopaque (2:1 ratio) and

centrifuged at 1200 x g for 20 min. Cells at the interface were collected and suspended in complete medium. Cells were pelleted by centrifugation at 400 x g for 10 min. Cells were resuspended and were pelleted as in the previous step. Finally, cells were suspended in complete medium and stored on ice until use.

3. Isolation of rat thymic lymphocytes

Thymic tissue was processed in the same manner as spleen as described above, except that the gradient centrifugation step was omitted.

4. Isolation of human peripheral blood lymphocytes (PBL)

PBL were isolated according to the method of Boyum (1964).

Principle

Diluted blood sample is layered over a density gradient medium, histopaque containing polysucrose and sodium diatrizoate. Erythrocytes form clumps in presence of polysucrose. The clumps are sedimented to the bottom of the tube upon centrifugation. Lymphocytes are retained at the interphase of plasma / histopaque.

Reagents

1. Histopaque, density = 1.077
2. Heparin, 1000 units / ml, prepared in sterile 0.9 % NaCl

Procedure

Venous blood collected into heparinized tubes (20 U/ml) was diluted 1:1 with sterile 0.9% NaCl. The diluted blood, 5.0 ml was layered over 2.5 ml of Histopaque and centrifuged at 1200 x g for 20 minutes. Cells at the interface were collected and suspended in medium. Cells were pelleted by centrifugation at 400 x g for 10 min. Resuspension and pelleting was repeated twice as described above. Finally, cells were suspended in complete medium and stored on ice until use.

5. Lymphocyte counting

Principle

Lymphocytes in cell suspensions prepared from lymphoid organs and peripheral blood are enumerated using Turk's solution. Gentian violet stains the nucleus, while dilute acetic acid lyses the RBC.

Reagents

1. Turk's solution: 0.01 % gentian violet (w/v) in 3 % (v/v) acetic acid

Procedure

Turk's solution was added to an aliquot of the cell suspension, mixed and loaded in to a haemocytometer. Cells were enumerated under 10 X magnification in white blood cell (WBC) grid areas. Average number of cells in the cell suspension was determined using the formula (Mishell and Shigii, 1980).

No. of cells/ml =Average No. of cells x dilution factor $x10^4$/ml

6. Determination of cell viability

Principle

Dead cells take up the dye, trypan blue while live cells exclude it, there by viable cells could be distinguished from non-viable dead cells, which are stained.

Reagents

1. Trypan blue
2. Sodium chloride (NaCl), 0.9%

Procedure

An aliquot of the lymphocyte suspension was gently mixed with an equal volume of 0.04 % (w/v) trypan blue in 0.9 % NaCl solution. After 3 min incubation, the cell suspension was placed under a coverslip on a microscopic slide. Quickly, the cell images under bright field in different frames (10 X magnification) were captured using a camera fitted to the microscope. A minimum of 300 cell images were enumerated using the recorded data for total cell number and dead cells (dye stained). The viability was expressed as % of total cell number. The percentage of viable cells was calculated using the following formula (Kruse et al., 1973).

$$\% \text{ viability} = \frac{\text{No. of unstained cells}}{\text{Total cell number}} \times 100$$

7. Lymphocyte proliferation assay using ^{3}H-thymidine incorporation into DNA

Principle

Lymphocytes were stimulated with relevant B and T cell specific mitogens under optimal culture conditions. After 48h of stimulation, the cells were pulsed with tritiated-

thymidine (^{3}H-Td) for 24 h and the cultures were processed using a semi-automatic cell harvester. Lysis of the cells results in the deposition of the macromolecular constituents on glass microfiber filters. The filter discs are counted for radioactivity using a liquid scintillation counting. The cells in "S" phase of the cell cycle incorporate the radioactive thymidine into DNA, whereas the resting cells do not. The results are expressed as cpm /culture (cell number used). Stimulation index is calculated as the ratio of average cpm of triplicate cultures in presence of mitogen divided by the average cpm of triplicate cultures in the absence of mitogen.

Reagents

1. Mitogens: 1 mg/ml solutions of Con A, LPS, PHA and PWM were prepared freshly in RPMI-1640, sterile filtered and stored at 4º C for use.
2. Complete RPMI-1640 medium: RPMI- 1640 medium with 5 % FBS.
3. ^{3}H-Thymidine: Diluted in RPMI to 25 μCi / ml.
4. Scintillation cocktail: 4 g PPO and 0.20 g POPOP in 1 litre of scintillation grade toluene.

Procedure

Mouse or rat splenic lymphocytes or human peripheral blood lymphocytes, 2 x 10^5, in triplicate were cultured with and without mitogens in 0.20 ml of complete medium in 96 well flat bottomed microtitre plates. The cultures were kept at 37º C in a humidified incubator with 5% CO_2. The cultures were pulsed with 0.5 μCi / well of ^{3}H-Td for the last 24 hours of the culture period and were harvested on to glass fibre filters after 72 hour using Skatron automatic cell harvester. The dried filters were transferred to toluene based scintillation cocktail, and the radioactivity was measured using Packard liquid scintillation counter (Kasyapa and Ramanadham, 1995).

8. Preparation of metallic and biological NP

8.1. Preparation of GNP

Principle

An aqueous solution of gold chloride is reduced by citrate to form metallic GNP. Citrate also acts as a surface capping agent to stabilize the GNP formed.

Procedure

GNP were prepared according to the method described earlier (Frens, 1973). Briefly, a suitable volume of 1 mM solution of gold chloride solution was kept in boiling water bath and sodium citrate solution is added to a final concentration of 4 mM. The solution undergoes color change, initially blue followed by deep red. At the end of 10 min period, the solution was brought to room temperature and was transferred to a centrifuge tube. The suspension was centrifuged at 10,000 x g for 10 min and the pellet was suspended in ultra pure water. The centrifugation step was repeated to sediment the NP. Finally, the GNP were suspended in ultra pure water and stored at 4º C.

8.2. Preparation of SNP

Principle

An aqueous solution of silver nitrate is reduced by citrate to form metallic SNP. Citrate also acts as surface capping agent to stabilize the SNP formed.

Procedure

The above mentioned chemical reduction method was used to prepare SNP according to the method described earlier (Lee and Meisel, 1982). In a typical preparation, a suitable volume of 1mM silver nitrate was kept in boiling water bath and sodium citrate solution was added to bring it to a final concentration of 4 mM. In about 20 minutes, the colorless silver nitrate solution turns to deep yellow colored solution indicating the formation of NP. The SNP were processed in the same manner as described above in the case of GNP.

The NP suspensions were sterile filtered using 0.45µm membrane filters prior to use in *in vitro* studies.

8.3. Preparation of CuNP

CuNP in powder form were suspended in ultrapure water to a concentration of 1 mg / ml. The suspension was sonicated for 30 min, each time for 2 min with an interval of 2 min, using a microprobe set to 35% of the maximal intensity in a sonicator (MSE instruments, UK). The suspension was suitably diluted in the desired solution and used after sterile filtration.

8.4. Preparation of BSA NP

Principle

Desolvation or coacervation process is commonly used for the preparation of NP of BSA. The desolvating agent changes the tertiary structure of the protein and increases

the hydrophobic nature. The protein tends to form into small aggregates called coacervates. The thermodynamically unstable coacervates are stabilized using glutaraldehyde as the cross-linking agent.

Reagents

1. BSA solution, 15 mg/ml in ultrapure water
2. Absolute ethyl alcohol
3. Glutaraldehyde solution, 8 %

Procedure

To a 2 ml solution of BSA which was kept under gentle stirring at 25ºC, 8ml of absolute ethanol was added dropwise. The desolvated protein solution was kept under stirring for 1 h. Then, an aliquot of glutaraldehyde was added and the stirring was continued for 16 h. Finally, the suspension was centrifuged at 10,000 x g for 30 min. The supernatant was discarded and the pellet was suspended in 2 ml of ultrapure water. The centrifugation step and resuspension of the pellet was repeated twice. Finally, the pellet was made up to 2 ml and stored at 4º C until use (Martınez et al., 2011).

8.5. Preparation of apo-transferrin NP

Principle

Apo-transferrin NP were prepared essentially according the method described earlier (Krishna et al, 2009). An aqueous solution of apo-transferrin was added to oil phase and a water-in-oil emulsion was prepared by ultra sonication. The NP thus formed were stabilized by freezing and thawing. The oil phase was removed using an organic solvent and the NP were suspended in aqueous phase.

Reagents

1. Apo-transferrin solution in phosphate buffered saline (PBS).
2. Olive oil.
3. Diethyl ether

Procedure

2.5 mg of apo-transferrin was dissolved in 0.20 ml of phosphate buffered saline, pH 7.2. The apo-transferrin solution was added dropwise to 30 ml of olive oil with continuous dispersion by gentle mixing at 4º C. The sample was sonicated using a micro probe (MSE Instruments, UK) with 30 seconds pulse. The sample sonication steps were

repeated 15 times with a gap of 1 minute between successive steps at 4º C. After sonication, the resulting mixture was immediately frozen in liquid nitrogen for 10 min and was then transferred to ice and incubated for 4 h. The NP formed were pelleted by centrifugation at 3000 x g for 10 min at 4º C and the pellet was extensively washed with diethyl ether and dispersed in PBS. The NP suspension was stored at 4º C until use.

8.6. Preparation of Chitosan NP

Principle

Positively charged chitosan forms a spontaneous complex or gel formation with negatively charged tripolyphosphate (TPP) through electrostatic interactions.

Reagents

1. Chitosan solution, 2 mg / ml in 1.2 % acetic acid(v/v)
2. TPP solution, 1 mg/ml

Procedure

To a 5 ml of chitosan solution, 2 ml of TPP was added drop wise with constant gentle stirring. Formation of chitosan NP was indicated by the formation of opalescent suspension. The NP were pelleted by centrifugation at 10,000g for 30 min. The NP were suspended in ultra pure water and the centrifugation step was repeated. Finally, the NP were suspended in 0.9% NaCl and stored at 4º C until use (Calvo et al., 1997b).

9. Characterization of NP

9.1. Visible spectroscopy

Principle

Metallic NP exhibit unique optical property due to interaction of their surface electrons with electromagnetic radiation is called surface plasmon resonance (SPR). Therefore, metallic NP have characteristic absorption maxima in the visible region of electromagnetic spectrum.

Procedure

The absorption spectrum of NP suspension was recorded from 400-700 nm using a UV-visible spectrophotometer (Shimadzu., Japan).

9.2. Transmission electron microscopy (TEM)

Principle

A beam of electrons is transmitted through an ultra-thin specimen and the interaction of sample with electron beam results in diffraction. At certain angles, the beam is diffracted strongly from the axis of incoming beam, while at others the beam is largely transmitted. An image is formed from the electrons transmitted through sample.

Procedure

A small drop of NP suspension was kept on carbon coated grids and the air dried samples were examined using the electron microscope (FEI model Tecnai G2S Twin, USA) at an accelerating voltage of 80 KV.

9.3. Scanning electron microscopy (SEM)

Principle

A beam of electrons passes through the sample and it interacts with its atoms and image is formed from signals generated as back scattered and secondary electrons. Samples topography and composition information is obtained.

Procedure

A drop of NP was spread and dried on a glass slide. This slide was placed and fixed on a specimen stub. The sample was coated with a conducting material using sputter coater and characterized for size and morphology by scanning electron microscope (FESEM ultra 55, carlzeiss, Germany) at 5 KV.

9.4. Nanoparticle Tracking Analysis (NTA)

Principle

A laser beam is passed through the sample chamber and properties of both light scattering and Brownian motion of the each particle is visualized via camera mounted onto optical microscope. The camera, which operates at 30 frames per second, captures the video file of the particle, which is under Brownian motion. The NTA software (2.3 build 0025) identifies the distance moved by each particle from frame to frame of the video and determines diffusion coefficient and consequently size of the particles. The average number of particles in each frame was used to calculate the concentration of the nanoparticle suspension.

Reagents

1. NP solution
2. Milli Q water
3. PBS

Procedure

The nanoparticle suspension was diluted with milli Q water and loaded in the Nanosight NS 500 instrument (Malvern Instruments Ltd, Malvern, UK). Samples were introduced into the integrated fluidics automatically. In all experiments, samples were measured for 90 seconds (25 frames per second), but the camera level (consists of shutter and gain), detection threshold was adjusted manually for each experiment. All measurements were done at room temperature and performed with the auto-adjustment-function for the parameter blur, minimum expected particle size and minimal track lengths.

10. Determination of metallic and biological NP concentration

The concentration of the GNP and SNP was determined gravimetrically. A known volume of the NP suspension was centrifuged at 10,000 x g in a Eppendorf tube and the supernatant was carefully removed and the pellet was air dried. The weight of the centrifuge tube with the pellet was recorded using an electronic balance and suitable corrections were made for the weight of the tube. At least 3 different batches of NP were analyzed. The concentration of CuNP was calculated from the dry weight of the sample. The concentration of nanoparticles was expressed as weight / volume (mg/ml).

For protein biological NP, biuret method was used to estimate the concentration of BSA and apo-transferrin NP. Anthrone method was used to determine the concentration of chitosan NP.

11. Estimation of Malondialdehyde (MDA)

Prinicple

MDA was measured according to the procedure of (Ohkawa et al., 1979). MDA forms a pink colored adduct upon boiling with thiobarbituric acid (TBA) under acidic conditions. The absorbance of the colored product was measured at 532 nm. A molar extinction coefficient of 1.53×10^5 $M^{-1}cm^{-1}$ was used to calculate the concentration.

Reagents

1. 0.50 % TBA in 15 % TCA and 8.1% Sodium dodecyl sulphate

Mouse splenic or human PBL, 0.2 x 10^6, were incubated in triplicate with GNP (200µg/ml), SNP (50µg/ml) and CuNP (10µg/ml) for 72 h. Then, the cell suspension was centrifuged at 6000 x g and the supernatant and the cell pellet were collected and preserved. One ml of TBA reagent was added to 0.2ml of supernatants and the mixture was kept in a boiling water bath for 15 minutes. The reaction was stopped by placing the mixture on ice. The precipitate was removed by centrifugation and the absorbance of the supernatant containing the MDA-TBA adduct was measured at 532 nm using a Spectrophotometer.

12. Maintenance of cell lines

SUP T1

The cell line was procured from National Center for Cell Science, Pune, India. The growth medium used for the propagation of this cell line was RPMI-1640 with 10% FBS. The cells were grown in tissue culture flasks kept in a CO_2 incubator maintained at 37° C and 5 % CO_2. The cells were seeded at a concentration of 0.2 x 10^6 cells / ml of the medium. When the cells reached a density of 2 x 10^6 cells / ml they were sub-cultured. Medium was renewed 2 to 3 times per week and the cultures were checked microscopically for any contamination using an inverted microscope.

U 266B1

It is a human myeloma cell line obtained from National Center for Cell Science, Pune, India. The growth medium used for the propagation of the cell line was RPMI-1640 with 10% FBS using the identical culture conditions described above. Medium was renewed 2 to 3 times per week.

13. MTT assay

MTT assay was done as described earlier (Mossman, 1983).

Principle

The yellow colored compound MTT, when incubated with cultured cells is reduced by mitochondrial dehydrogenase enzymes of the living cells only to a purple colored formazan product. The absorbance of the formazan is measured using an ELISA reader at 570 nm and 630 nm. The absorbance at 630 nm is subtracted from 570 nm value to correct for the background absorbance.

Reagents

1. 5 mg / ml MTT in PBS, prepared freshly
2. 4% isopropanol in 1 M HCl

Procedure

Cells, 5 x 10^4, in 0.10 ml of complete medium were incubated with metallic NP in 96 well microtitre plates for 24 h. At the end of the incubation period, 20 µl of MTT was added to each well. The plate was incubated for 4 h at 37º C. At the end of incubation period, 100 µl of 4% isopropanol in 1M HCl was added to the wells and mixed several times to solubilize the formazan compound. The absorbance was measured at 570/630 nm in dual wavelength mode using a microplate reader (Multiskan EX, Labsystems, Finland).

14. Preparation of Rhodamine (Rho) labeled BSA and Chitosan

14.1. Rho-BSA conjugate (Rho-BSA)

Principle

Rhodamine is conjugated to BSA using RITC at alkaline pH. Excess fluorochrome is removed by dialysis. The degree of conjugation of the fluorochrom to the protein is determined by measuring the absorbance at 280 nm and 580 nm in a UV-visible spectrophotometer.

Reagents

1. Bicarbonate buffered saline - 0.05 M bicarbonate buffer, 0.9 % NaCl, pH 9.2
2. RITC, 5 mg / ml in methanol
3. BSA solution in bicarbonate buffered saline, 10 mg / ml
4. PBS, 0.02 M phosphate buffer – 0.9 % NaCl, pH 7.2

Procedure

An aliquot of BSA is treated with RITC to a final concentration of 100 µg / ml and the mixture was kept under gentle mixing at room temperature for 4 h. Then, solution was transferred to a dialysis bag and dialyzed against PBS for 24 h in dark. Several buffer changes were made to ensure complete removal of the fluorochrome. The conjugate was stored at 4ºC. An aliquot of the conjugate is suitably diluted in PBS and the absorbance was measured at 280 nm and 580 nm (Goding , 1976).

14.2. Rho-chitosan conjugates (Rho-chitosan)

Principle

Chitosan is labeled with rhodamine using RITC according to the method described earlier (Ma et al., 2008).

Chitosan in acidic medium is made to react with RITC in methanol. The conjugate is precipitated with NaOH and the excess fluorochrome is removed.

Reagents

1. Chitosan solution 5 mg/ ml in 0.5 % acetic acid
2. RITC, 5 mg / ml in methanol

Procedure

A suitable aliquot of chitosan with RITC to a final concentration of 100 µg / ml was kept under gentle stirring for 24 hours at room temperature. Chitosan was precipitated using 10 N NaOH and the pellet was suspended in ultra pure water. The suspension was centrifuged at 10,000 x g for 20 min and the pellet was re-suspended in water and the centrifugation step was repeated. Finally, the conjugate was suspended in 0.5% acetic acid and dialyzed against ultra pure water for 4 hours. The conjugate was stored at 4º C. An aliquot of the conjugate is suitably diluted in PBS and the absorbance was measured at 280 nm and 580 nm.

15. Preparation of NP coated with Rho- BSA and Rho- chitosan conjugates

Principle

The rhodamine labeled conjugates were coated on the surface of NP by passive adsorption process. The stability of the coated ligand on the NP was characterized.

Reagents

1. Rho-BSA and Chitosan, 1 mg / ml
2. Metallic NP suspension
3. Tris-buffered saline (TBS), 20 mM Tris-HCl in 0.9 % NaCl, pH 7.20

Procedure

An aliquot of GNP/ SNP/ CuNP suspension was centrifuged at 10,000 g for 10 min in a microfuge tube. The supernatant was discarded and the pellet was suspended in 0.40 ml of tris-buffered saline, pH 7.20. To this, 0.1ml of the rhodamine conjugated BSA or chitosan is added and incubated at room temperature for 1 h. Then, the mixture was centrifuged at 10,000 x g and the pellet was suspended in TBS and centrifuged as above. This step was repeated once and finally the NP are suspended in TBS and kept at 4ºC until use. All the operations were carried out in dark.

16. Estimation of rat cytokines by Enzyme linked immunosorbent assay (ELISA)

Principle

The rat IL-2, IL-4, IFN-gamma and TNF-alpha were estimated using sandwich amplified ELISA. The microwell strips were pre-coated with either a polyclonal or monoclonal against the relevant cytokines - IL-2, IL-4, IFN-gamma and TNF-alpha separately. The rat sample or varying concentrations of standard recombinant cytokines were added to the wells. The cytokine present in the sample or the standard binds to coated antibodies. A biotin-conjugated anti-rat cytokine antibody was added which binds to the cytokines, captured by first anti-rat antibody. The unbound biotin-conjugated anti-cytokine antibody was removed by wash step and streptavidin-horse radish peroxidase conjugate was added, which binds to biotin conjugated anti- cytokine antibody following incubation. Finally, substrate solution was added and the reaction was stopped using the stop solution. The absorbance of the colored product was measured in an ELISA reader which is directly proportional to the amount of cytokines present in the sample or standard.

Reagents

1. Assay buffer: PBS with 1 % Tween 20 and 10 % BSA, diluted to 1x from a 20x stock.
2. Wash buffer: PBS with 1 % Tween 20, diluted to 1x from 20 x stock.

3. Standard IL-2, IL-4, IFN-gamma and TNF-alpha, recombinant lyophilized proteins reconstituted in ultra pure water. IL-2 : 4000 pg /ml, IL-4 : 200 pg / ml, IFN-gamma : 4000 pg / ml and TNF-alpha : 5000 pg /ml.
4. Sample diluent: supplied by the manufacturer and used to dilute standard and sample.
5. Micro-well plate with strips coated with monoclonal antibody to rat IL-2, IL-4, IFN-gamma or polyclonal antibody to TNF-alpha.
6. Biotin labeled monoclonal or polyclonal antibody conjugate, diluted 1:100 with assay buffer and used within 30 minutes
7. Streptavidin-Horse radish peroxidase (S-HRP): Diluted 1:200 in assay buffer and used within 30 minutes
8. Substrate solution: Tetramethyl benzidine (TMB)
9. Stop solution: 1 M phosphoric acid

Procedure

The micro-well strips were washed twice with the addition of 400 µl of wash buffer into each well. The buffer was allowed to sit in the wells for 10-15 seconds. Wells were aspirated and the excess wash buffer was removed by tapping them on an absorbent pad. All the standards and samples were done in duplicate. The standards were prepared by serial dilution by adding 100 µl of standard to 100µl of diluent in duplicate wells and mixed. Dilutions were done by transferring 100µl prepared first dilution in to next set of wells. Finally, 100µl from the wells of the last dilution was discarded. 100µl of sample diluent was taken in duplicate into blank wells. Each sample, 50 µl of sample was diluted with 50µl of sample diluent and added to wells. Then diluted biotin-conjugate, 50µl was added to all wells. The micro-well strips were covered and incubated for 3 hours at room temperature. Wells were emptied and were washed thrice carefully with 400 µl of wash buffer. Diluted S-HRP conjugate, 100µl was added to all the wells. The micro-well strips were covered and incubated for 1 hour at room temperature. Wells were emptied and washed thrice with 400 µl of wash buffer. Substrate solution (TMB), 100 µl was added to all the wells and incubated for 10 minutes at room temperature. Finally, 100µl of stop solution was added to all wells. Absorbance was read at 450 nm within 30 minutes of stopping the reaction. The results were calculated from the standard graph and were expressed as pg/ml.

17. Biochemical analysis

Collected blood samples from control and treated group of animals were centrifuged at 2000 rpm for 10 minutes and plasma was separated. The plasma was subjected to various biochemical tests to know the levels of ALP, ALT, AST, urea and creatinine.

18. Statistical analysis

Data were expressed as mean ± SEM. Statistical significance was evaluated by one- way ANOVA followed by post-hoc Tukey's test using Sigma plot 11 software (Systat, San Jose, CA). Difference of mean values between control and treated groups was considered significant at p value <0.05.

Chapter 3

Preparation and characterization of metallic and biological NP

Introduction

Preparation and characterization is a prerequisite to study cellular effects of NP *in vitro* and *in vivo.* NP have been synthesized essentially using two approaches - self-assembly of atoms/molecules/clusters of a material or by reduction in size of the starting material (Kwok and Chan, 2014). Both approaches make use of several physical and chemical methods. Due to ease of synthesis and low cost, the chemical methods have been widely used. However, recently, biological methods are also being explored for the synthesis of metallic NP (Singh et al., 2016).

After NP are synthesized, characterization is necessary prior to their use. Information about physico-chemical properties of NP are useful in prediction and determination of their behavior in biological system (Johnston et al., 2012). Physiological interactions of NP from molecular to systemic level can influence their role in diagnostic accuracy and therapeutic efficacy. It is well documented that physico- chemical properties of NP such as size, shape and surface charge affect their circulation, biodistribution as well as their interactions with cells (Duan et al., 2013). Characterization is very much essential for validation and improvement of synthesis protocols and to realize the potentials of NP (Hall et al., 2012). Characterization not only determines the bio-medical applications but also predicts the safety and toxicity of NP (Luyts et al., 2013). Several methods have been reported for characterization of NP, each one having certain advantages and disadvantages. Some of the widely used techniques for characterization of NP are presented in Table 3.1.

In the present study metallic (gold, silver and copper) and biological (bovine serum albumin, apo-transferrin and chitosan) NP were prepared by chemical methods and characterized using UV-visible spectroscopy, transmission electron microscopy (TEM), scanning electron microscopy (SEM) and nanoparticle tracking analysis (NTA).

Methods

Preparation of metallic and biological NP

GNP and SNP were prepared by chemical reduction method using tri-sodium citrate as described in materials and methods (Chapter 2). CuNP were procure

Table 3.1: Comparison of NP characterization techniques

S.No	Techniques	Physico-chemical characteristics analyzed	Advantages	Disadvantages
1	Dynamic light scattering (DLS)	Hydrodynamic size distribution	Non destructive method. Rapid and reproducible. Measures in any solvent of interest. Good accuracy for monodispersed samples. Modest cost.	Limited size resolution. Limited use for poly-dispersed sample measurement. Assumption of spherical shape of samples.
2	Scanning electron microscopy (SEM)	Size distribution, shape, aggregation and dispersion.	Direct measurement of size distribution and shape. High resolution.	Conducting sample or coating of conducting material on sample. Dry sample, Measurement in non-physiological condition. High cost.Cryogenic method required for NP-bioconjugates.
3	Transmission electron microscopy (TEM)	Size distribution, shape, aggregation and dispersion.	Direct measurement of size distribution and shape. High resolution	Ultrathin samples required. Measurement in non-physiological condition. High Cost
4	Atomic force microscopy (AFM)	Size distribution, shape, aggregation, dispersion and surface properties.	3D sample mapping. Sub-nanoscale topographic resolution. Measurement of samples in dry or aqueous environment.	Overestimation of lateral dimensions. Time consuming. Limited to exterior of NP
5	UV-visible spectroscopy	NP size, aggregation, stabilization and surface chemistry	Simple sample preparation. Low cost.	Used only in NP with surface plasmon resonance.
6	Nanoparticles tracking analysis (NTA)	Hydrodynamic size distribution and agglomeration.	Avoids intensity bias towards large particles. Provides information about number of NP.	Only visualization of NP.

commercially and used. All three metallic NP were characterized by UV-visible spectroscopy, TEM, and NTA.

Biological NP- apo-transferrin, bovine serum albumin and chitosan NP were prepared by sol-oil, desolvation and ionic gelation methods respectively and characterized by SEM and NTA as described in materials and methods.

Gravimetric method for determination of NP concentration

GNP and SNP were prepared by chemical reduction method. 30ml of nanoparticles suspension (GNP and SNP) was sedimented by centrifugation at 11000 xg for 20 minutes. The dry weight of nanoparticles sediment was measured gravimetrically. A clean empty eppendorf tube was taken and weighed. NP sediment was taken into eppendorf tube and dried at 37ºC for 3 hours to remove water. Eppendorf tube with NP sediment weighed again. The dry weight of the NP sediment was obtained subtracting the initial weight from final weight of the eppendorf tube. Concentration of NP was expressed as weight/volume.

Results

1. **Yield and concentration of NP**

   GNP and SNP were prepared several times and yield of the NP was calculated from initial weight of the gold chloride and silver nitrate taken for preparation. The weight of NP obtained in each experiment was determined gravimetrically. Results are presented in Table 3.2. Gold chloride, 10 mg and silver nitrate, 5 mg were taken for preparing NP in each experiment. The data showed that 73% of initial weight of gold chloride was converted to GNP and 60% of silver nitrate was converted to SNP

2. **Characterization of GNP**

   Absorption spectrum of GNP in the visible range revealed a maximum at 518 nm, representative of characteristic surface plasmon resonance (Figure 3.1). TEM images of GNP are presented in Figure 3.2. Particles showed a spherical shape and calculated diameter was in the range of 13-15nm. Hydrodynamic diameter of GNP along with particle number in the suspension as analyzed by NTA is presented in

Figure 3.3. Data from a representative experiment is shown in the figure. Unimodal distribution was noted. Data of four sample preparations analyzed independently depicting mean, mode and median are presented in Table 3.3. The predominant modal hydrodynamic diameter was 28 ± 1.6 nm with a particle number of 0.59 ± 0.06 $x10^9$/µg.

3. Characterization of SNP

A characteristic absorption maximum at 420 nm was observed in the absorption spectrum of SNP recorded in visible range (Figure 3.4). TEM images of SNP are presented in Figure 3.5. The particles showed spherical morphology with a diameter range of 40-80 nm. Hydrodynamic diameter of SNP along with particle number in the suspension as analyzed by NTA is presented in Figure 3.6. Data from a representative experiment is shown in the figure. Predominantly unimodal distribution was noted. Data of four samples analyzed independently depicting mean, mode and median are presented in Table 3.4. The predominant modal hydrodynamic diameter was 66 ± 2.7 nm with a particle number of 0.48 ± 0.03 $x10^9$/µg.

4. Characterization of CuNP

Absorption spectrum of CuNP suspension is presented in Figure 3.7. A broad absorption maximum around 505 nm was observed. TEM images revealed, near spherical morphology with diameter range of 23-33 nm (Figure 3.8). Hydrodynamic diameter of CuNP along with particle number in the suspension as analyzed by NTA is presented in Figure 3.9. Data from a representative experiment is shown in the figure. A multimodal distribution of particles was observed. At least three particle populations were identified. Data of three independent experiments depicting mean, mode and median are presented in Table 3.5. The average modal diameter was 134 ± 26.0 nm and particle concentration of 0.05 ± 0.004 $x10^9$/µg.

5. Characterization of apo-transferrin NP

Scanning electron micrograph depicting apo-transferrin NP morphology is presented in Figure 3.10. The particles were spherical in shape with a size range of

40-50nm in diameter. Data from a representative NTA analysis is shown in Figure 3.11. NP population showed a predominantly unimodal distribution. Data of three samples analyzed independently is given in Table 3.6. Average modal diameter was 104 ± 5.6 nm and the mean particle number was 16.8 ± 0.8 $x10^6$/ µg.

6. Characterization of BSA NP

Scanning electron micrograph of BSA NP is presented Figure 3.12. The particles were spherical in shape with a size range of 80-120 nm. Data from a representative NTA analysis is shown in Figure 3.13. NP population showed a predominantly unimodal distribution. Data of two independent experiments is given in Table 3.7. Average hydrodynamic size was 114 nm and number of particles was 11.75 $x10^6$/ µg.

7. Characterization of chitosan NP

Scanning electron micrograph of chitosan NP is presented in Figure 3.14. The particles showed a spherical shape with a size range of 120-150nm Representative NTA analysis data is depicted in Figure 3.15. The hydrodyanamic size showed a wide range from 50-500 nm with a multimodal distribution. Data of three independent experiments is presented in Table 3.8. Modal hydrodynamic diameter of the major NP population was 172 ± 17.5 nm and the number of particles was 8.0 ± 0.4 $x10^6$/ µg.

Table 3.2: Estimation of dry weight of GNP and SNP by gravimetric method (Values presented are from 3 independent experiments). Gold chloride, 10 mg and Silver nitrate, 5 mg were used in all the three experiments.

Expt. No	GNP (mg)	SNP (mg)
1	8	3.0
2	7	3.1
3	7.5	3.0
Mean ± SEM	7.5 ± 0.3	3.0 ± 0.03

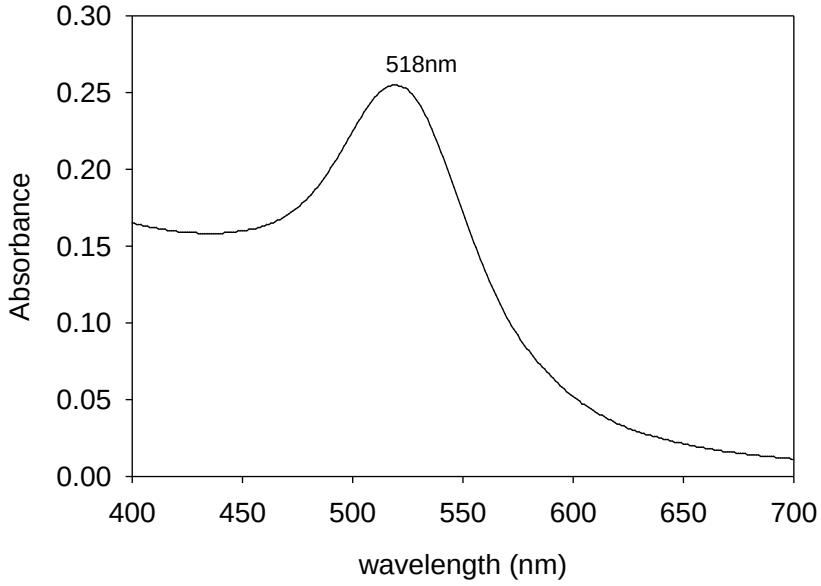

Figure 3.1: Absorption spectrum of GNP. A suspension of 50 µg / ml in ultrapure water was scanned at room temperature. Plot shown is representative of one out of three experiments.

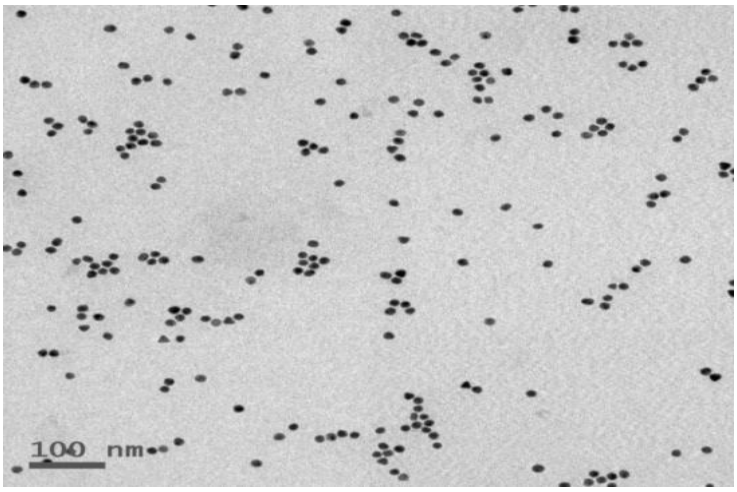

Figure 3. 2: Transmission electron micrograph of GNP. 5 µl of 200 µg/ml suspension was used and representative data of one out of three independent experiments is presented.

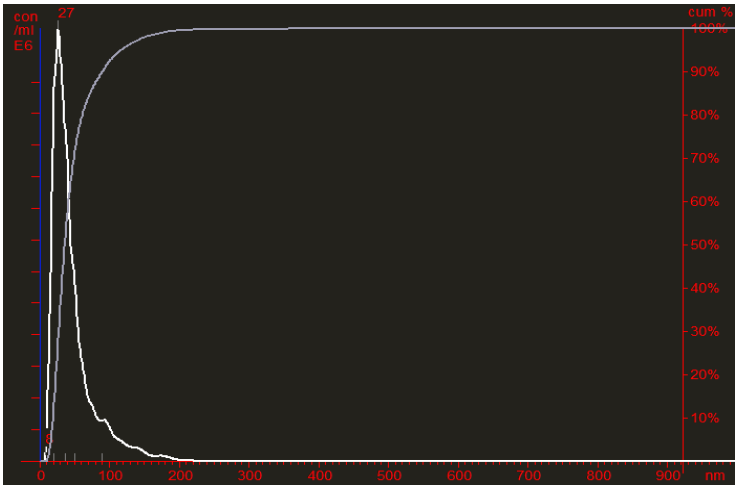

Figure 3.3: Nanoparticle tracking analysis of GNP. A suspension of 2 µg/ml in ultrapure water was analyzed at room temperature. X- axis: Diameter (nm) and Y-axis: Particle number (x 10^6). Representative data of one out of four independent experiments is presented.

Table 3.3: Distribution of size and particle number of GNP analyzed using NTA

S.No	Diameter (nm)			x 10^9/µg
	Mean	Mode	Median	
1	58	27	49	0.48
2	61	32	48	0.76
3	42	25	33	0.57
4	42	27	35	0.54
Mean ± SEM	50 ± 5.0	28 ± 1.5	40 ± 4.2	0.59 ± 0.06

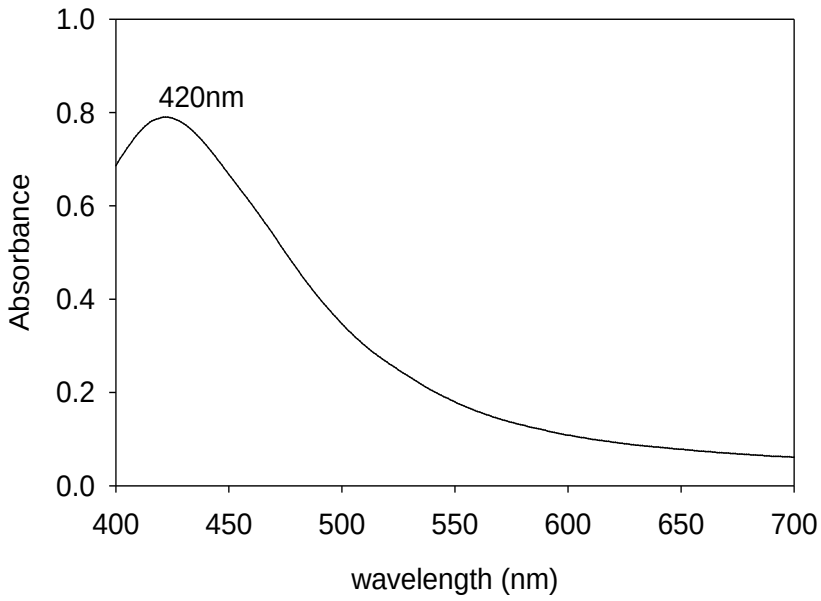

Figure 3.4: Absorption spectrum of SNP. A suspension of 50 µg / ml in ultrapure water was scanned at room temperature. Plot shown is representative of one out of three experiments.

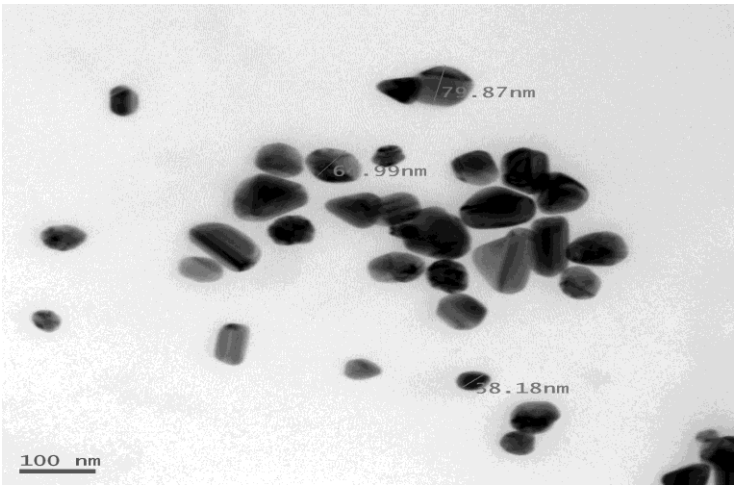

Figure 3.5: Transmission electron micrograph of SNP. 5 µl of 200 µg/ml suspension was used and representative data of one out of three independent experiments is presented.

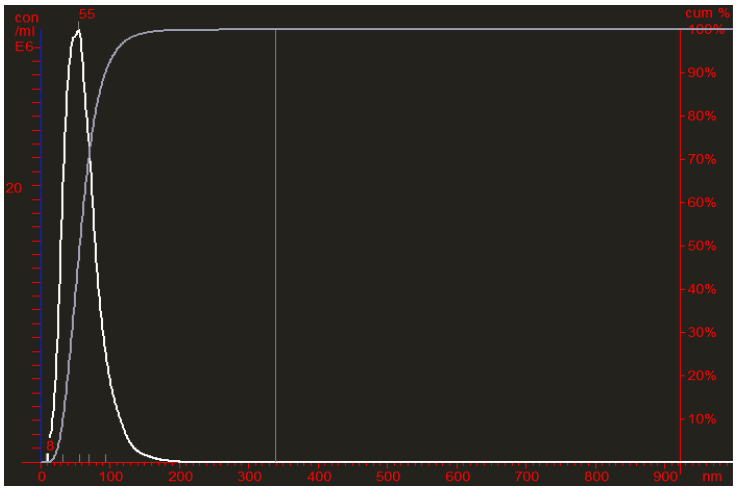

Figure 3.6: Nanoparticle tracking analysis of SNP. A suspension of 2 µg/ml in ultrapure water was analyzed at room temperature. X- axis: Diameter (nm) and Y-axis: Particle number (x 10^6). Representative data of one out of three independent experiments is presented.

Table 3.4: Distribution of size and particle number of SNP analyzed using NTA

S.No	Diameter (nm)			x 10^9/µg
	Mean	Mode	Median	
1	78	72	73	0.54
2	79	69	72	0.53
3	69	57	65	0.41
4	77	69	72	0.44
Mean ± SEM	76 ± 1.8	66 ± 2.7	70 ± 1.5	0.48 ± 0.03

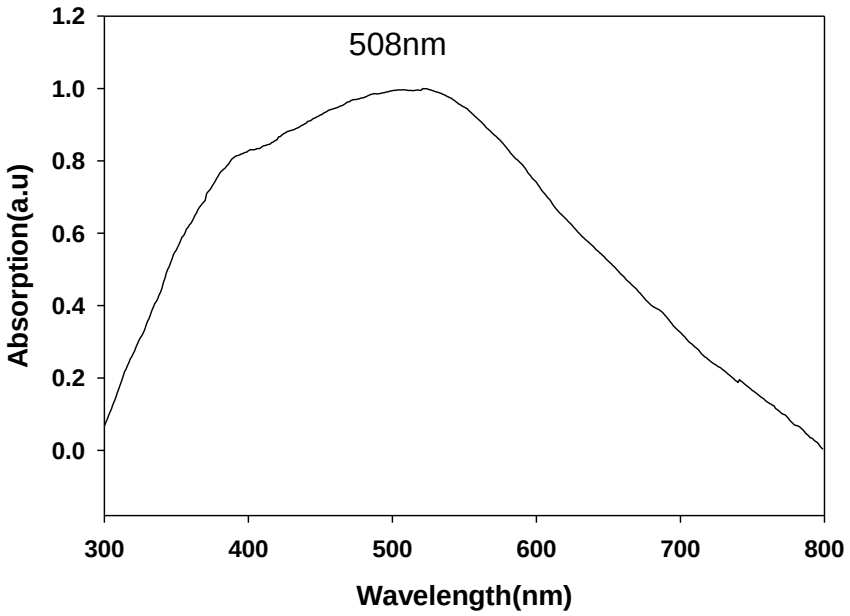

Figure 3.7: Absorption spectrum of CuNP. A suspension of 50 µg / ml in ultrapure water was scanned at room temperature. Plot shown is representative of one out of three experiments.

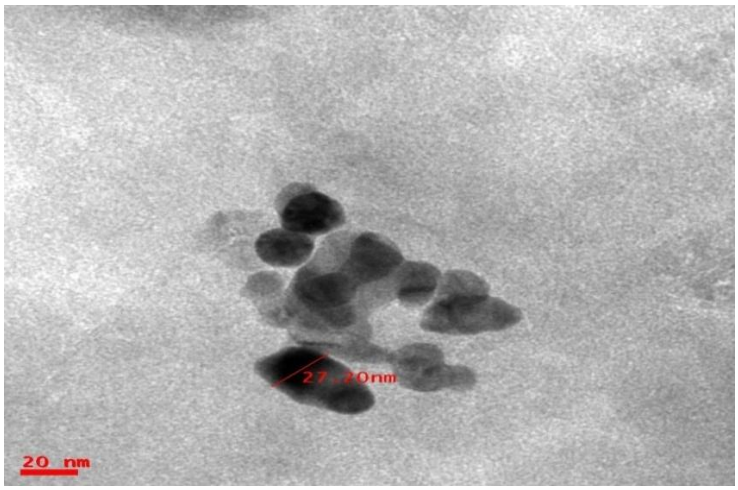

Figure 3.8: Transmission electron micrograph of CuNP. 5 µl of 200 µg/ml suspension was used and representative data of one out of three independent experiments is presented.

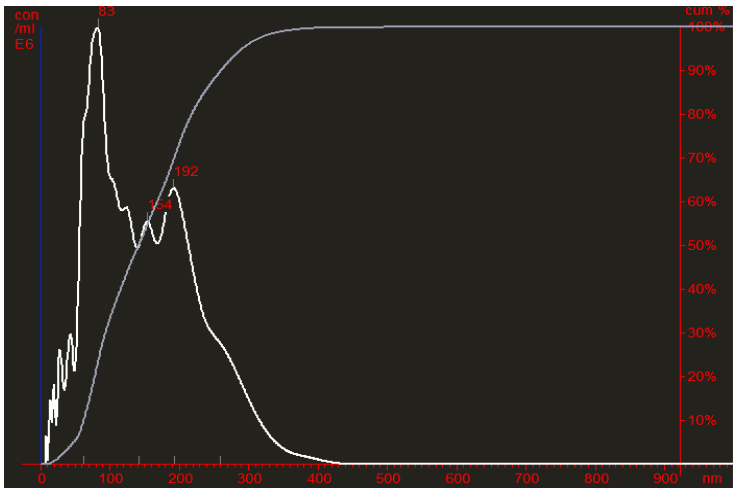

Figure 3.9: Nanoparticle tracking analysis of CuNP. A suspension of 2 µg/ml in ultrapure water was analyzed at room temperature. X- axis: Diameter (nm) and Y-axis: Particle number (x 10^6). Representative data of one out of three independent experiments is presented.

Table 3.5: Distribution of size and particle number of CuNP analyzed using NTA

S.No	Diameter (nm)			x 10^9/µg
	Mean	Mode	Median	
1	204	170	183	0.054
2	196	149	185	0.065
3	152	83	142	0.052
Mean ± SEM	184 ± 16	134 ± 26.0	170 ± 14	0.057 ± 0.004

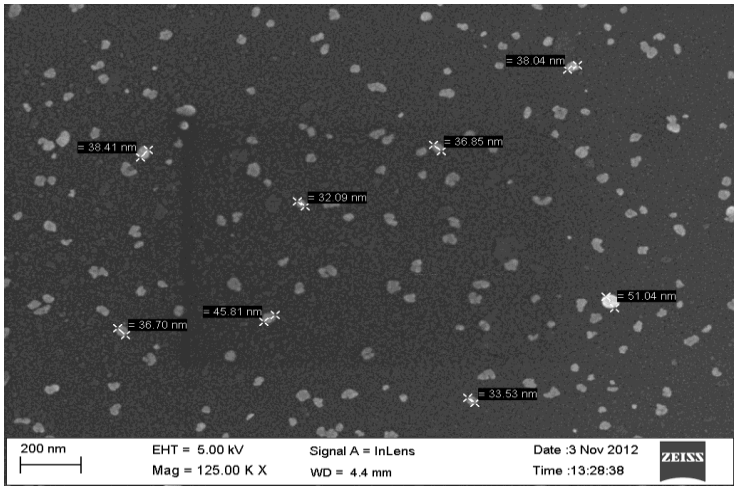

Figure 3.10: Scanning electron micrograph of apo-transferrin NP. A suspension of 100 µg/ml in phosphate buffered saline (PBS), pH 7.4 was used for scanning at room temperature.

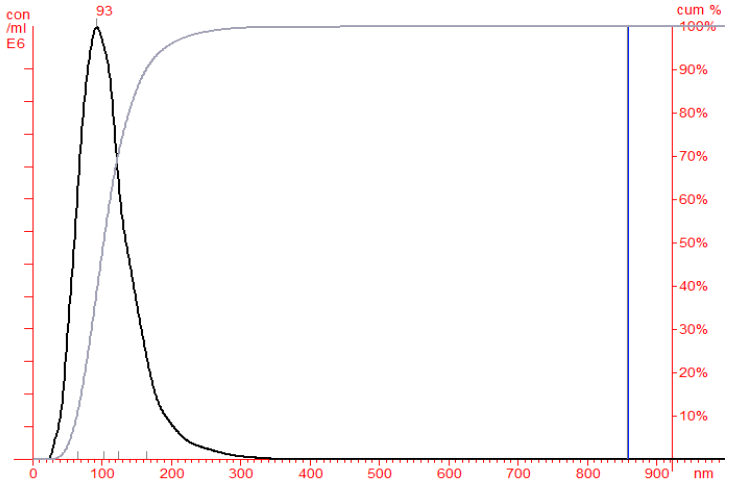

Figure 3.11: Nanoparticle tracking analysis of apo-transferrin NP. A suspension of 100 µg/ml in PBS was analyzed at room temperature. X- axis: Diameter (nm) and Y-axis: Particle number (x 10^6). Representative data of one out of three independent experiments is presented.

Table 3.6: Distribution of size and particle number of Apo-transferrin NP analyzed using NTA

S.No	Diameter (nm)			x 10^6/µg
	Mean	Mode	Median	
1	111	93	103	18.3
2	132	111	124	15.6
3	130	109	122	16.8
Mean ± SEM	124 ± 6.6	104 ± 5.6	116 ± 6.6	16.8 ± 0.8

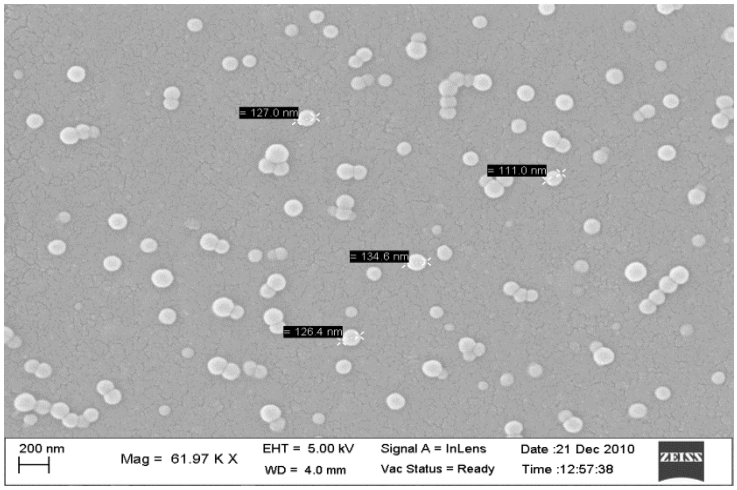

Figure 3.12: Scanning electron micrograph of BSA-NP. A suspension of 100 µg/ml in PBS was used for scanning at room temperature.

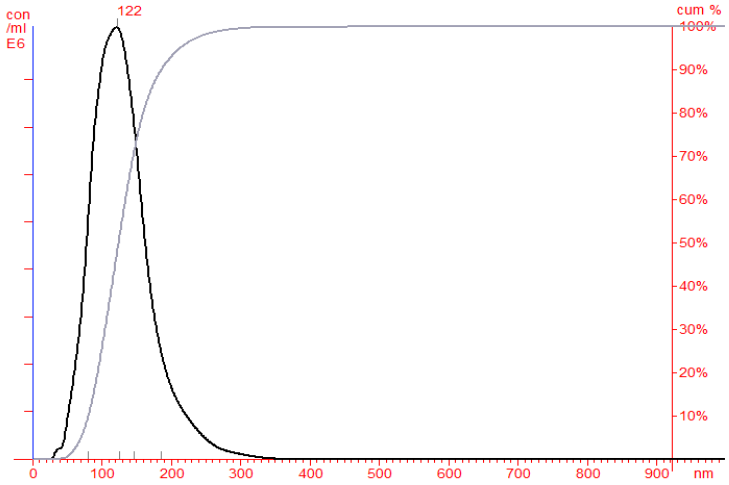

Figure 3.13: Nanoparticle tracking analysis of BSA- NP. A suspension of 100 µg/ml in PBS was analyzed at room temperature. X- axis: Diameter (nm) and Y- axis: Particle number (x 10^6). Representative data of one out of three independent experiments is presented.

Table 3.7: Distribution of size and particle number of BSA - NP analyzed using NTA

S.No	Diameter (nm)			x 10^6/µg
	Mean	Mode	Median	
1	131	122	125	11.7
2	130	105	121	11.8
Mean	130.5	113.5	123	11.75

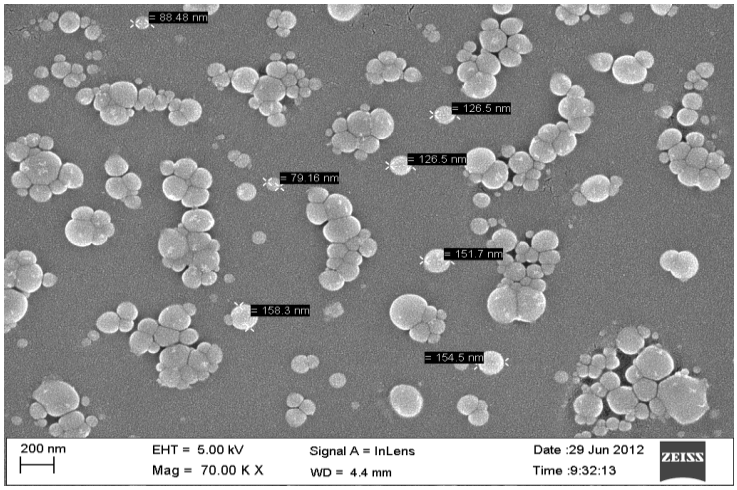

Figure 3.14: Scanning electron micrograph of chitosan NP. A suspension of 100 µg/ml in PBS was used for scanning at room temperature.

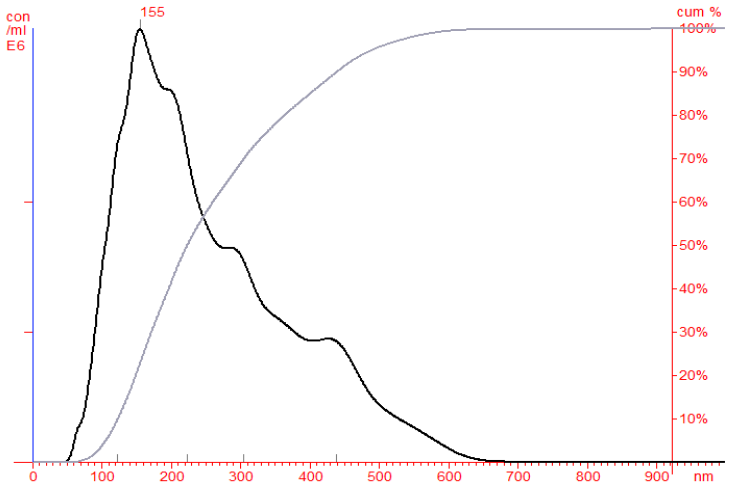

Figure 3.15: Nanoparticle tracking analysis of chitosan NP. A suspension of 100 µg/ml in PBS was analyzed at room temperature. X- axis: Diameter (nm) and Y-axis: Particle number (x 10^6). Representative data of one out of three independent experiments is presented.

Table 3.8: Distribution of size and particle number of chitosan NP analyzed using NTA

S.No	Diameter (nm)			x 10^6/µg
	Mean	Mode	Median	
1	281	154	254	8.5
2	256	155	224	7.3
3	272	207	252	8.2
Mean ± SEM	270 ± 7.3	172 ± 17.5	243 ± 9.7	8.0 ± 0.4

Discussion

Several physical and chemical methods have been employed for the synthesis of metallic NP. The major physical methods are – 1. Pulsed laser ablation, 2. Sonochemical reduction, 3. Microwave irradiation, 4. Gamma irradiation etc. The notable chemical methods are- 1. Chemical reduction of metal salts, 2. Thermal decomposition of metal salts, 3. Electrochemical synthesis etc. An ideal method for metallic NP synthesis should have the features- 1. Size and shape of the particle can be controlled, 2. Yields monodisperse suspension, 3. Reproducible, 4. Low cost, 5. Few steps and less bye products, 6. Reaction at low temperature.

Amongst the various methods for preparation of metallic NP, chemical reduction is preferred as it is a simple, reproducible and low cost protocol. It is well established that in chemical reduction process, size, shape and stability of NP are strongly influenced by the experimental conditions, rate of reducing agent interaction with metal ions and adsorption processes of stabilizer (Sharma et al., 2009; Sengupta et al., 2005). Hence, the synthesis of NP having controlled size, shape, stability and properties has become an essential prerequisite in nanotechnology research. Sodium borohydride, tri-sodium citrate, ascorbate, and elementary hydrogen are other commonly used reducing agents (Iravani et al., 2014).

Citrate reduction method used in the present work is a well established protocol (Turkevich et al., 1951, Frens, 1973). Citrate has been proposed to serve both as a reducing agent and a stabilizer. It has been reported that the size of GNP formed is dependent on the concentration of citrate used for reduction (Zabetakis et al., 2012). In the present studies, GNP were prepared using a gold chloride: citrate, molar ratio of 1:4. The yield of GNP formation was highly reproducible with a process yield of 73 %. SNP were also prepared using citrate reduction with a yield of 60 %.

Synthesis of stable CuNP is a challenging task as they undergo rapid oxidation in air or aqueous medium (Umer et al., 2012). In the present studies, commercially prepared CuNP were used. A small percentage of the commercial preparation also contains CuO NP.

Metallic NP absorbs the characteristic visible electromagnetic waves by the collective oscillation of the electrons at the surface and this phenomenon is called surface

plasmon resonance (SPR). The striking colors of the metallic NP are due to the interaction with visible light. The optical properties of the NP mainly depend on their size, shape and dielectric constant of the surrounding medium. Due to this plasmon absorption, the gold, silver and CuNP solutions appear in purple, greenish yellow and red color respectively. The surface plasmon absorption peak wavelengths are unique to the type of metal nanoparticles (Jain et al., 2008). In the present study, metallic NP surface plasmon absorption peak was observed by UV-visible spectroscopy.

Biological NP are prepared from the natural biopolymers using various methods (Allouche, 2013). Similar to metallic NP, synthetic method of biological NP is also guided by criteria which yields a NP with desirable size, morphology, stability, retention of biological activity, etc.,. Majority of protocols fall in to two categories, a 'one-step ' or a ' two- step' procedure. Two-step protocols are based on a initial emulsification step followed by formation of NP by a mechanism which involves polymerization, gelation or precipitation. In one-step methods, NP formation is achieved by desolvation, nanoprecipitation, or drying processes without any prior emulsification step. The choice of a particular method is crucial to prepare NP with desirable properties necessary for its specific application. Keeping in view, the criteria discussed above, NP were prepared using BSA, apo-transferrin and chitosan in the present work. Standard protocols published in recent years have been used to prepare NP.

Albumin-based NP are generally prepared by the emulsification, desolvation or coacervation methods. In the present study, desolvation method was used for the preparation of BSA NP. In desolvation, protein aggregates are formed in aqueous solution by addition of alcohol and then the insufficiently stabilized protein aggregates are cross-linked by glutaraldehyde. The condensation reaction between lysine and arginine of albumin and aldehyde of glutaraldehyde imparts the stability to NP (Martinez et al., 2011). Apo-transferrin NP were prepared by sol-oil method (Gandapu et al., 2011). Ionotropic gelation method was used to prepare chitosan NP. In ionotropic gelation, intermolecular and intra molecular linkages are formed between the tripolyphosphate (TPP) and chitosan (Calvo et al., 1997).

Characterization of NP is an essential prerequisite prior to their use in biological system. Information regarding size, shape, number and state of aggregation of NP is

required for their use *in vitro* and *in vivo*. A variety of characterization techniques have been reported which are described in the introduction of this chapter. Metallic and biological NP that have been prepared were characterized using four techniques – 1) Visible spectroscopy, 2) Transmission electron microscopy for metallic NP, 3) Scanning electron microscopy for biological NP and 4) Nanoparticle tracking analysis (NTA).

Metallic NP absorbs light at a particular wavelength of the electromagnetic spectrum due to surface plasmon resonance (SPR). The absorption spectra are unique and specific to each metallic NP (Eller and Haastrup, 2011). Absorption spectrum of NP suspension is recorded in aqueous media wherein the particles exist in monodisperse state. Limited information can be derived from the absorption spectrum of NP regarding size, concentration and aggregation state. GNP and SNP showed SPR peak absorption at 512 and 420 nm as reported earlier (Jain et al., 2008). However, in case of CuNP, a very broad absorption was observed in the range of 450-550 nm.

Shape of metallic NP was determined using TEM. Despite its disadvantages, TEM provides reliable data on the morphology and size (diameter) of metallic NP in their dry state. TEM analysis carried out different batches of GNP and SNP preparations showed spherical morphology and in the size (diameter) range of 15 nm for GNP and 40-60 nm for SNP. In case of CuNP, average diameter was 30 nm, which is in accordance with the value reported by the manufacturer. Hence, TEM analysis has provided information with respect to morphology and average dry size of the three metallic NP.

Biological NP (BSA, apo-transferrin and chitosan) were analyzed using SEM. Apo-transferrin and BSA NP were found to be in monodisperse state and having spherical morphology. Distribution of particles based on size was narrow in case of apo-transferrin and broad with BSA and chitosan NP indicating formation of agglomerates in the latter.

In the present work, all the NP preparations were characterized by NTA to determine the hydrodynamic size and particle number. Hydrodynamic size is probably the actual size of the particle as it exists in aqueous suspension. NTA visualizes the NP individually and avoids intensity bias towards the aggregates or large particles (Filipe et al., 2010). Not only diameter, but the particle number is estimated with accuracy. It is important to note that in cell culture system (*in vitro*) as well in tissue milieu (*in vivo*), particle number is more relevant than the concentration as cell-particle interaction takes place between two

geometrically spherical entities. Cellular interaction with a substance in solution is usually expressed in terms of concentration (µg, mg / µmole, mmole etc). This may not be valid for a substance in particle form. Hence, estimation of particle number per unit mass of NP suspension is a salient feature of the present work.

Reproducible estimates of hydrodynamic size of metallic as well as biological NP along with number of particles could be obtained using NTA. Size distribution analysis of particles also provided valuable information regarding possible aggregation occurring in some NP preparations. CuNP showed a multimodal distribution of size indicating formation of aggregates in suspension which may interact differently with cells.

The salient findings of this chapter are as follows:

1) GNP and SNP could be prepared using citrate reduction protocol. Yield of particles was reproducible. Data obtained on SPR of three metallic NP was comparable to published reports.
2) All three metallic NP showed a spherical morphology using TEM. The hydrodynamic size of particles obtained using NTA was higher than that observed with TEM. Particle number per unit mass and information on state of aggregation could be obtained with NTA.
3) Biological NP (apo-transferrin, BSA and chitosan) were prepared and characterized for shape, particle number and aggregation.

Chapter 4

Effect of NP on proliferative response and viability of primary B and T lymphocytes: *in vitro* studies

Introduction

Use of metallic and biological NP in consumer and medical products has been on the increase due to their anti-bacterial, anti-fungal, anti-viral and anti-cancerous activities (Arvizo et al., 2012; Zazo et al., 2016; Landriscina et al., 2015). This has resulted in significant enhancement in exposure of humans to NP. Hence, in addition to the beneficial effects of NP, concerns about their possible harmful side effects have to be addressed. Due to putative novel properties exhibited by NP compared to soluble counterparts, it is generally assumed that they may affect the biological systems *in vitro* and *in vivo* (Albanese et al., 2012; Rivera-Gil et al 2013; Mu et al., 2014). Assessment of adverse effects during the pre-clinical evaluation can indicate the potential concerns before a NP based product can enter into clinical trials (in order to avoid unwanted reactions in the clinic). Reliable *in vitro* studies are required to test their effects on biological system. *In vitro* tests using primary cells and established cell lines offer initial complementary approach prior to *in vivo* studies. Low cost, less time for experimentation and less animal use are some of the advantages of *in vitro* compared to *in vivo* studies. *In vitro* analyses can provide information on mechanisms of NP mediated interactions with cells (Horie et al., 2012). It has been proposed that in *vitro* studies along with *in vivo* studies offer a comprehensive assessment of toxicity of NP (Fischer and Chan, 2007).

Lymphocyte activation

Mature B and T lymphocytes in circulation and secondary lymphoid organs get activated upon encounter with immunogens. The process of lymphocyte activation followed by differentiation is an important event in the initiation and maintenance of adaptive immune response. Immunogens which are recognized as "non-self" (foreign) are processed and presented by two major pathways – extracellular (exogenous) and intracellular (endogenous) mediated by the antigen-presenting cells. Presentation of processed antigen in the context of appropriate MHC molecules on the surface of relevant antigen-presenting cells is an important event prior to antigen recognition. Interaction of native or processed antigen in association with MHC molecules (and accessory receptors) with specific antigen receptors and co-receptors on B and T lymphocytes triggers a series of events resulting in activation.

The activation phenomena which occur in B and T lymphocytes are briefly described below.

B-cell antigen receptor

B cell antigen receptor is composed of monomeric IgM and IgD molecules non-covalently associated with two accessory molecules Igα and Igβ linked through disulfide linkages (Campbell and Cambier 1990; Chen et al., 1990; Parkhouse, 1990). Another receptor called Ig $_{\gamma}$ which is identical in structure with Igβ except for the cytoplasmic tail has also been shown to be present on B cells (Friedrich et al., 1993). B cell antigen receptor has two functions- firstly, it can efficiently take up antigen by receptor-mediated endocytosis, thereby allowing it to be processed and presented to helper T cells (Myers, 1991).Secondly, the antigen receptor recognizes antigen and transduces signals across the membrane to the cell interior, necessary for B cell activation (Pleiman et al., 1994).

B-lymphocyte activation

Majority of B lymphocytes in circulation and secondary lymphoid tissues are in resting state (G0 phase) of cell cycle prior to their encounter by a specific antigen. Resting B cells are small, quiescent, non-dividing cells with low metabolic activity (Monroe and Cambier, 1983). Upon antigenic stimulation, B cell undergoes several morphological and metabolic changes (Anderson et al., 1977). B cell activation takes place in two modes - T cell dependent and T cell independent. Activation of B cells by T cell dependent antigens requires participation of T cells which render the relevant help in the form of a variety of soluble mediators secreted by activated helper T cells. These cytokines in turn aid in clonal expansion and differentiation of antigen specific B cells (DeFranco, 1987). Activated B cells enter in to primary follicles of secondary lymphoid organs, where they undergo rapid proliferation and form germinal centers (GC). Subsequently, in the germinal centers, plasma cells and long lived memory cells are generated, which drive potent antibody secretion (primary response). Upon re-exposure to the same antigen again, memory cells initiate a secondary antibody response characterized by immunoglobulin class switching and affinity maturation.

Binding of antigen to the membrane Ig receptor causes their cross linking which in turn results in activation of a variety of tyrosine kinases (Flaswinkel and Reth, 1994). The cross-linking of Ig receptors also results in activation of phospholipase C_{γ}, which catalyzes formation and conversion of phosphatidyl inositol-4,5 bisphosphate to inositol 1,4,5 trisphosphate (IP3) and diacyl glycerol(DAG) (Carter et al., 1991: Nishizuka, 1992). IP3 diffuses in to the cytosol and mediates Ca^{2+} release from endoplasmic reticulum (Khan et

al., 1992). DAG mediates translocation and activation of different forms of protein kinase C (PKC) (Mischak et al., 1991). Elevated levels of Ca^{2+} are also necessary for activation of PKC. Activated PKC phosphorylates a variety of proteins that help in further cellular activation (Burke et al., 1989).

During B lymphocyte activation, secondary messengers like cAMP and cGMP are also produced and participate in signal transduction. It has been shown that cAMP acts synergistically with LPS in proliferation of B cells *in vitro* (Kasyapa and Ramanadham**,** 1995).

B cell activation through the antigen receptor is shown to require many soluble factors that are secreted by other cells in the milieu. Mature B cells depend on cytokines derived from the activated T lymphocytes in a tightly regulated manner (Miyajima et al., 1992). Activated helper T cells secrete an array of interleukins- IL-2, IL-4, IL-5, IL-6 etc., which are required for the proliferation and differentiation of committed B lymphocytes (Jelnik et al., 1986; Hirano et al., 1986).

T lymphocyte activation

T cells play a major role in cell mediated immunity and also promote the production of antibodies from B cells. Activation of T cells is mediated by T-cell antigen receptor complex (TCR). $CD4^+$ T cells recognize processed antigen presented in association with MHC class II molecules, whereas processed antigens presented in association with MHC I molecules are recognized by $CD8^+$ T cells. $CD4^+$ T cells are the major source of interleukins essential for helper function. Cytotoxic $CD8^+$ T cells are required for killing of virus-infected and malignant cells. Cytokine profile present during contact with dendritic cells determines $CD4^+$ T-cell fate (Kapsenberg, 2003). $CD4^+$ T or T_H0 cells are classified in to T_H-1 and T_H-2 cells, each of which produces distinct cytokines (Mossman et al., 1986). T_H-1 cells produce IFN-gamma, IL-2 and TNF-alpha. These cytokines regulate the various facets of cell-mediated immunity, which mainly includes inflammation. T_H-2 cells produce interleukin-4, IL-5, IL-6, and IL-13, but IL-10 is secreted by both T_H-1 and T_H-2 cells. IFN-gamma produced by T_H-1 cells helps in the T_H-1 development and inhibits proliferation of T_H-2 cells, whereas IL-2 produced by T_H-2 cells inhibits activation of T_H-1 cells. T_H-2 cells induce proliferation of mast cells and eosinophils and also promote humoral immunity by B cells. IFN-gamma and IL-4 are the main markers of T_H-1 and T_H-2 cells respectively (Abbas et al., 1996).

Assessment of lymphocyte activation *in vitro and in vivo*

Plant lectins and bacterial products with mitogenic activity have been extensively used to study lymphocyte activation. Antigenic stimulation is usually oligo clonal in nature. Frequency of activated cells is relatively small in the overall population of lymphoid cells available for interaction. Due to this, biochemical phenomena that occur in antigen activated cells can not be well studied. Lectins which stimulate the lymphocytes in a polyclonal manner serve as "surrogate antigens". It has been shown that interaction and recognition of various mitogenic substances 'bypass' the requirement for antigen processing and presentation. Gross morphological and biochemical characteristics of mitogen stimulated lymphocyte responses *in vitro* are very similar to antigen induced immune reactions *in vivo*. Therefore, it is well accepted that measurement of mitogen induced lymphocyte proliferative response can be used as a tool to assess lymphocyte activation and immunocompetence (Janossy and Greaves, 1971).

B lymphocytes, T lymphocytes and monocytes circulate through blood and lymph, and therefore are likely to come in contact with NP. Interaction of immune cells with NP may influence their functions such as proliferation, secretion of cytokines and immunoglobulins. Functional analysis can be studied *in vitro* by incubating desired lymphocyte population with NP in tissue culture. Effect of metallic (gold, silver and copper) and biological (apo-transferrin, bovine serum albumin and chitosan) NP on the mitogen-induced proliferative response and viability of murine splenic, rat splenic and thymic and human PBL were studied *in vitro*.

Methods

Metallic NP

Gold, silver and copper NP prepared and characterized as described in Chapter 3 were used in the present experiments. All the NP preparations were sterile filtered before use.

Biological NP

Apo-transferrin, bovine serum albumin and chitosan NP prepared and characterized as described in Chapter 3 were used in the present experiments.

Determination of NP number

Number of metallic and biological NP was determined by NTA as described in materials and methods.

Lymphocyte preparation

Lymphocytes from mouse spleen, rat spleen & thymus and human peripheral blood were prepared as described in materials and methods.

Lymphocyte proliferation assay

Effect of metallic and biological NP on B and T cell mitogen- induced proliferative response was determined using ^{3}H-Td incorporation assay as described in materials and methods. Average of triplicate cultures was calculated. Mitogen induced proliferative response was expressed in terms of stimulation index which was calculated as:

$$\text{Stimulation index (SI)} = \frac{\text{Average cpm in the presence of mitogen (or mitogen + NP)}}{\text{Average cpm with cells only}}$$

Considering the stimulation index of cells stimulated with mitogen as 100%, the proliferative response for experimental samples treated with mitogen and / or NP was calculated and expressed as % of control.

Determination of cell viability

Viability of lymphocytes was determined as described in materials and methods.

Estimation of malondialdehyde (MDA) levels

The final product of lipid peroxidation in cells is MDA, which was estimated using thiobarbituric acid assay as described in materials and methods. Concentration of MDA was calculated using molar extinction coefficient of $1.55 \times 10^{5}\ M^{-1}cm^{-1}$ and was expressed as nmoles / ml.

Preparation of supernatants of metallic NP incubated in tissue culture medium and their effect on mitogen induced lymphocyte proliferative response

Metallic NP were incubated in triplicate in RPMI-1640 medium containing 5 % FCS for 72 hours. Then, the samples were centrifuged at 10,000 x g for 20 min to sediment the NP. Supernatants were collected in separate sterile tubes and used to culture mouse splenic lymphocytes and human PBL to determine lymphocyte proliferative response as described in materials and methods.

Results

Aggregation of metallic NP in tissue culture

In order to analyze the aggregation status of metallic NP in presence of tissue culture medium, absorption spectra of GNP and SNP were recorded in the wavelength range of 400-700 nm. The data are presented in Figures 4.1 and 4.2. Absorption maximum of GNP obtained in RPMI-1640 containing 5 % FCS at initiation of incubation was similar to that observed at 72 hours. This indicates that the physical state of NP in suspension was maintained in tissue culture medium for a period of 3 days. Similar results were obtained with SNP (Figure 4.2). No reproducible spectra could be recorded with CuNP despite several repetitive experiments.

Effect of GNP on mitogen induced proliferative response

Mouse splenic lymphocytes were incubated with 5 - 200µg GNP /ml in presence of optimal concentrations of LPS or Con A. Cultures set up with mitogens alone served as controls. The concentrations of GNP used corresponded to particle number of 3-120 x 10^9/ml. Con A induced proliferative response was significantly inhibited from 25 µg GNP /ml in a dose dependent manner ($p < 0.05$, Figure 4.3). LPS stimulated proliferative response was significantly inhibited from 50 µg GNP/ ml in a dose dependent manner.

Human PBL were treated with the same concentrations of GNP as mentioned above in the presence of PWM or PHA. Proliferative response stimulated by PWM as well as PHA was inhibited in presence of GNP in a dose dependent manner (Figure 4.4).

Rat splenic and thymic lymphocytes were also treated with different concentration of GNP (5-200µg/ml or 3-120x10^9/ml) in the presence of mitogens. GNP decreased the LPS and ConA induced proliferative response in a dose dependent manner (Figure 4.5). ConA induced rat thymic lymphocyte proliferative response also decreased in a dose dependent manner in the presence of GNP (Figure 4.6).

Effect of SNP on the mitogen induced proliferative response

Mouse splenic lymphocytes were treated with 5-50 µg SNP / ml (2.4 – 24 x 10^9 particles / ml) in presence of LPS and Con A. Proliferative response was significantly inhibited in a dose dependent manner (Figure 4.7).

PHA or PWM stimulated human PBL were treated with concentrations of SNP mentioned above. Proliferative response was unaffected at 5 µg SNP /ml, but was significantly decreased from 12.5- 50 µg SNP / ml, in a dose dependent manner (Figure 4.8).

Rat splenic and thymic lymphocytes were treated with SNP using the concentrations mentioned above. Proliferative response induced by LPS and Con A was inhibited by SNP in a dose dependent manner (Figure 4.9). Rat thymic lymphocyte proliferative response stimulated by Con A was also inhibited by 12.5 – 50 µg SNP / ml (Figure 4.10).

Effect of CuNP on the mitogen induced proliferative response

Mouse splenic lymphocytes stimulated with LPS or Con A were treated with CuNP in the concentration range of 1-10 µg / ml or 57-570 $x10^6$ particles / ml. Mitogen induced proliferative response was inhibited significantly by CuNP in dose dependent manner (Figure 4.11).

Human PBL stimulated with PWM or PHA were also treated with CuNP using the same concentrations mentioned above. Proliferative response decreased in a dose dependent manner (Figure 4.12).

Rat splenic and thymic lymphocytes also were treated with above said concentrations of CuNP in presence of LPS and Con A. CuNP decreased the mitogen induced proliferative response in dose dependent manner (Figure 4.13). Con A stimulated proliferative response of thymocytes was significantly inhibited by 2.5 – 10 µg CuNP / ml (Figure 4.14).

Effect of metallic NP on ^{3}H-thymidine incorporation by unstimulated lymphocytes

^{3}H-thymidine incorporation into DNA by unstimulated (without mitogen) mouse splenic lymphocytes and human PBL was measured after culturing them with metallic NP. GNP had no effect on the incorporation at all concentrations tested in mouse splenic lymphocytes as well as in human PBL (Figure 4.15). Thymidine incorporation by mouse splenic lymphocytes and human PBL was inhibited by 50 µg SNP / ml (Figure 4.16). In CuNP treated unstimulated lymphocytes from mouse as well as human, thymidine incorporation was significantly decreased at 5 and 10 µg /ml (Figure 4.17).

Effect of metallic NP on viability of mouse splenic lymphocytes and human PBL

Viability of lymphocyte populations incubated in culture with the three metallic NP was determined using trypan blue dye exclusion method. In order to

enumerate a large number of cells after dye addition, microscopic images were captured rapidly using a camera as described in materials and methods. Representative images depicting live and dead cells are presented in Figure 4.18.

Viability of mouse splenic lymphocytes as well as human PBL was unaffected at 25-100 µg GNP / ml. Only at 200µg GNP / ml, viability was marginally decreased compared to untreated controls significantly (Table 4.1). Mouse splenic lymphocytes and human PBL were treated with different doses of SNP ranging from 5-50µg / well corresponding to 2.4-24 $x10^9$ particles / ml. Viability was significantly reduced at 25 and 50 µg SNP / ml in both populations of lymphocytes (Table 4.2). Upon treatment with CuNP, viability of splenic lymphocytes and human PBL was inhibited in a dose dependent manner (Table 4.3).

Effect of supernatants obtained from metallic NP incubated in culture medium on mitogen stimulated proliferative response

Metallic NP were incubated in complete culture medium: 25 & 200µg GNP /ml(G1,G2), 12.5 & 50µg SNP /ml(S1,S2) and 2.5 & 10µg CuNP /ml(C1,C2) for 72 hours and NP-free supernatants then prepared as described in materials and methods. Mouse splenic lymphocytes and human PBL were cultured in fresh medium and NP- free supernatants. Proliferative response was measured in presence of mitogens and results are presented in Figures 4.19-4.21. GNP supernatants had no effect on proliferative response of both cell populations (Figure 4.19). Similarly, proliferative response of mouse splenic and human PBL was also not affected by SNP supernatants (Figure 4.20). However, mitogen induced proliferative response of both lymphocyte populations was significantly inhibited in presence of supernatants of CuNP incubated cultures (Figure 4.21). The inhibition was more pronounced in human PBL than in mouse lymphocytes.

Malondialdehyde concentration in supernatants of mouse splenic lymphocytes and human PBL treated with metallic NP

Mouse splenic lymphocytes and human PBL were incubated in culture with GNP 200µg GNP /ml, 50µg SNP /ml and 10µg CuNP/ml for 72 hours. Then, supernatants were collected and MDA concentration was determined. MDA levels in

supernatants of GNP and SNP treated murine splenic lymphocytes were similar to controls (Figure 4.22). MDA concentration was significantly higher in supernatant of CuNP treated cells compared to controls.

Human PBL were also treated with metallic NP and concentrations of MDA estimated in the supernatants are presented in Figure 4.24. MDA concentration in GNP and SNP treated PBL supernatants was similar to controls. CuNP treated PBL supernatants had significantly increased MDA levels compared to controls (Figure 4.23).

Effect of biological NP on mitogen induced proliferative response of mouse splenic lymphocytes and human PBL

Apo-transferrin NP

Mouse splenic lymphocytes were incubated with 25 & 100 µg of apo-transferrin NP /ml (corresponding to 420 & 1680 $x10^6$ particles / ml) in presence of LPS and Con A. Proliferative response in apo-transferrin NP treated lymphocytes was similar to controls (no NP addition) (Figure 4.24). Similar results were obtained with PWM and PHA stimulated human PBL treated with apo-transferrin NP (Figure 4.25).

BSA NP

Effect of BSA NP on mitogen induced proliferative response of mouse splenic lymphocytes and human PBL was determined using 25 and 100 µg / ml (300 and 1200 $x10^6$ particles / ml). The results are presented in Figures 4.26 & 4.27. BSA NP had no effect on proliferative response of both lymphocyte populations.

Chitosan NP

Mouse splenic lymphocytes were incubated with 50 and 200 µg/ml of chitosan NP for 72 h in the presence of LPS and Con A. Proliferative response was significantly inhibited with both concentrations of chitosan NP tested (Figure 4.28).

Human PBL were also treated with chitosan NP with above said concentrations for 72 h in the presence of PHA and PWM. Mitogen induced proliferative response was significantly decreased in presence of chitosan NP (Figure 4.29).

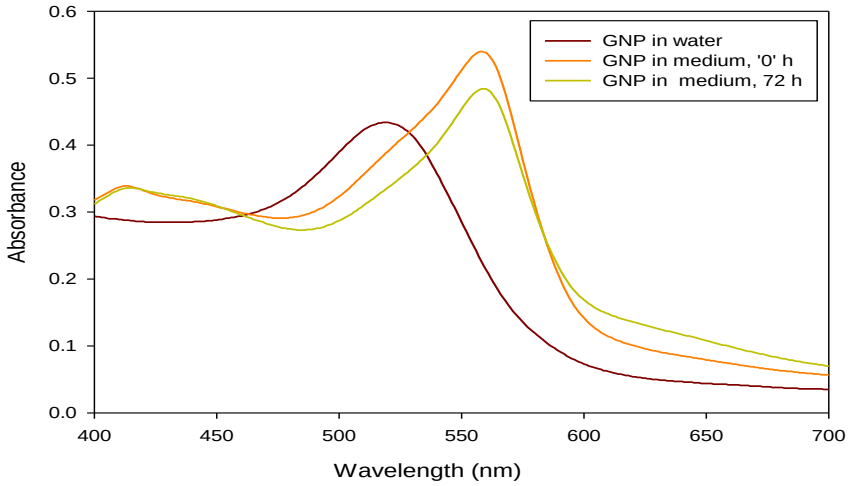

Figure 4.1 : Absorption spectrum of GNP in tissue culture medium

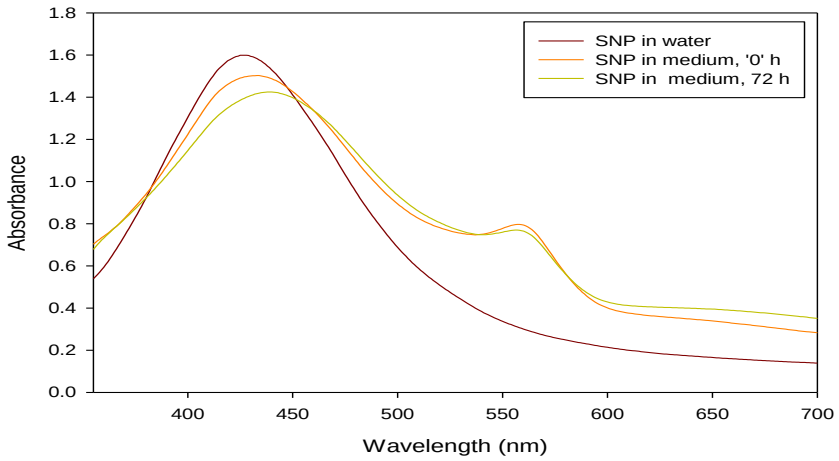

Figure 4.2: Absorption spectrum of SNP in tissue culture medium

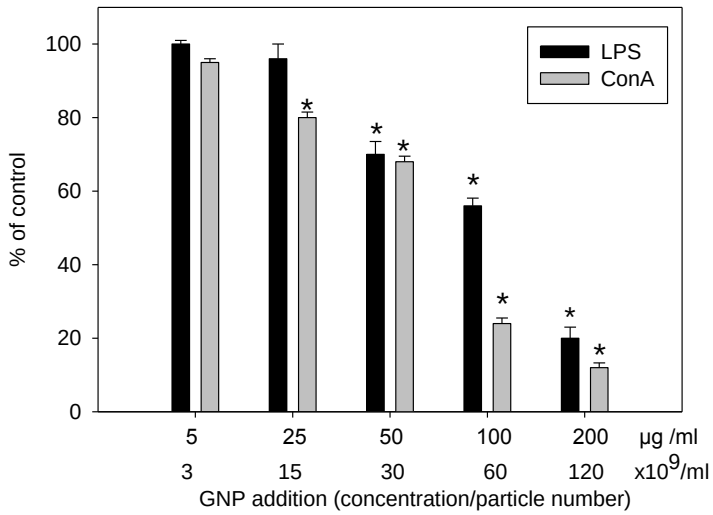

Figure 4.3: Effect of GNP on LPS or Con A induced proliferative response of mouse splenic lymphocytes. Data presented are mean ± SEM of three experiments. Mean stimulation indices with mitogens alone (control): LPS: 23 ± 1.0, Con A: 25 ± 1.0 were normalized to 100%. *p < 0.05, NP treated vs. control.

.

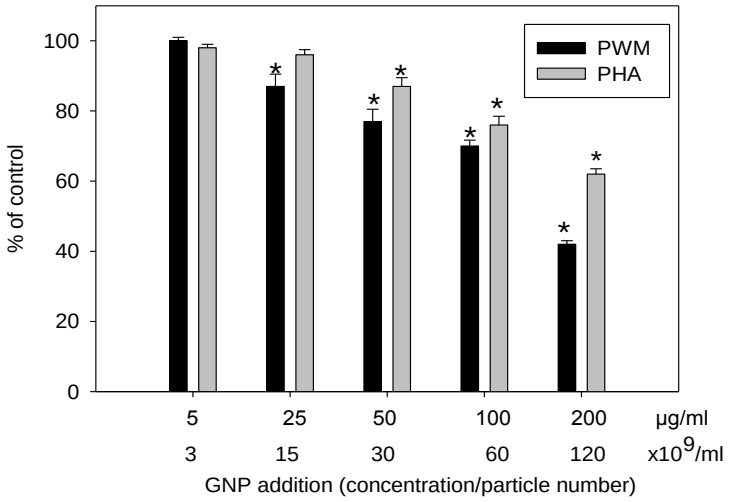

Figure 4.4: Effect of GNP on PWM or PHA induced proliferative response of human PBL. Data presented are mean ± SEM of three experiments. Mean stimulation indices with mitogens alone (control): PHA: 58 ± 2.0 and PWM: 24 ± 1.0 were normalized to 100%. * p < 0.05, NP treated vs. control.

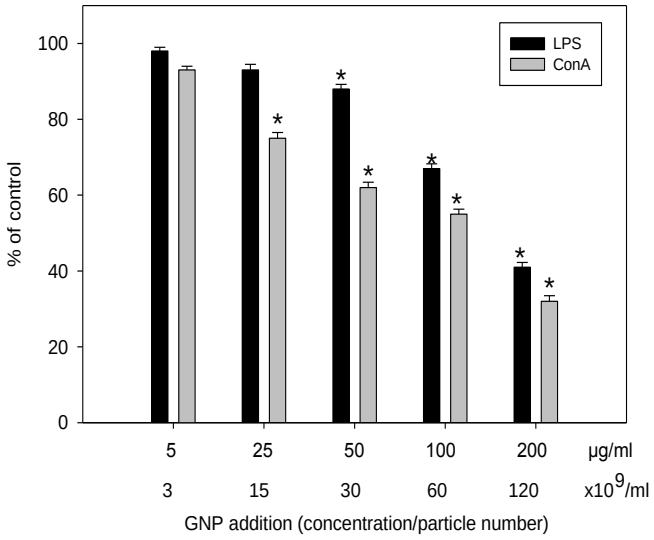

Figure 4.5: Effect of GNP on LPS or Con A induced proliferative response of rat splenic lymphocytes. Data presented are mean ± SEM of three experiments. Mean stimulation indices with mitogens alone (control): LPS: 2.5 ± 0.2 and Con A: 22 ± 1.5 were normalized to 100%. * p < 0.05, NP treated vs. control

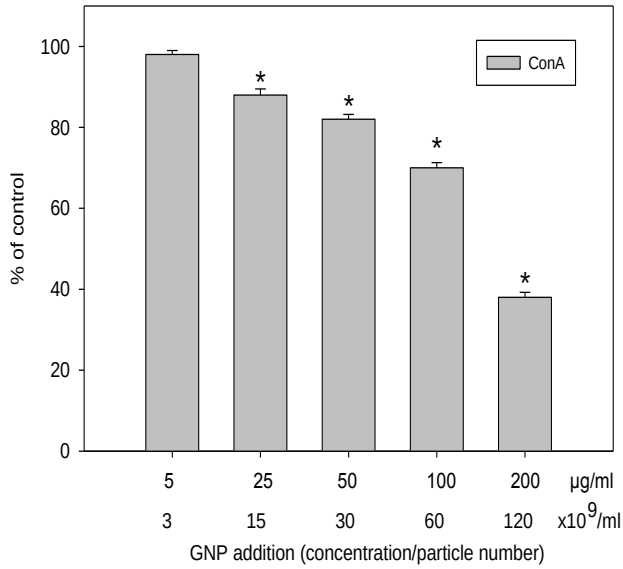

Figure 4.6: Effect of GNP on Con A induced proliferative response of rat thymic lymphocytes. Data presented are mean ± SEM of three experiments. Mean stimulation index with mitogen alone (control): Con A: 62 ± 3.5 was normalized to 100%. * p < 0.05, NP treated vs. control.

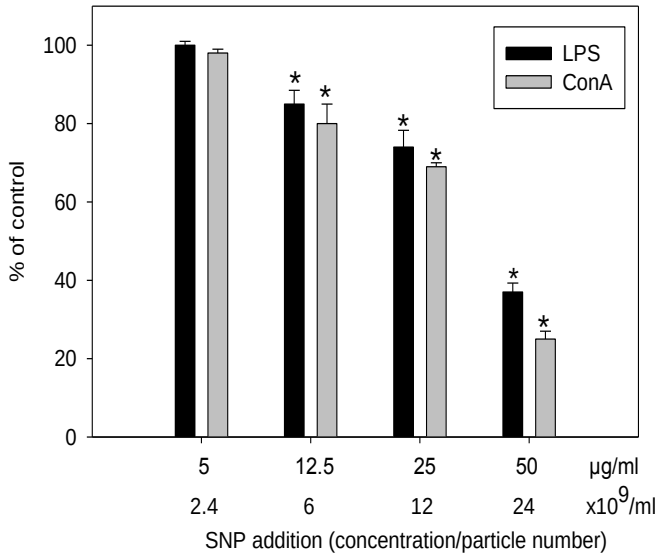

Figure 4.7: Effect of SNP on LPS or Con A induced proliferative response of mouse splenic lymphocytes. Data presented are mean ± SEM of three experiments; Mean stimulation indices with mitogens alone (control): LPS: 23 ± 1.0, Con A: 25 ±1.0 were normalized to 100% value. *p < 0.05, NP treated vs. control.

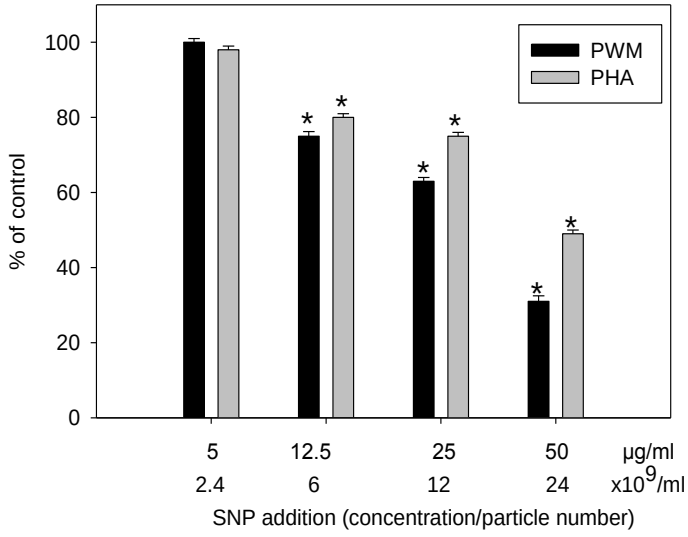

Figure 4.8: Effect of SNP on PWM or PHA induced proliferative response of human PBL. Data presented are mean ± SEM of three experiments. Mean stimulation indices with mitogens alone (control): PHA: 58 ± 2.0 and PWM: 24 ± 1.0 were normalized to 100%. * p < 0.05, NP treated vs. control.

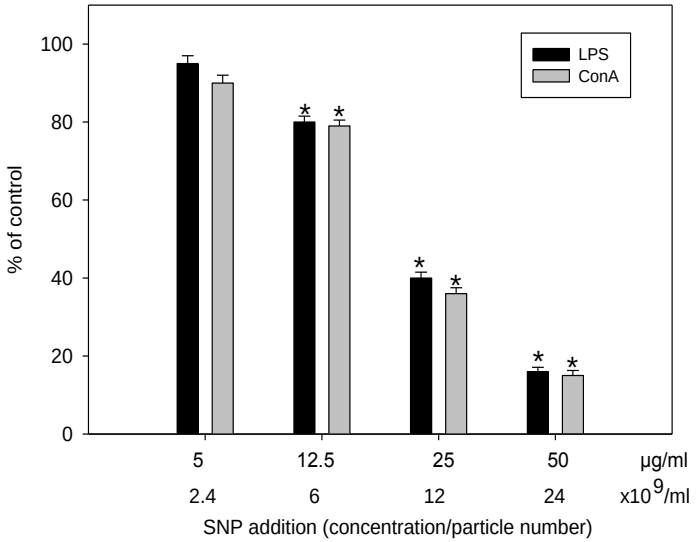

Figure 4.9: Effect of SNP on LPS or Con A induced proliferative response of rat splenic lymphocytes. Data presented are mean ± SEM of three experiments. Mean stimulation indices with mitogens alone (control): LPS: 2.5 ± 0.2 and Con A: 22 ± 1.5 were normalized to 100%. * p < 0.05, NP treated vs. control.

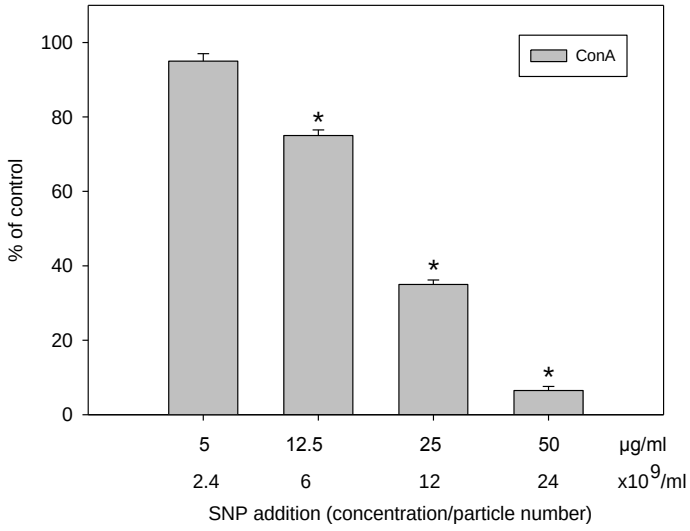

Figure 4.10: Effect of SNP on Con A induced proliferative response of rat thymic lymphocytes. Data presented are mean ± SEM of three experiments. Mean stimulation index with mitogen alone (control): Con A: 62 ± 3.5 was normalized to 100%. * p < 0.05, NP treated vs. control.

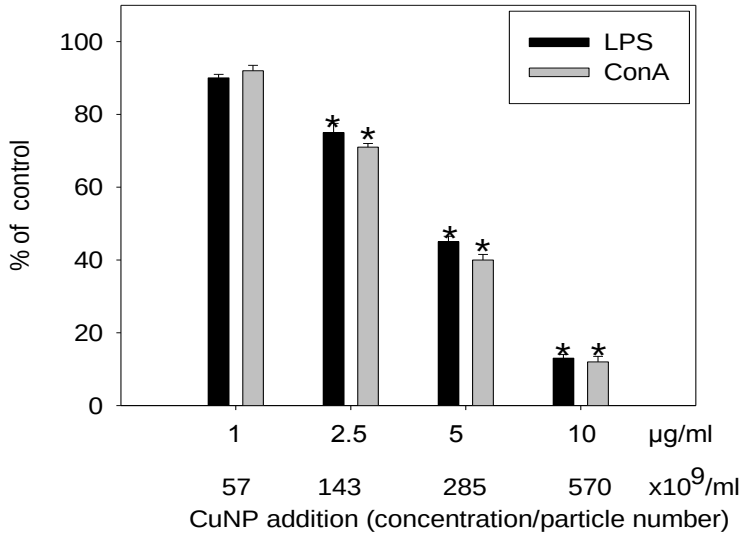

Figure 4.11: Effect of CuNP on LPS or Con A induced proliferative response of mouse splenic lymphocytes. Data presented are mean ± SEM of three experiments. Mean stimulation indices with mitogens alone (control): LPS: 23 ± 1.0, Con A: 25 ± 1.0 were normalized to 100%. *p < 0.05, NP treated vs. control.

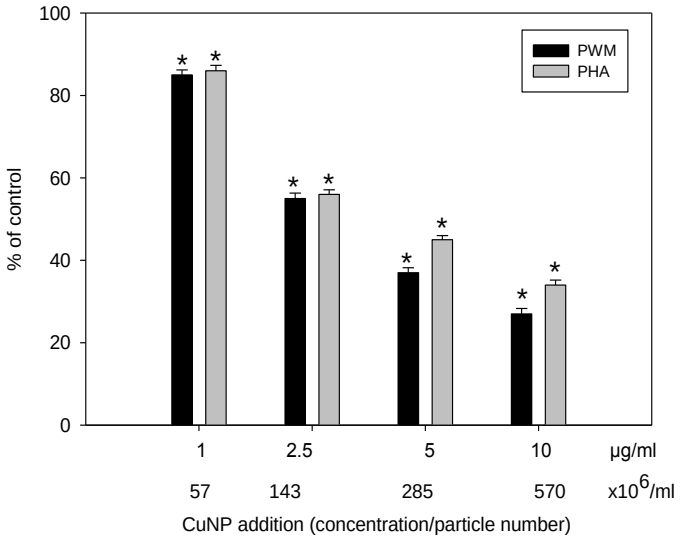

Figure 4.12: Effect of GNP on PWM or PHA induced proliferative response of human PBL. Data presented are mean ± SEM of three experiments. Mean stimulation indices with mitogens alone (control): PHA: 58 ± 2.0 and PWM: 24 ± 1.0 were normalized to 100%. * p < 0.05, NP treated vs. control.

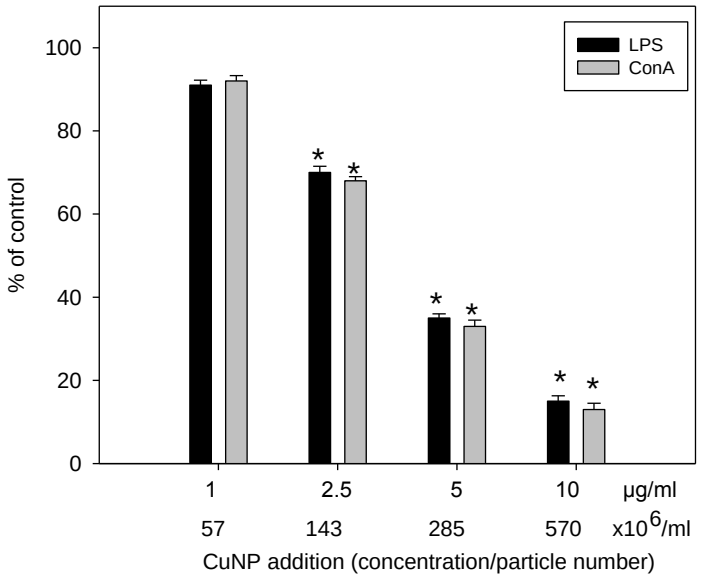

Figure 4.13: Effect of CuNP on LPS or Con A induced proliferative response of rat splenic lymphocytes. Data presented are mean ± SEM of three experiments. Mean stimulation indices with mitogens alone (control): LPS: 2.5 ± 0.2 and Con A: 22 ± 1.5 were normalized to 100%. * p < 0.05, NP treated vs. control.

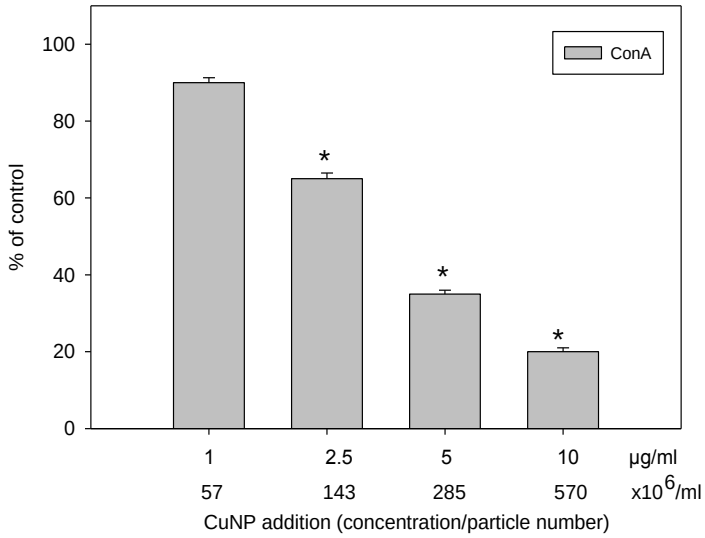

Figure 4.14: Effect of CuNP on Con A induced proliferative response of rat thymic lymphocytes. Data presented are mean ± SEM of three experiments. Mean stimulation index with mitogen alone (control): Con A: 62 ± 3.5 was normalized to 100%. * p < 0.05, NP treated vs. control.

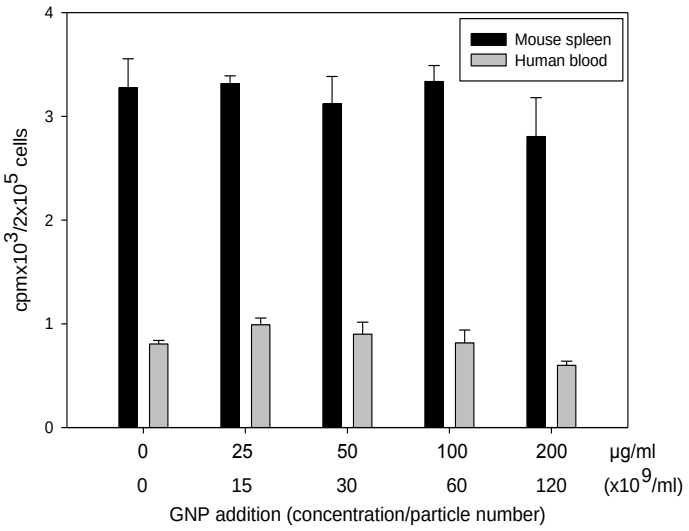

Figure 4.15: Effect of GNP on [^{3}H]-thymidine incorporation by unstimulated lymphocytes. Data presented are Mean ± SEM of three experiments.

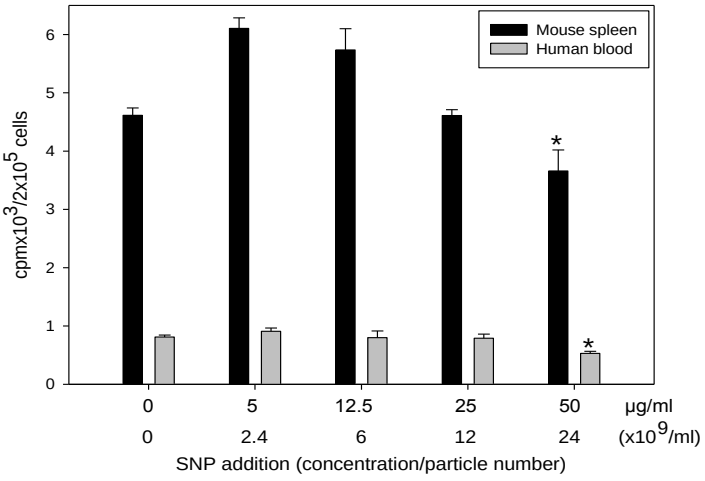

Figure 4.16: Effect of SNP on [^{3}H]-thymidine incorporation by unstimulated lymphocytes. Data presented are Mean ± SEM of three experiments. * p< 0.05, NP treated vs. control.

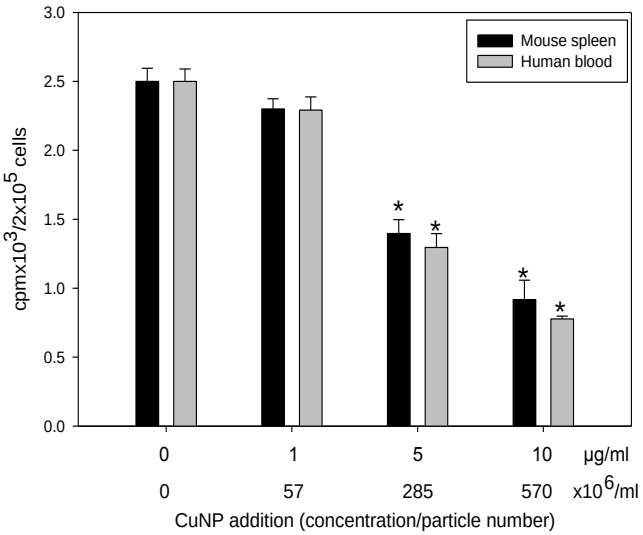

Figure 4.17: Effect of CuNP on [^{3}H]-thymidine incorporation by unstimulated lymphocytes. Data presented are Mean ± SEM of three experiments. * p< 0.05, NP treated vs. control.

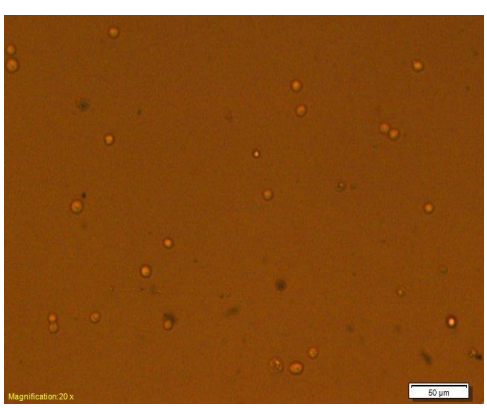

A)

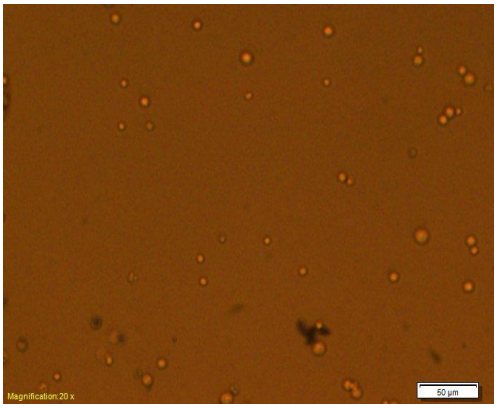

B)

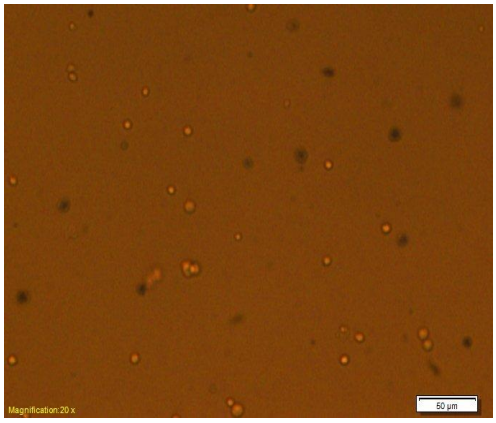

C)

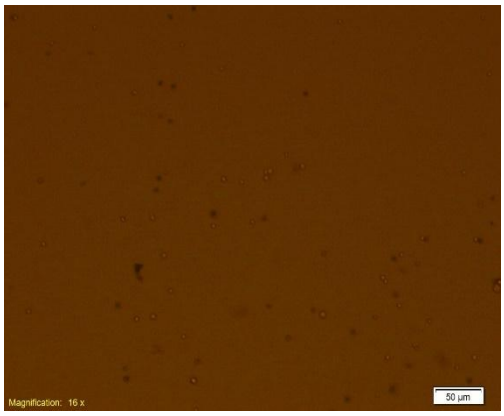

D)

Figure 4:18: Enumeration of viable and dead lymphocytes using trypan blue dye exclusion. Microscopic pictures of a representative experiment are shown. Lymphocyte preparations treated with NP were - A: No treatment, B: GNP, C: SNP, D: CuNP

Table 4.1: **Viability of lymphocytes treated with GNP for 72 h. Data presented are mean ± SEM of three experiments. * p < 0.05, treated vs. control**

NP Concentration (µg/ml)	Particle number ($x10^9$/ml)	Mouse splenic lymphocytes Viability (%)	Human PBL Viability (%)
0.0	0.0	92 ± 2.0	92 ± 2.0
25	15	92 ± 1.0	92 ± 1.0
50	30	88 ± 1.0	92 ± 2.0
100	60	84 ± 3.0	88 ± 2.0
200	120	81 ± 2.0*	82 ± 2.0*

Table 4.2: Viability of lymphocytes treated with SNP for 72 h.**Values shown are means ± SEM of three experiments; * p <0.05, control vs. treated.**

NP Concentration (µg/ml)	Particle number ($x10^9$/ml)	Mouse splenic lymphocytes Viability (%)	Human PBL Viability (%)
0.0	0.0	92 ± 2.0	92 ± 2.0
5	2.4	88 ± 2.0	91 ± 1.0
12.5	6	84 ± 3.0	88 ± 2.0
25	12	72 ± 2.0*	82 ± 1.0*
50	24	66 ± 1.0*	80 ± 2.0 *

Table 4.3: Viability of lymphocytes treated with CuNP for 72 h. Values shown are means ± SEM of three experiments; * p <0.05 control vs. treated.

NP Concentration (µg/ml)	Particle number ($x10^6$/ml)	Mouse splenic lymphocytes	Human PBL
		Viability (%)	
0.0	0.0	92 ± 2.0	92 ± 2.0
2.5	143	73 ± 2.0*	73 ± 2.0 *
10	570	50 ± 0.5*	62 ± 0.5*

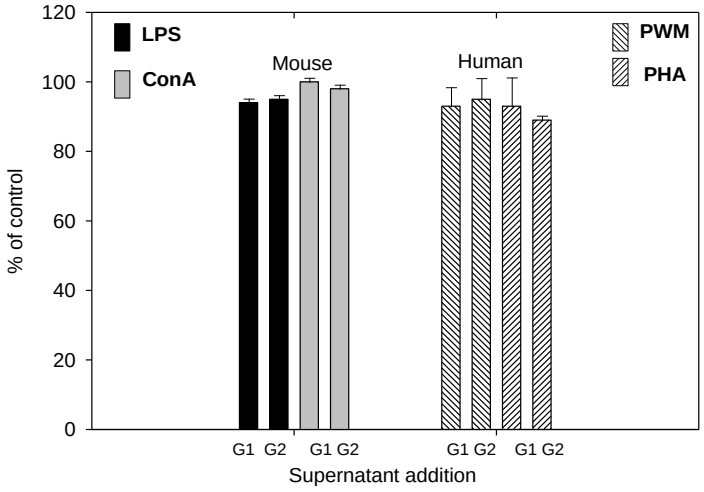

Figure 4.19: Mitogen stimulated proliferative response of lymphocytes cultured in NP-free supernatants obtained from GNP incubated in complete medium for 72 hours: G1- 50µg/ml, G2-200µg/ml. Mean stimulation indices with mitogens (control): LPS: 4.5 ± 0.2, Con A: 3.5 ± 0.10, PHA: 21.0 ± 1.2 and PWM: 54 ± 3.0 are normalized to 100 % value. Data presented are Mean ± SEM of three experiments.

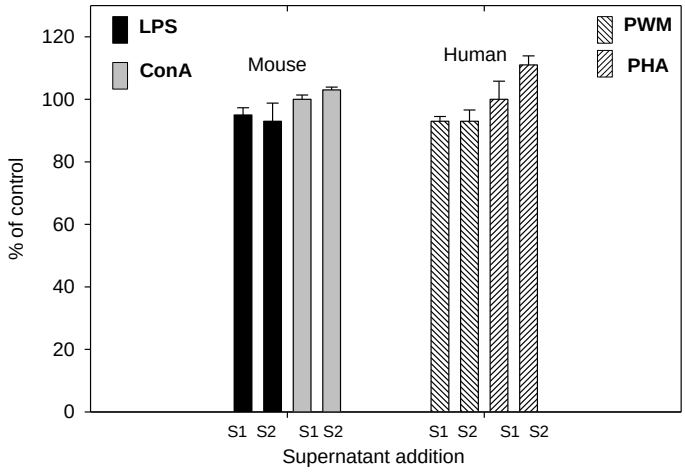

Figure 4.20: Mitogen stimulated proliferative response of lymphocytes cultured in NP-free supernatants obtained from SNP incubated in complete medium for 72 hours: S1- 12.5µg/ml, S2-50µg/ml. Mean stimulation indices with mitogens (control): LPS: 4.5 ± 0.2, Con A: 3.5 ± 0.10, PHA: 21.0 ± 1.2 and PWM: 54 ± 3.0 are normalized to 100 % value. Data presented are Mean ± SEM of three experiments.

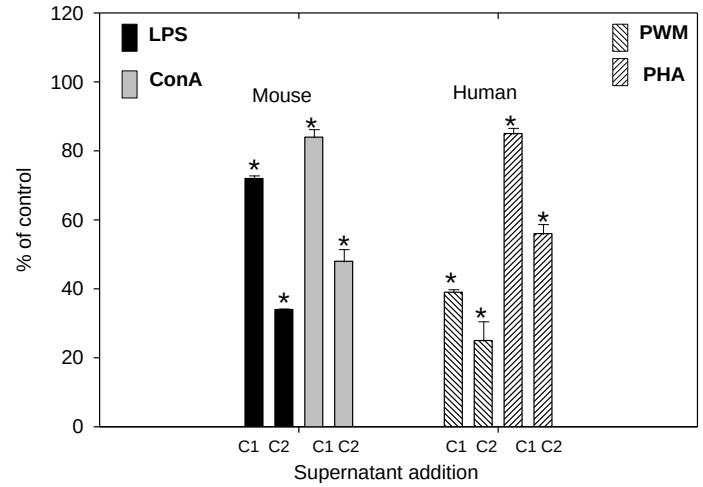

Figure 4.21: Mitogen stimulated proliferative response of lymphocytes cultured in NP-free supernatants obtained from CuNP incubated in complete medium for 72 hours: C1- 2.5µg/ml, C2-10µg/ml. Mean stimulation indices with mitogens (control): LPS: 4.5 ± 0.2, Con A: 3.5 ± 0.10, PHA: 21.0 ± 1.2 and PWM: 54 ± 3.0 are normalized to 100 % value. Data presented are Mean ± SEM of three experiments. * p< 0.05, treated vs. control.

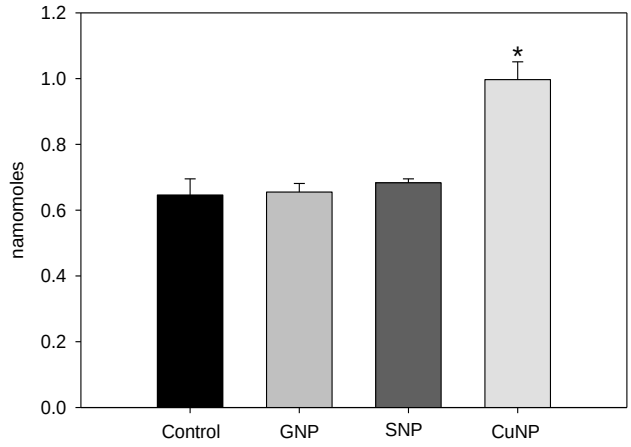

Figure 4.22: MDA concentration in supernatants of mouse splenic lymphocytes treated with metallic NP. GNP: 200, SNP: 50 and CuNP:10 µg/ml were used. Data presented are mean ± SEM of three experiments. * p< 0.05, treated vs. control.

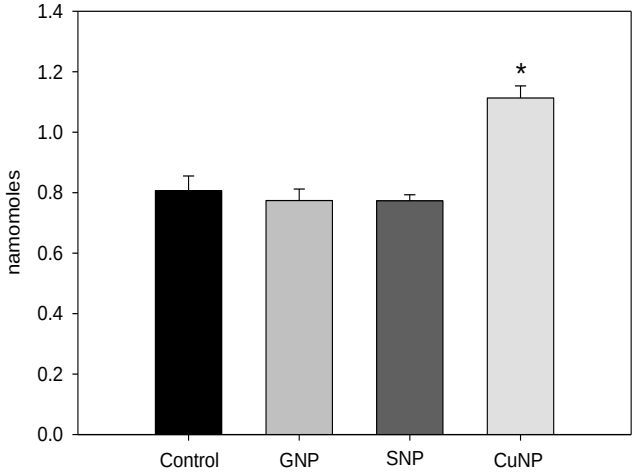

Figure 4.23: MDA concentration in supernatants of human PBL treated with metallic NP. GNP: 200, SNP: 50 and CuNP: 10 µg/ml were used. Data presented are mean ± SEM of three experiments. * p< 0.05, treated vs. control.

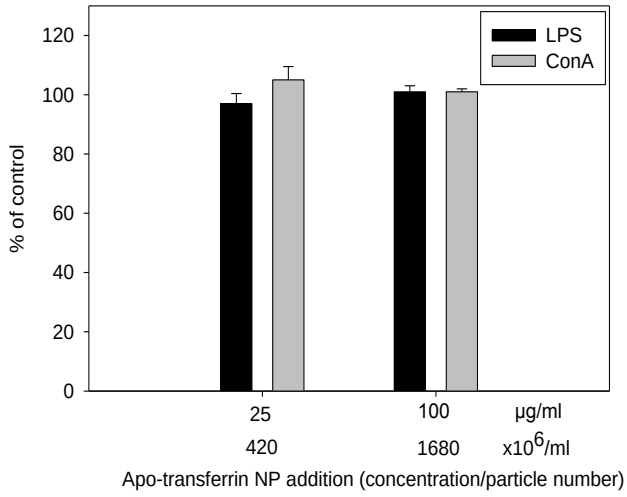

Figure 4.24: Effect of apo-transferrin NP on LPS or Con A induced proliferative response of mouse splenic lymphocytes. Mean stimulation indices with mitogens (control): LPS: 30 ± 2.5, Con A: 19 ±1.0 were normalized to 100%. Data shown are mean ± SEM of three experiments.

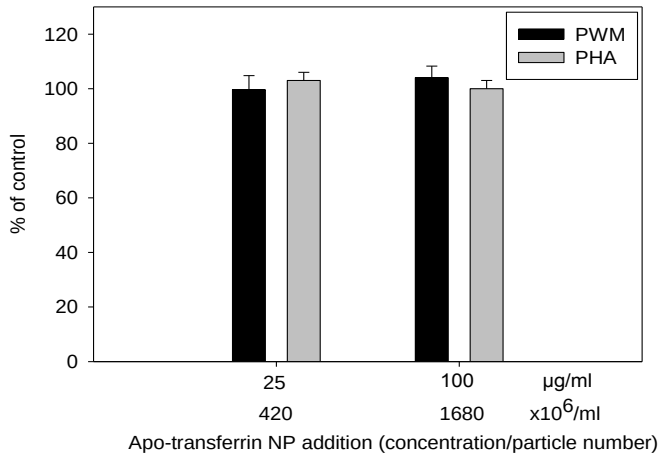

Figure 4.25: Effect of apo-transferrin NP on PWM or PHA stimulated proliferative response of human PBL. Mean stimulation indices with mitogens(control): PHA: 55 ± 2.5 and PWM: 28 ± 1.5 were normalized to 100%. Data shown are mean ± SEM of three experiments.

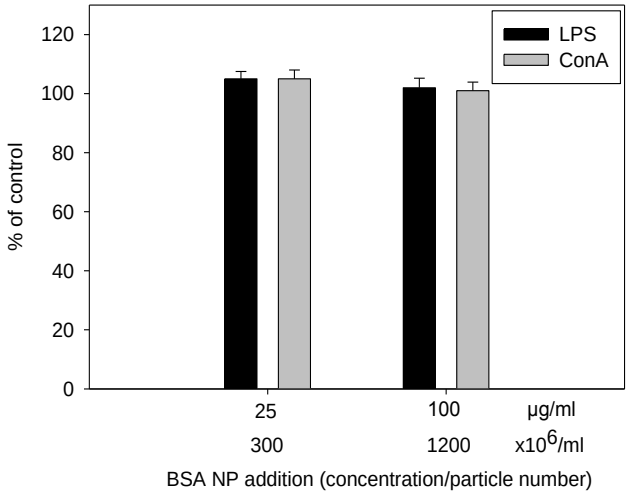

Figure 4.26: Effect of BSA NP on LPS or Con A induced proliferative response of mouse splenic lymphocytes. Mean stimulation indices with mitogens (control): LPS: 30 ± 2.5, Con A: 19 ±1.0 were normalized to 100%. Data shown are mean ± SEM of three experiments.

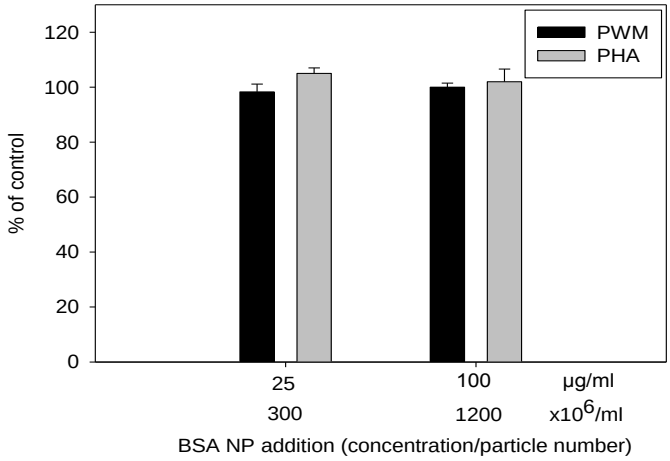

Figure 4.27: Effect of BSA NP on PWM or PHA stimulated proliferative response of human PBL. Mean stimulation indices with mitogens(control): PHA: 55 ± 2.5 and PWM: 28 ± 1.5 were normalized to 100%. Data shown are mean ± SEM of three experiments.

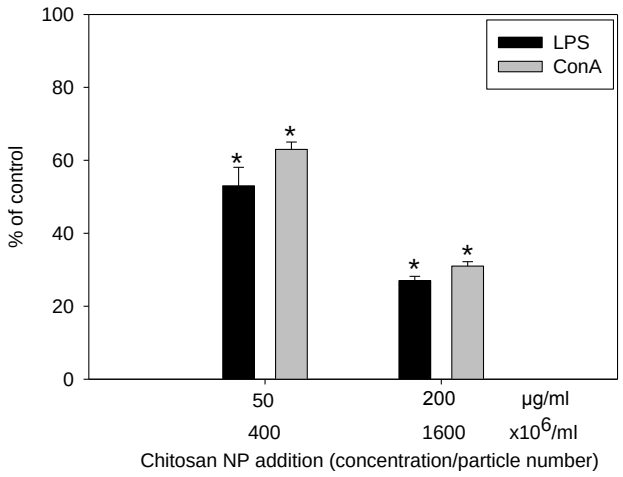

Figure 4.28: Effect of chitosan NP on LPS or Con A induced proliferative response of mouse splenic lymphocytes. Mean stimulation indices with mitogens (control): LPS: 30 ± 2.5, Con A: 19 ±1.0 were normalized to 100%. Data shown are mean ± SEM of three experiments. *p< 0.05, NP treated vs. control.

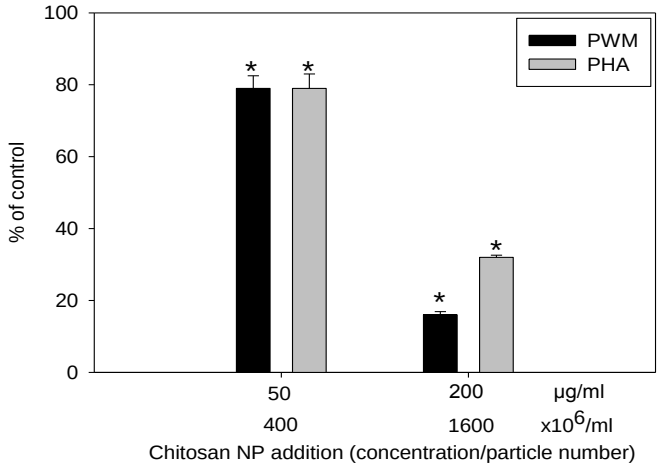

Figure 4.29: Effect of chitosan NP on PWM or PHA stimulated proliferative response of human PBL. Mean stimulation indices with mitogens (control): PHA: 55 ± 2.5 and PWM: 28 ± 1.5 were normalized to 100%. Data shown are mean ± SEM of three experiments. *p< 0.05, NP treated vs. control.

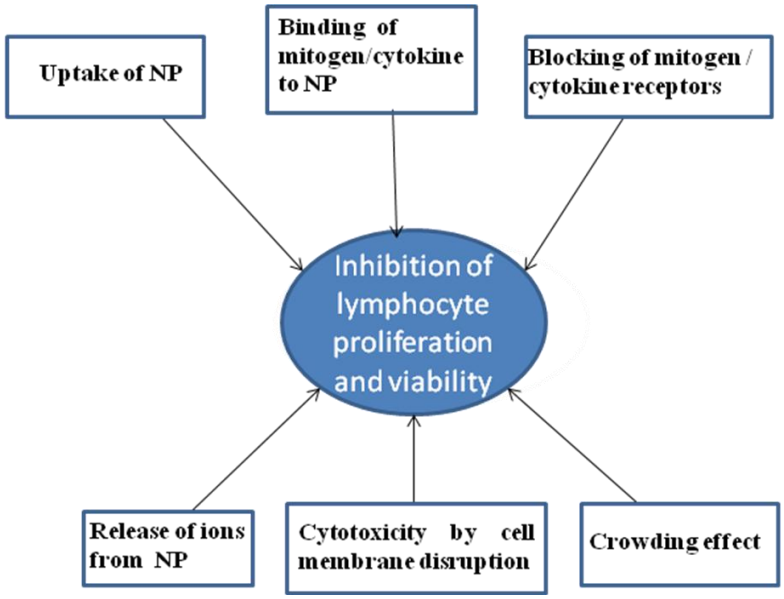

Figure 4.30: Possible mechanisms of metallic NP mediated inhibition of lymphocyte activation *in vitro*

Discussion

To test the effect of metallic NP on proliferative response of lymphocytes, they were incubated together in tissue culture medium for 3 days. It is necessary that NP are in mono dispersed state to effectively interact with lymphocytes. However, one major problem encountered with NP in suspension is their tendency to form aggregates depending on pH, ionic strength, charge, temperature etc. of the medium. The aggregates then sediment to the bottom of the tissue culture well and will be unavailable for interaction with lymphocytes. It has been demonstrated that the SPR spectrum of NP in visible range is significantly altered when they are aggregated compared to monodispersed state (Blakey et al., 2013; Prathna et al., 2011; Albanese and Chan, 2011) Aggregation of NP in tissue culture medium containing 5 % FCS was assessed by measuring the absorption spectrum in the visible range (400-700 nm). The results showed that GNP and SNP were indeed in monodispersed state after 3 days in culture. However, with CuNP, the results obtained were ambiguous indicating formation of aggregates in tissue culture medium.

Metallic NP have been proposed for wide use in biomedical imaging, cancer therapy and as anti-microbial agents (Almeida et al., 2014; Lara et al., 2011; Nune et al., 2009). In order to use NP as carriers of drugs and other biologically active ligands in vivo, it is necessary to evaluate their biocompatibility (Hanini et al., 2011). Investigations of immunomodulatory effects are essential for designing safe NP for use in imaging and clinical applications (Jiao et al., 2014). In the present work, putative immunomodulatory effects of GNP, SNP and CuNP on mitogen-induced proliferative response and viability were evaluated *in vitro*. Murine splenic lymphocytes and human PBL stimulated by T- and B-cell-specific mitogens were used as the models.

Significant inhibition of mitogen-stimulated proliferation of splenic lymphocytes (mouse, rat), thymic lymphocytes (mouse) and human PBL was noted by treatment with GNP, SNP and CuNP, at a concentration of ≥ 25, ≥ 5 and ≥ 2.5 μg/ml, respectively. Mitogen induced proliferative response of mouse splenic lymphocytes and human PBL was not affected upon treatment with apo-transferrin and BSA NP up to a concentration of 200 μg/ ml. However, chitosan NP treatment inhibited mitogen-stimulated response at 50 and 200 μg/ml. This inhibition may be due to interaction of chitosan with mitogens rather

than an effect on lymphocyte activation per se (Li et al., 2014). GNP <200 µg/ml had no effect on viability of either mouse lymphocyte or human PBL population. Viability of both populations of lymphocytes was decreased at 25–50 µg SNP/ml and 2.5-10 µg CuNP/ml. GNP had no effect on [^{3}H]-Td incorporation by unstimulated human or mouse lymphocytes at all test concentrations. With SNP, significant inhibition in incorporation was only noted at 50 µg/ml. However, with CuNP, significant inhibition in incorporation was observed at ≥ 5 µg CuNP/ml. From all this it can be surmised that in case of GNP and SNP, any observed inhibition of mitogen-induced proliferative responses would not be due to any effects of the NP on [^{3}H]-Td entry into cells / incorporation into cell DNA per se. In case of CuNP, at higher concentrations, it is possible that free copper ions released from NP might have some effect on DNA synthesis of mitogen activated cells (Li et al., 2013).

Enhancement of PHA-induced proliferative responses by human PBL due to GNP has been reported before (Liptrott et al., 2014). In an *in vivo* study using mice, orally administered GNP were able to differentially affect *ex-vivo* lymphocyte proliferative responses—stimulatory at low doses and inhibitory at high doses (Małaczewska, 2015). Dose-dependent increases in proliferative indices for $CD3^+$ and $CD4^+$ T-cells and no change in $CD8^+$ T cells were seen in human PBL treated *in vitro* with GNP (12nm diameter) at concentrations of 1–25 µg/ml (Guevel et al., 2015). A few studies have reported that SNP were cytotoxic and/or modulated immune responses (Greulich et al., 2011; Van der Zande et al., 2012). Differential effects on PHA-stimulated lymphocyte proliferative responses were also seen using SNP coated with polyvinyl–pyrrolidone + citrate; these SNP were stimulatory at l µg/ml but inhibitory at 10–40 µg/ml (Huang et al., 2016). In the present work, results suggested that SNP caused inhibitory (cytostatic) effects at low concentrations but cytotoxic effects at very high concentrations. No studies are available on the effect of CuNP on lymphocyte proliferation and viability. Exposure of nano copper to mice, decreased spleen index when compared to untreated mice (Chen et al., 2006).

The findings reported here further indicate that metallic NP could potentially modulate lymphocyte function *in situ* in terms of inhibiting their activation by mitogens. The precise mechanisms by which NP bring about this inhibitory effect are not clear. As the NP are not internalized by lymphocytes, it is possible that the effects are mediated via their uptake, mopping of mitogen/cytokines by binding to them, blocking of receptors

(mitogen/cytokine), induction of cytotoxicity by cell membrane disruption, crowding effect and release of ions from NP (Figure 4.30). It has been proposed that ions released from metallic NP can bring about cellular and molecular toxicities, including cell death (Zhao et al., 2014). Estimation of MDA levels in NP treated against untreated mouse and human lymphocytes showed significant elevation of MDA only in CuNP treated when compared to the untreated lymphocytes. This suggests that CuNP play significant role in immunomodulation of lymphocytes. CuNP has been shown to induce oxidative stress via Fenton type of reaction (Ibrahim et al., 2015).

In order to evaluate whether free gold or silver or copper ions released from NP play a role in the inhibition of proliferative responses, particle-free supernatants were collected from GNP, SNP and CuNP that had been incubated in culture medium. Mitogen-induced proliferative responses of splenic lymphocytes and human PBL cultured in supernatants of GNP and SNP were identical to those of cells cultured in fresh medium. However, supernatants of CuNP showed significant inhibition of mitogen induced proliferative response. It has been shown by others that SNP release ions at negligible concentrations into culture medium containing serum (Loza et al., 2014). GNP have been shown to be stable in terms of release of ions into culture medium at pH 7.0 (Sabella et al., 2014). Thus, the effects on mitogen-induced proliferation by the GNP and SNP were not likely due to the release of ions from the parent particles. Dissolution of copper from NP in culture medium has been shown to be moderate in first 24 h followed by slight increase over 72h. Size of NP and temperature were found to influence the dissolution of copper (Li et al., 2015). Inhibition of proliferative response in supernatants of CuNP suggests that it could be due to the effect of free copper ions released from NP. It has been proposed that toxicity of CuNP could be due to copper dissociated from particles under physiological conditions (Lee et al., 2016). On the other hand, one cannot rule out that the ions released from NP were being bound up by the serum proteins during the 72 hour culture period. If that were the case, this does not rule out the potential for liberated ions to have acted on the cells in the initial 48 hour incubation period before the tritiated thymidine was added. Clearly, further studies are needed to ascertain how GNP/SNP/ CuNP are acting to inhibit mitogen induced lymphocyte activation.

Biopolymer NP are being used as excellent carriers in the site-directed *in vivo* delivery of drugs, genes, vaccines and other macromolecules. The benefits of the biopolymeric NP are their biodegradability and non-toxicity (Mahapatro and Singh, 2011).

Biodegradable NP protects the degradation of therapeutic proteins such as insulin from harsh environment in the gastro-intestinal tract and delivers the proteins into systemic circulation efficiently when administered through oral route (Bakhru et al., 2013).

BSA is an abundant serum protein that has been shown to be biocompatible, biodegradable, non-toxic and non-immunogenic (Yu et al., 2014). Due to these features, BSA NP have been used as a carrier for many drugs and antigens. Use of albumin NP as cancer drug carrier is due to their advantage in passive and active targeting (Yu et al., 2015). In many studies, albumins NP were reported as excellent carriers for anti-cancerous drugs and to have no serious side effects (Elzoghby et al., 2012). Apo-transferrin NP have also been investigated as drug delivery vehicles. Apo-transferrin NP loaded with curcumin have been shown to be taken up efficiently by cells and inhibit HIV-1 replication *in vitro* (Gandapu et al 2011). Apo-transferrin NP have been demonstrated to increase absorption and significantly reduce toxicity of anti-cancer drug, doxorubucin following oral administration to rats (Golla et al., 2013).

Due to their biodegradability, biocompatability, non-toxicity and low immunogenicity, chitosan NP have been extensively advocated for biomedical use (Jain et al., 2016). Chitosan NP have been demonstrated to possess anti-bacterial, anti-fungal and anti-cancer activities (Yao et al., 2013). Chitosan has muco-adhesive property and mediates opening of tight junctions. Because of these features, chitosan NP have been used as carriers for oral delivery of macromolecules. Chitosan NP have been used as promising targeted drug delivery vehicles as the loaded therapeutics are protected from degradation in the gastro-intestinal tract (Chen et al., 2013a, 2014). Chitosan NP display higher toxicity against tumour than normal cells (Qi et al., 2005). Positive charge of chitosan NP increases their intracellular uptake and influences their escape from lysosomes and in perinuclear localization (Yue et al., 2011). Also, positive charge of amino groups in chitosan NP can interact with tumour cell membrane which is more negatively charged than membrane of normal cell (Zhang et al., 2010b). It has been reported that chitosan binds to mitogens such as LPS and produce a stable complex due to its polycationic and hydrophobic substituents (Davydova et al., 2008). Due to their versatile use in biomedical applications, it is important to study the effect biological NP for possible effects on immune cells.

In the present study, the effect of blank (with no loaded cargo) BSA, apo-transferrin and chitosan NP on lymphocyte activation was investigated *in vitro*. Proliferative response was measured in presence of a T or B cell mitogen and biological NP mentioned above. Both BSA and apo- transferrin NP had no effect on mitogen induced proliferative response of mouse or human lymphocytes. But, lymphocyte proliferative response was significantly inhibited by chitosan NP. Preliminary work carried out has shown that chitosan NP binds to mitogens avidly. It is possible that binding of mitogens to chitosan NP reduces their optimal concentration necessary for lymphocyte activation. In summary, the biological NP had no effect on mitogen induced lymphocyte activation *per se*.

The following are the salient observations of the work presented in this chapter:

1) GNP, SNP and CuNP inhibited mitogen induced proliferative response of lymphocyte population from mouse, rat and human peripheral blood in a dose-dependent manner.

2) Metallic NP inhibited lymphocyte viability, the observed effect with CuNP > SNP > GNP.

3) Possible mechanisms for the observed inhibition of activation by GNP and SNP were discussed. In case CuNP, release of free copper ions and induction of oxidative stress seem to be involved.

4) Amongst biological NP, chitosan NP exhibited an indirect effect on lymphocyte activation through interaction with mitogen. BSA and apo-transferrin NP had no effect on lymphocyte proliferative response and hence seem to be immune-compatible.

Chapter 5

Effect of metallic NP on malignant B and T lymphocyte cell lines

Introduction

Drug delivery based on nanotechnology has been gaining importance in clinical medicine. Controlled release, prolonged half-life in circulation, enhanced uptake in to cells etc., have been demonstrated with drugs conjugated to NP as compared to free form (Bertrand et al., 2010). In addition, NP have been shown to improve drug efficacy in cancer treatment by increasing solubility, stability and loading capacity. Modification in pharmacokinetics, decrease in toxicity and specific targeting to tumour have also been demonstrated with NP-drug conjugates (Dawidczyk et al., 2014; Seigneuric et al., 2010). Prior to use of drug-NP conjugates *in vivo*, pre-clinical evaluation is carried out *in vitro* using primary cells as well as established cell lines. The results obtained using cell lines *in vitro* is useful to design experiments for pre-clinical studies *in vivo* using animal models (McCauley et al., 2013; Florento et al., 2012).

GNP of 5 nm size have been shown to inhibit proliferation and induce apoptosis in human leukemia cell line, K562 (Namvar et al., 2015). Treatment of multiple myeloma cell lines in culture with GNP of 5nm size inhibited their proliferation by affecting a cell cycle arrest in G1 phase (Bhattacharya et al., 2007). Glucose capped GNP of 7 nm size were found to be non-toxic to human T cell lines (Kaur et al., 2013). Little or no cytotoxicity was observed in RAJI B Lymphoma cells or Jurkat cells upon treatment with 15 nm size GNP at a concentration of 2.5 µg/ cm^2 (Knight et al., 2007).

Exposure of Jurkat cells to 10-100nm of SNP for 24 h showed that toxicity in terms of formation of micronuclei and DNA damage was inversely proportional to the size of the particle (Butler et al.,2015). In Jurkat cells, viability was found to be inhibited in a dose-dependent manner upon treatment with SNP at concentration of 2.5-10 ppm (Parnsamut and Brimson, 2015). Dose dependent inhibition of viability of K562 was observed with copper oxide NP treatment (Shafagh et al., 2015). Studies described above suggest that effect of metallic NP like GNP, SNP and CuNP have been investigated on malignant T and B cell lines. Size of NP used was less than 20 nm. In the present work, effect of GNP, SNP and CuNP of defined size and particle number has been investigated using U266B1 and SUP-T1 as model cell lines.

Materials and methods

Preparation and characterization of metallic NP

Metallic NP were prepared and characterized as described in materials and methods.

Cell lines

The cell lines used were U266 B1, a human myeloma cell line (B lymphocyte) which secretes monoclonal IgE and IL-6 and SUPT-1, a human T lymphoblastic lymphoid cell line expressing CD4. Maintenance and sub-culture of the cell lines was carried out as described in materials and methods.

MTT assay

Effect of metallic NP on proliferation of U266B1 and SUP-T1 cell lines was assessed by MTT assay as described in materials and methods. Proliferation of experimental samples treated with NP was calculated and expressed as % of control.

Results

GNP

SUP-T1 and U266 B1 cell lines were treated with 5 - 200µg GNP / ml corresponding to 3-120 x 10^9 particles / ml for 24 h. Results of MTT assay as a measure of proliferative response are presented in Figures 5.1 and 5.2. In SUPT-1 cells, proliferation was significantly inhibited at all doses from 25- 200 µg GNP /ml. The response was also dose-dependent. In case of U266 B1 cells, there was no effect of 5 and 20 µg GNP / ml on proliferation. But, proliferation was inhibited by 50-200 µg GNP/ ml.

SNP

SUP-T1 and U266 B1 cell lines were treated with 5 – 100 µg SNP / ml corresponding to 2.4 – 48 x 10^9 particles / ml. Proliferation of SUPT-1 cells was inhibited by 12.5 – 100 µg SNP / ml (Figure 5.3). U266 B1 cell proliferation was unaffected by 5-25 µg SNP / ml. Significant inhibition of proliferation was observed at 50 and 100 µg SNP / ml (Figure 5.4).

CuNP

U266B1 and SUP-T1 cell lines were incubated with 1 – 10 µg CuNP / ml (57-570 x 10^6 particles / ml) for 24 h. Proliferation of SUPT-1 cells was inhibited in a dose-dependent manner at all the concentrations of CuNP tested (Figure 5.5). Similarly, CuNP inhibited proliferation of U266B1 cells at 2.5 – 10 µg / ml (Figure 5.6).

In summary, all the metallic NP affected the proliferation of SUPT-1 and U266 B1 cells *in vitro*. The cytotoxic effect of CuNP > SNP > GNP. T cell lymphoma, SUPT-1 was observed to be more susceptible to inhibitory effect of NP compared to B cell lymphoma U266 B1.

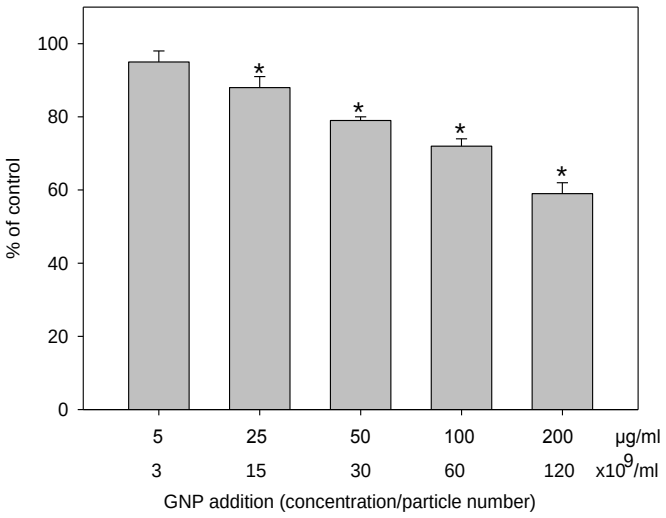

Figure 5.1: Effect of GNP on proliferation of SUPT-1 cell line. Data presented are mean ± SEM of three experiments. Absorbance of cells with no NP: 0.595 ± 0.045 was normalized to 100 %(control). * p < 0.05, NP treated vs. control.

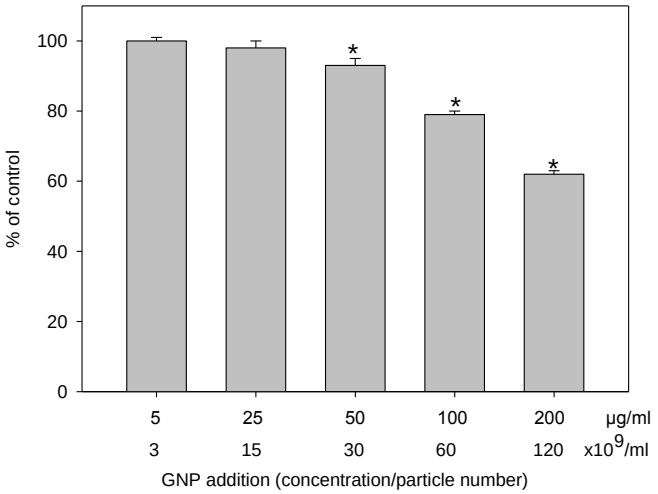

Figure 5.2: Effect of GNP on proliferation of U266 B1 cell line. Data presented are mean ± SEM of three experiments. Absorbance of cells with no NP: 0.540 ± 0.043 was normalized to 100 %(control). * p < 0.05, NP treated vs. control.

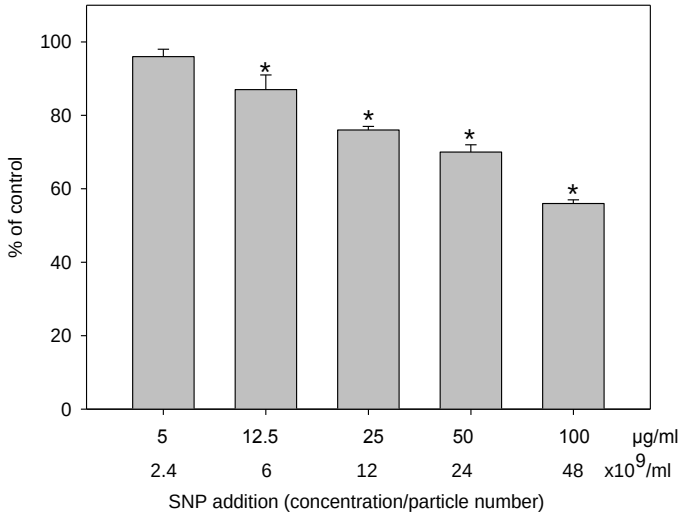

Figure 5.3: Effect of SNP on proliferation of SUPT-1 cell line. Data presented are mean ± SEM of three experiments. Absorbance of cells with no NP: 0.595 ± 0.045 was normalized to 100 %(control). * p < 0.05, NP treated vs. control.

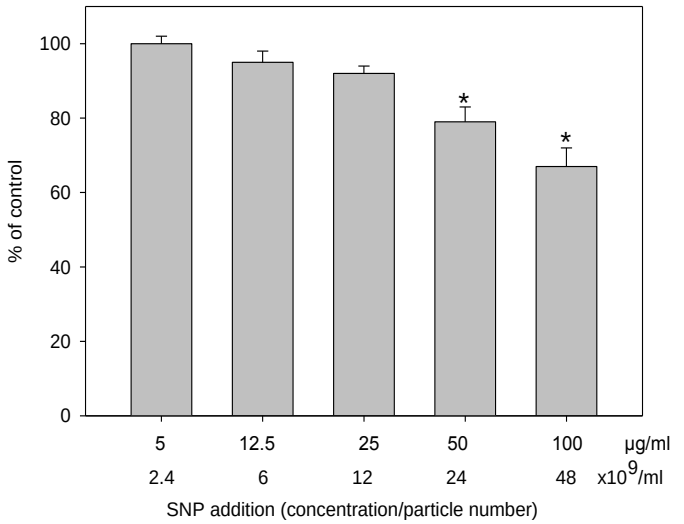

Figure 5.4: Effect of SNP on proliferation of U266 B1 cell line. Data presented are mean ± SEM of three experiments. Absorbance of cells with no NP: 0.540 ± 0.043 was normalized to 100 %(control). * p < 0.05, NP treated vs. control.

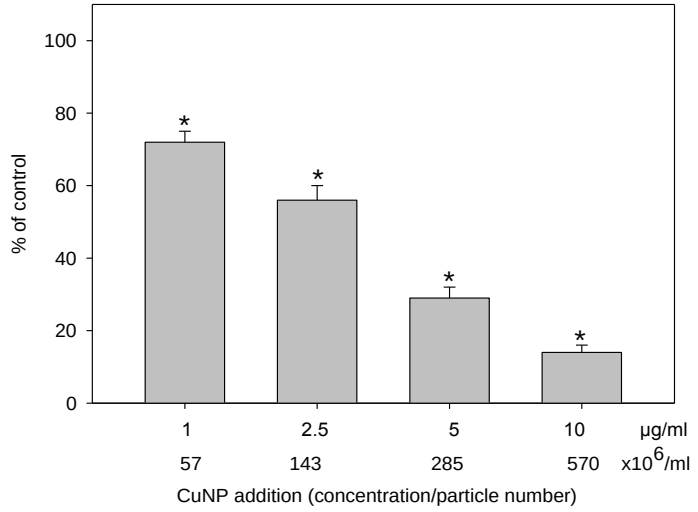

Figure 5.5: Effect of CuNP on proliferation of SUPT-1 cell line. Data presented are mean ± SEM of three experiments. Absorbance of cells with no NP: 0.595 ± 0.045 was normalized to 100 %(control). * p < 0.05, NP treated vs. control.

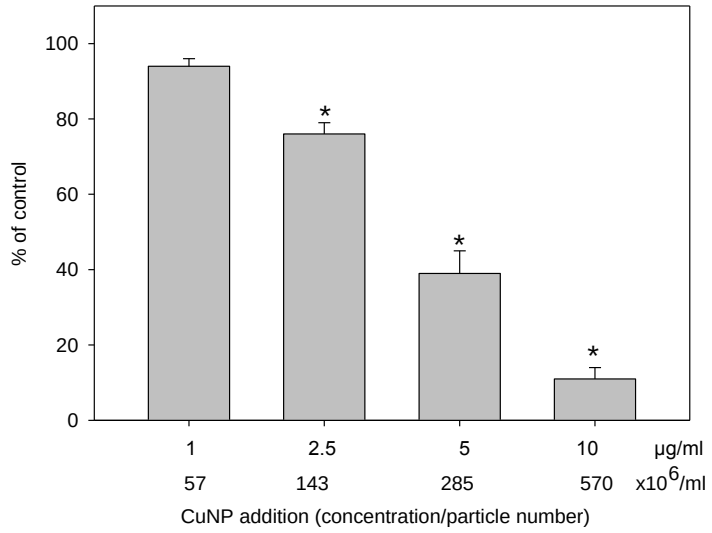

Figure 5.6: Effect of CuNP on proliferation of U266 B1 cell line. Data presented are mean ± SEM of three experiments. Absorbance of cells with no NP: 0.540 ± 0.043 was normalized to 100 %(control). * p < 0.05, NP treated vs. control.

Discussion

Studies on effect of metallic NP on mitogen activated primary murine and human lymphocytes *in vitro* revealed that proliferation was inhibited in a dose-dependent manner (Chapter 4). Entry of resting lymphocytes in to cell cycle and proliferation is brought about by an array of intracellular signaling events involving second messengers, cytokines etc. Malignant cell lines of lymphoid origin proliferate in tissue culture in a similar manner as primary cells, albeit in the absence of a stimulus from antigen / mitogen (Norian et al., 2015, Shaffer et al., 2002). Metallic NP have been tested for their potential anti-proliferative activity *in vitro* using a variety of cell lines (Fraga et al., 2013, Asharani et al., 2009). Further, metallic NP coated with anti-cancer drugs and bioactive ligands have been tested in vitro as effective drug delivery vehicles (Dreaden et al., 2009; Benyettou et al., 2015). It is desirable to use a NP which has anti-proliferative activity on malignant cells per se. Hence, putative anti-proliferative activity of GNP, SNP and CuNP using SUPT-1 and U266 B1 as model cell lines was evaluated.

Bare GNP has been shown to inhibit viability of malignant cell lines - RAJI B lymphoma, Jurkat (Knight et al., 2007), OPM-1, RPMI-8266 (Bhattacharya et al., 2007) and K562 (Namvar et al., 2015). However, GNP coated with either biotin or glucose were found to be non-toxic to K562 (Connor et al., 2005) and Jurkat cell lines (Kaur et al., 2013). It has been proposed that coating of GNP with biomolecules renders them non-toxic to cells. Choice of functionalization of GNP may also determine its biomedical applications (Tiwari et al., 2011). In non T and B cell lines such as PC-3, MCF-7, HT1080 and A549, GNP has been shown to inhibit viability (Patra et al., 2007; Vijayakumar and Ganesan, 2012; Choi et al., 2012; Karuppaiyaa et al., 2013). In the present experiments, GNP of 28 nm size (hydrodynamic diameter) inhibited proliferation of T and B cell lines. The effect was dose-dependent at 25-200 µg GNP / ml. It is to be noted that proteins, mainly albumin present in fetal calf serum get adsorbed to GNP when they are suspended in tissue culture medium. Anti-proliferative effect observed with GNP is in agreement with earlier reports (Bhattacharya et al., 2007; Knight et al., 2007; Namvar et al., 2015). Toxicity of GNP may due induction of apoptosis via the mitochondrial intrinsic pathway through caspases 3 and 9 activation (Namvar et al., 2015) and upregulation of cell cycle proteins p21 and p27 (Bhattacharya et al., 2007).

Effect of SNP on viability of malignant cell lines has been investigated using varying particle size and concentration. In Jurkat cells treated with 0.5-1.0 mg / litre of SNP, significant loss of viability has been reported (Eom and Choi, 2010). Dose and size dependent loss of viability was observed upon treatment of Jurkat cells with 2.5-15 ppm SNP and 10-20 nm size particles (Parnsamut and Brimson, 2015; Butler et al., 2015). These observations suggest that concentration and size play an important role in SNP induced toxicity of malignant lymphoid cells. Loss of viability was observed in HepG2 and U937 cell lines upon treatment with SNP (Faedmaleki et al., 2014; Parnsamut and Brimson, 2015). In the present study, SNP of 40-80 nm size inhibited the viability of U266B1 and SUP-T1 in a dose-dependent manner. Mechanism of SNP induced toxicity are due to induction of apoptosis via oxidative stress, decreased ERK signaling, activation of p38 mitogen activated protein kinase through nuclear factor-E2 related factor and nuclear factor-kappaB signaling pathways, induction of DNA damage and cell cycle arrest (Parnsamut and Brimson, 2015; Eom and Choi, 2010)

Treatment of U937, Hela, HepG2 and MCF-7 cell lines with CuNP resulted in inhibition of cell viability in dose- dependent manner (Jose et al., 2011; Siddiqui et al., 2013; Laha et al., 2014). In K562 cells treated for 24h with 2-25 µg / ml of copper oxide NP, cell viability was inhibited (Shafagh et al., 2015). In the present study, CuNP inhibited proliferative response at 1 – 10 µg/ml. Both B and T cell lines used seems to be susceptible to cytotoxic effect of CuNP as reported earlier (Jose et al., 2011; Siddiqui et al., 2013; Laha et al., 2014). It has been shown that CuNP induced toxicity involves reactive oxygen generation, induction of apoptosis, upregualtion of p53 and increase in Bax/Bcl-2 ratio (Shafagh et al., 2015)

The salient findings of the work presented in this chapter are:

1) All the three metallic NP used in the experiments inhibit proliferation of T-and B-cell lines in a dose-dependent manner.
2) Amongst the metallic NP, cytotoxic potential of CuNP > SNP > GNP.

Chapter 6

Tissue localization of metallic NP using *ex-vivo* imaging following oral administration to rats

Introduction

Metallic NP have been used in various areas of clinical medicine such as diagnosis, targeted drug delivery and cancer therapy (Jeong et al., 2014; Austin et al., 2014). All these applications, NP have to be administered *in vivo*. Accumulation and persistence of NP in the body tissues may lead to enhanced interaction with cells and manifestation of potential toxic effects (Johnston et al., 2010). Bio-distribution of metallic NP is of concern as some of them have been shown to be rapidly cleared from blood by cells of reticulo-endothelial system and persist in tissues / organs for long time period (Duan and Li et al., 2013; Dobrovolskaia et al., 2008). *In vivo* studies are helpful to understand the interaction of NP with biological systems (Almeida et al., 2011). Tissue distribution of NP defines their therapeutic effect (Li and Huang, 2008).

Traditionally, biodistribution studies of NP were carried out using TEM or autoradiogrphy with radiolabeled probes. Both these techniques provide qualitative or in some cases semi-quantitative information about localization of NP. Mass spectrometric methods have also been developed to study biodistribution which allows for quantification of the constituent element of NP (Liu et al., 2012). There are other imaging modalities, which give the information about the biodistribution of NP, but each imaging modality has its own pros and cons. advantages and disadvantages of each technique used to study the bio-distribution of NP are summarized in the Table 6.1.

Fluorescence imaging particularly near infrared (NIR) fluorescence imaging is used to overcome the limitations of optical imaging. Near infrared fluorescence imaging minimizes background interference and improves tissue depth penetration and image sensitivity (Hilderbrand and Weissleder, 2010). Organic NIR fluorescent dyes have been widely used as probes due to their photo-stability, ease of synthesis and amenability for conjugation with biomolecules such as proteins. Coating of NIR dye conjugated proteins on the surface of NP or loading of NIR dyes in the NP have been used for imaging (Luo et al., 2010). Surface of NP can be effectively coated using small ligands, polymers, lipids etc, through covalent and non-covalent interactions (Nam et al., 2013). Rhodamine dyes are highly fluorescent, resistant to photo-bleaching and have quantum yield emission maximum near to infrared red range of 500-600 nm. They have good solubility in organic solvents and have less toxicity (Jeon et al., 2010). Rhodamine derivatives have been widely used for labeling biomolecules (Shibata et al., 2008).

Table 6.1: Techniques used to study biodistribution of NP

Techniques	Label used	Information obtained	Advantages	Disadvantages	References
Radio labeling	Radionuclides	Qualitative and quantitative	Minimally invasive.High penetration and negligible tissue attenuation related issues. Small amount of material is required. Low background noise.	Health hazard. Environmentally Unsafe. Synthesis and disposal of radioactive compounds are expensive.	(Liu et al., 2012; Llop et al., 2013)
Transmission electron microscopy (TEM)	None	Qualitative and semi quantitative information	Detect and identify the NP location in tissues and cells. NP size and shape information can be obtained	Tedious sample preparation Requires uniform thin sample. High cost.	(Tsutsumi and Yoshioka, 2011; Alger et al., 2014)
Inductively coupled plasma - mass spectrometry (ICP-MS)	None	Quantitative information	High sensitivity. Simultaneous detection of multiple elements. Short analysis time.	Digestion step is needed, which destroys the physical properties of NP. Difficult to distinguish between the elements that are inherent to the nanomaterials and those that are released from dissolution. High cost. It is an end point measurement	(Tsutsumi and Yoshioka, 2011; Alger et al., 2014).
Computed tomography (CT)	Contrast agents	provides anatomical, physiological and molecular information	Non-invasive. Provides subtle differences between different soft tissues.	Low specificity and sensitivity. Exposure to X-ray radiation expo	(Fass, 2008; Ding and Wu,2012)
Magnetic resonance imaging (MRI)	Contrast agents	Provides anatomical, physiological and molecular information	Non invasive. Good contrast between the different soft tissues of the body. Ionizing radiation is not needed. Provide 3 D representation of organs.	Low sensitivity. Long acquisition time. High cost.	(Ding and Wu,2012; Thomas et al.,2013)
Positron emission tomograpghy (PET)	Radionuclides.	Provides anatomical, physiological and molecular information	Non invasive. High sensitivity	Lack of detailed and high resolution anatomy. Require radio-nuclide facilities	(Ding and Wu,2012;Thomas et al.,2013)
Optical imaging (fluorescence imaging)	Fluorophores	Provide information on global tissue accumulation	Low cost. Non toxic. Non-invasive	Auto-fluorescence. Gives limited anatomical information. Sensitivity reduces with increase in image depth	(Liu et al., 2012; Thomas et al.,2013)

Administration of GNP orally for 8, 16 and 30 days to the rats showed accumulation of GNP as clusters in the cytoplasm of macrophages and lymphocytes regardless of duration of the administration (Zlobina et al., 2013). Dual-radiolabeled [^{14}C] citrate-[^{198}Au] GNP when orally administered to rats showed highest accumulation in the liver followed by spleen, lungs and blood (Rambanapasi et al., 2015). GNP oral administration in rats for 14 days, showed slight accumulation of NP in kidney, whereas, high ionic gold were observed in kidney, liver, lung and spleen (Jo et al., 2015). In mice, GNP, after 14-28 days of oral administration, were detected in blood cells and bone marrow (Zhang et al., 2010a).

Oral administration of SNP or $AgNO_3$ to rats for 28 days showed that liver and spleen are the targets for either SNP or silver salt and no difference was found in the distribution of silver in either agent administered animals (Van der Zande et al., 2012). SNP or Silver acetate administered orally to Wistar Hannover Galas rats for 28 days showed accumulation of either form of silver in ileum, liver, and kidney tissues. Oral exposure of SNP for 30 to 45 days resulted in the accumulation of SNP in liver and kidney tissues (Jimenez-Lamana et al., 2014).

Single oral dose of CuNP or Cu ions to rats resulted in the lower levels of Cu in CuNP than Cu ion treated groups in blood and liver, kidney and spleen. Compared to the control, the Cu levels in both CuNP or Cu ions were higher in liver, kidney, and spleen (Lee et al., 2016). CuNP administration orally to mice showed that target organs are kidney, liver and spleen (Chen et al., 2006).

In the present study, *ex-vivo* imaging was performed using Rho-BSA/chitosan conjugate coated on the surface of metal NP to study the biodistribution of NP in organs such as spleen, thymus, liver and kidneys.

Materials and methods

Chemicals

GNP, SNP and CuNP prepared and characterized in Chapter 3 were used. BSA, chitosan and RITC were purchased from Sigma chemicals (India).

Animals

Female rats, 6 weeks of age were obtained from National Center for Laboratory Animal Sciences, National Institute of Nutrition, Hyderabad. Rats were housed in the Animal facility of University of Hyderabad for few days before use. The rats were fed pelleted rat diet and were given water *ad libitum*.

Imaging equipment

Small animal in vivo imaging system – Model " In-Vivo MS FX PRO" supplied by Carestream Health, USA was used for imaging of tissues. The imaging system is a CCD-based pre-clinical fluorescence imager equipped with software for acquisition and analysis of images (Bruker MI Software).

Preparation of Rho-BSA and Rho-chitosan conjugates

BSA and Chitosan were covalently coupled with RITC using a standard protocol as described in Materials and Methods (Chapter 2).

Characterization of Rho-labeled conjugates by Fluorescence spectroscopy: Rho-BSA, Rho-chitosan and GNP, SNP and CuNP coated with Rho-conjugates were characterized using fluorescence spectroscopy.

Preparation of Rho-BSA and Rho-chitosan conjugates coated on to the surface of Metallic NP

Rho-BSA and Rho-chitosan conjugates were coated on the surface of metallic NP using adsorption process. Uncoated conjugates were removed by 3 times centrifugation at 10000 x g for 15 minutes. Concentration of BSA and chitosan present in the supernatants was determined using standard protocols (Lowry et al., 1951; Scott Jr., and Melvin, 1953).

Oral administration of Rho-BSA and Rho-chitosan coated metallic NP to rats

Rats were housed in individual cages and were kept on overnight fasting (16 h) prior to conjugate / NP administration. Water was supplied ad libitum. Uncoated metallic NP, Rho-BSA, Rho-chitosan conjugates and metallic NP coated with Rho-conjugates were administered separately to individual rats. A dose of 1 mg / Kg body weight in a volume of 0.20 ml of Tris- buffered saline, pH 7.40 was administered orally using a gavage needle

fitted to a 1 ml syringe. Feed was given to rats 2 h after oral administration of conjugates / NP. Rats were sacrificed using mild ether anesthesia and liver, spleen, thymus, kidney were dissected out. Contaminating blood and fat adhering to tissues was carefully removed. Tissues were kept on ice in individual sterile petri dishes until use.

***Ex-vivo* imaging using small animal *in vivo* imaging system**

Excitation and emission filters suitable for rhodamine were selected. Tissues were transferred to clean tissue culture petri dishes (Corning) and were placed on the imaging platform of imaging system chamber. The following settings were used to acquire images.

1. Exposure / time : Standard, 30 sec
2. No. of exposures: 1
3. x and y binning: 4 pixels each
4. Illumination source: multi wavelength
5. Camera setting: F stop- 2.62, FOV- 180 mm, Fixed plane - 15 mm.
6. Excitation / emission filter : 550 nm / 600 nm

   Images were processed by ROI analysis and the mean fluorescence intensity was computed by Bruker MI software.

Results

Fluorescence spectra of Rho-BSA, Rho-chitosan conjugates, bare NP and conjugates coated on the NP surface:

Rho-BSA and Rho-chitosan conjugates and conjugate coated NP (GNP, SNP and CuNP) were investigated for the presence of rhodamine dye by fluorescence spectroscopy. Both conjugates (Figures 6.1 & 6.2) showed emission maximum at 580 nm, which is a characteristic feature of Rhodamine B isomer used and hence, confirmed its presence in the conjugates. Bare NP (GNP, SNP and CuNP) did not exhibit any fluorescence under the same conditions employed above (Figures 6.3- 6.5). This observation confirmed that NP per se does not emit any fluorescence in the region of emission spectrum of rhodamine.

Fluorescence spectra of Rho-BSA coated NP are presented in Figures 6.6 – 6.8. Spectrum of Rho-BSA coated GNP showed an absorption maximum similar to Rho-BSA conjugate. Fluorescence spectra of Rho-BSA coated SNP and CuNP also were similar to that of the free conjugate. This observation strongly indicated that the Rho-BSA conjugate is bound to all the three metallic NP. Fluorescence emission spectra of Rho-chitosan coated NP are presented in Figure 6.9- 6.11.

***Ex-vivo* imaging of tissues following administration of Rho-BSA and Rho-chitosan coated NP**

Liver, kidney and lymphoid organs, (thymus, spleen) harvested from rats administered GNP, SNP and CuNP coated with Rho-BSA and Rho-chitosan conjugate were imaged *ex-vivo*. Soluble conjugates and bare (uncoated) NP were used as controls. Fluorescence images of thymus from rats that received Rho-BSA coated metallic NP are presented in Figure 6.12. Relative fluorescence intensity scale is also depicted in the figure for reference. All three coated NP showed significant accumulation in the thymus. However, the fluorescence observed with soluble Rho-BSA conjugate is many fold less compared to fluorescence observed in conjugate coated NP images. This observation strongly suggests significant accumulation of NP in thymus 24 hours following oral administration. Fluorescence images of spleen are presented in Figure 6.13. The fluorescence intensity was less compared to that observed in thymus, indicating a marginal localization of NP in spleen.

Fluorescence images of liver and kidney are presented in Figures 6.14 and 6.15 respectively. Low fluorescence intensity was noted in the liver tissue from rats which received soluble Rho-BSA conjugate. The intensity was significant in livers of conjugates coated NP administered rats.

Fluorescence images of thymus, spleen, liver and kidneys from rats administered Rho-chitosan coated NP along with relevant controls are presented in Figures 6.16 – 6.19. The results obtained with Rho-chitosan conjugate were similar to those observed with Rho-BSA conjugate. Fluorescence intensity of free conjugate localization was less with both the conjugates used. No fluorescence was noted in any of the tissues obtained from bare NP administered rats.

Fluorescence intensity was computed by imaging software and is presented in Tables 6.2 and 6.3 for Rho-BSA and Rho-chitosan respectively. Intensity in all the tissues of conjugate coated NP administered rats was higher by at least 10 fold compared to intensity observed in tissues of soluble conjugate administered rats. Hence, the results strongly indicate that the higher intensity was due to accumulation of NP and probably not due to uptake of free conjugate by the tissue.

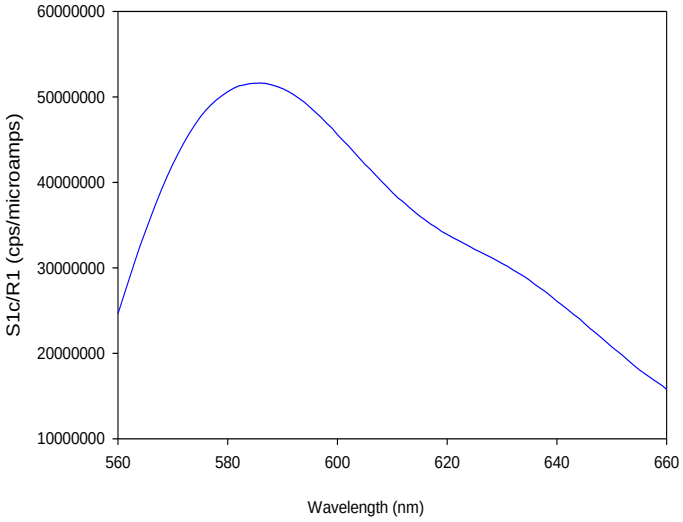

Figure 6.1: Fluorescence spectrum of Rho-BSA conjugate

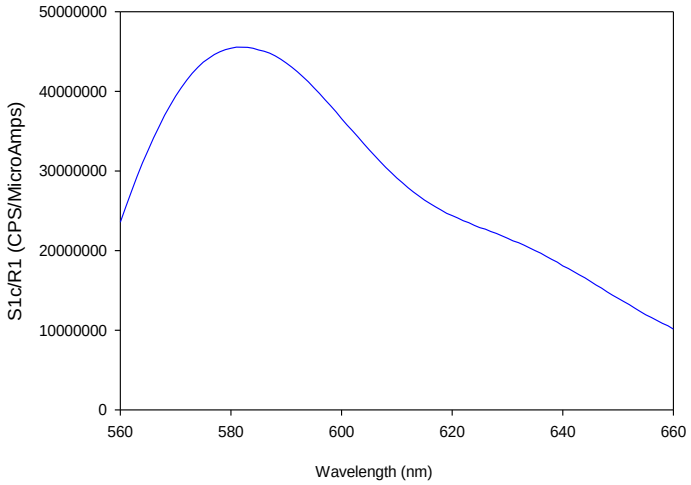

Figure 6.2: Fluorescence spectrum of Rho-chitosan conjugate

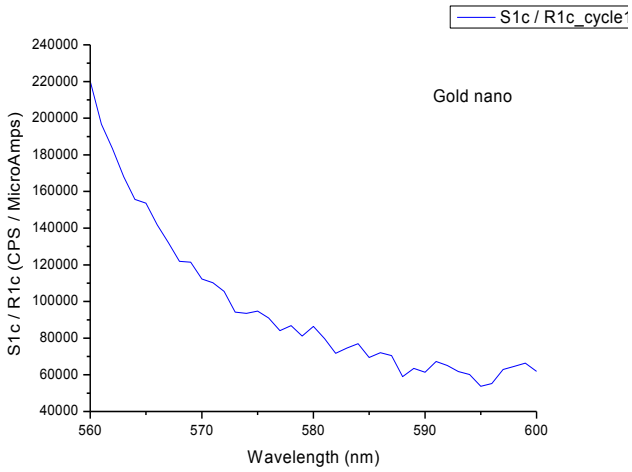

Figure 6.3: Fluorescence spectrum of GNP

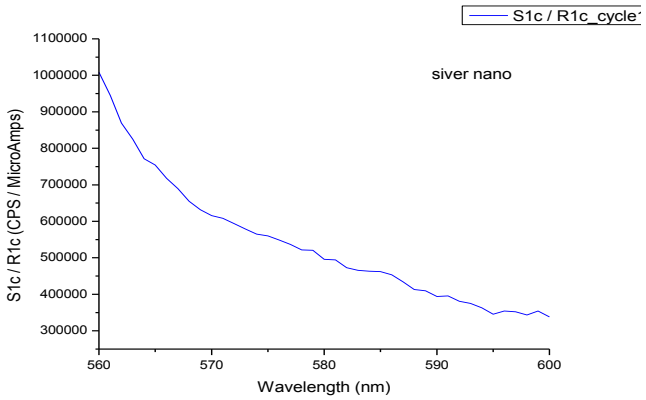

Figure 6.4: Fluorescence spectrum of SNP

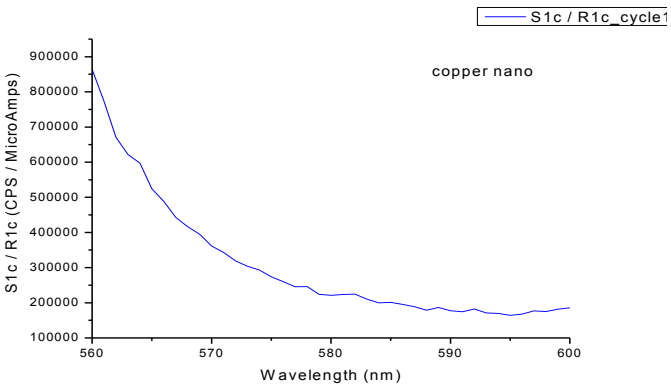

Figure 6.5: Fluorescence spectrum of CuNP

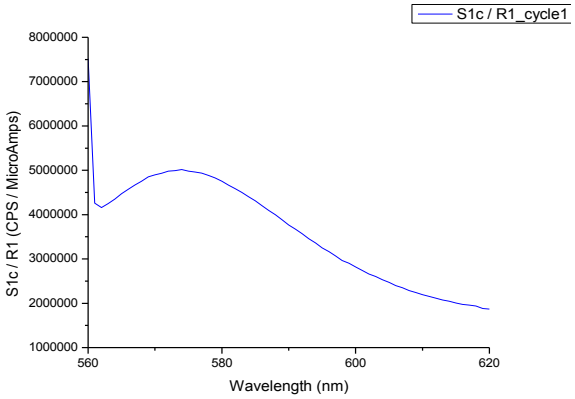

Figure 6.6: Fluorescence spectrum of Rho-BSA coated GNP

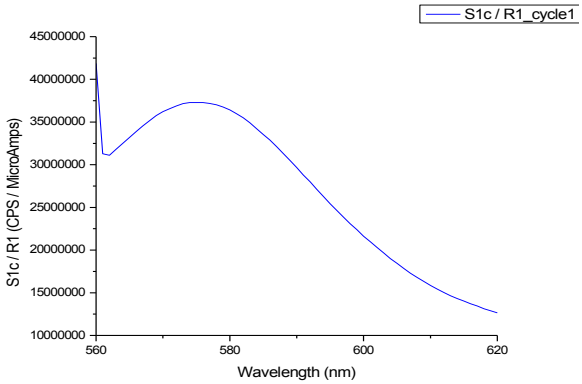

Figure 6.7: Fluorescence spectrum of Rho-BSA coated SNP

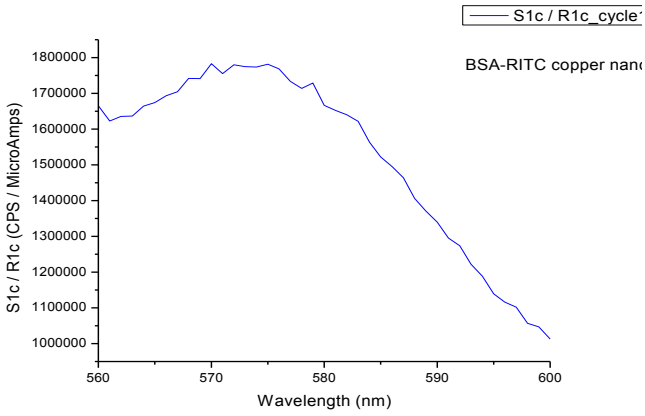

Figure 6.8: Fluorescence spectrum of Rho-BSA coated CuNP

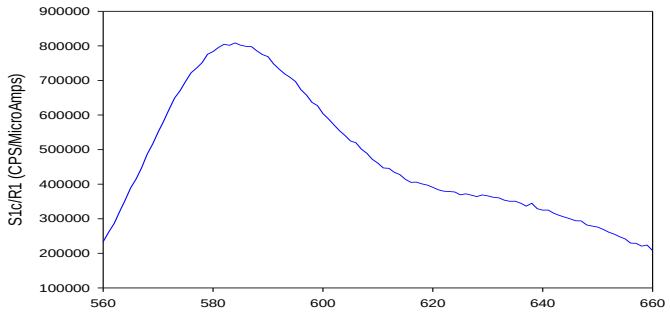

Figure 6.9: Fluorescence spectrum of Rho-chitosan coated GNP

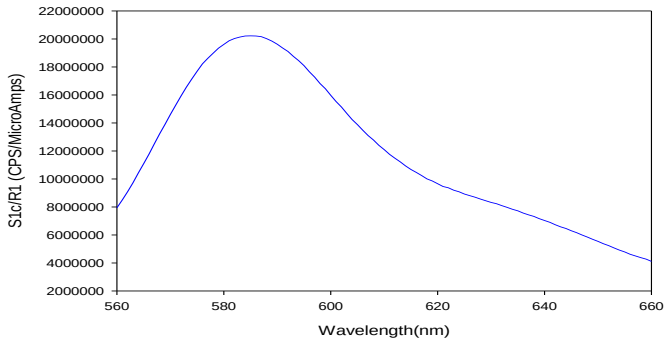

Figure 6.10: Fluorescence spectrum of Rho-chitosan coated SNP

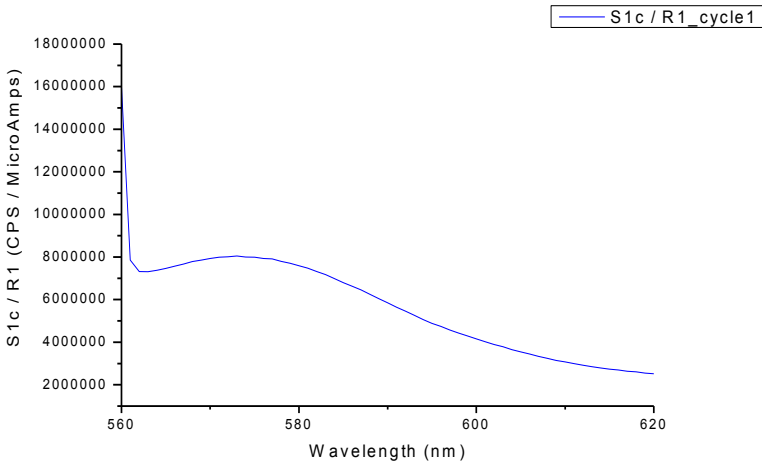

Figure 6.11: Fluorescence spectrum of Rho-chitosan coated CuNP

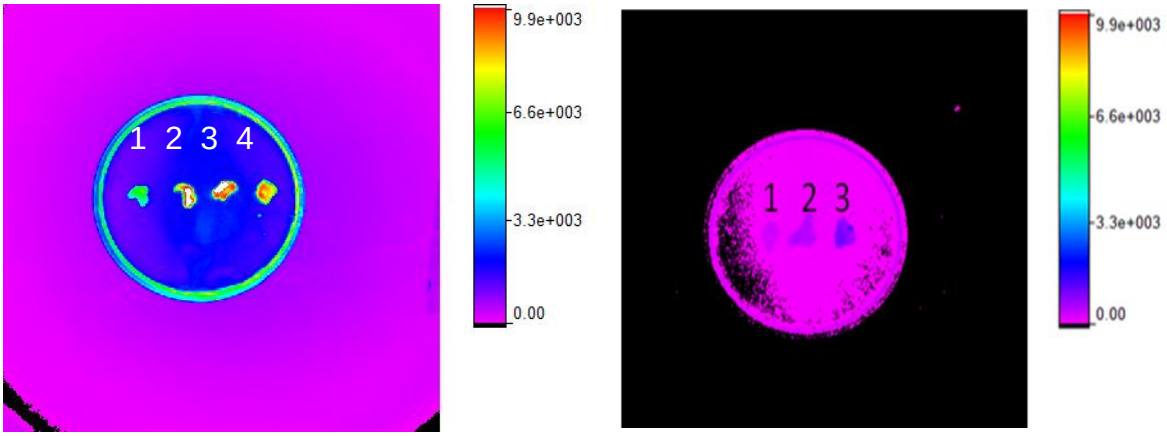

(A) **(B)**

Figure 6.12: *Ex-vivo* imaging of thymus from rats administered Rho-BSA coated NP (A), or bare NP (B).
A: 1. Rho-BSA conjugate; 2. Rho-BSA GNP; 3. Rho-BSA SNP; 4. Rho-BSA CuNP
B: 1. GNP; 2. SNP; 3. CuNP

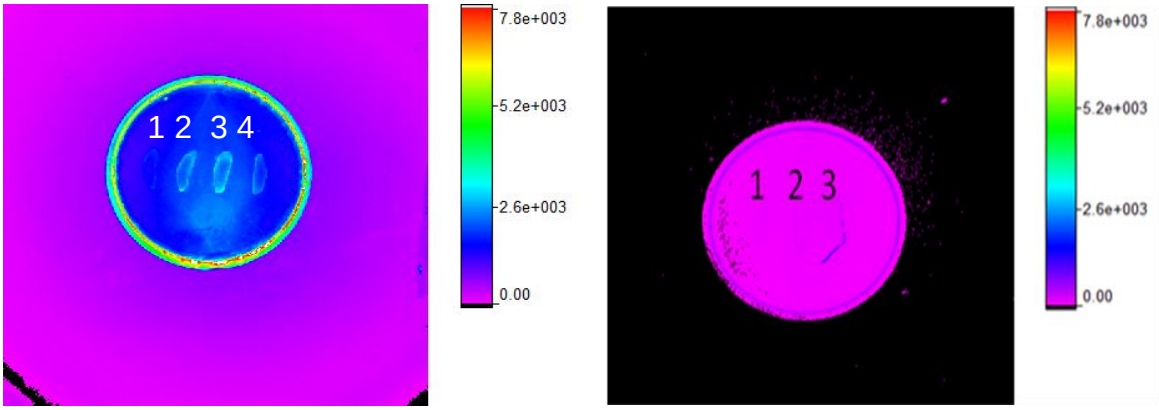

(A) **(B)**

Figure 6.13: *Ex-vivo* imaging of spleen from rats administered Rho-BSA coated NP (A), or bare NP (B).
A: 1. Rho-BSA conjugate; 2. Rho-BSA GNP; 3. Rho-BSA SNP; 4. Rho-BSA CuNP
B: 1. GNP; 2. SNP; 3. CuNP

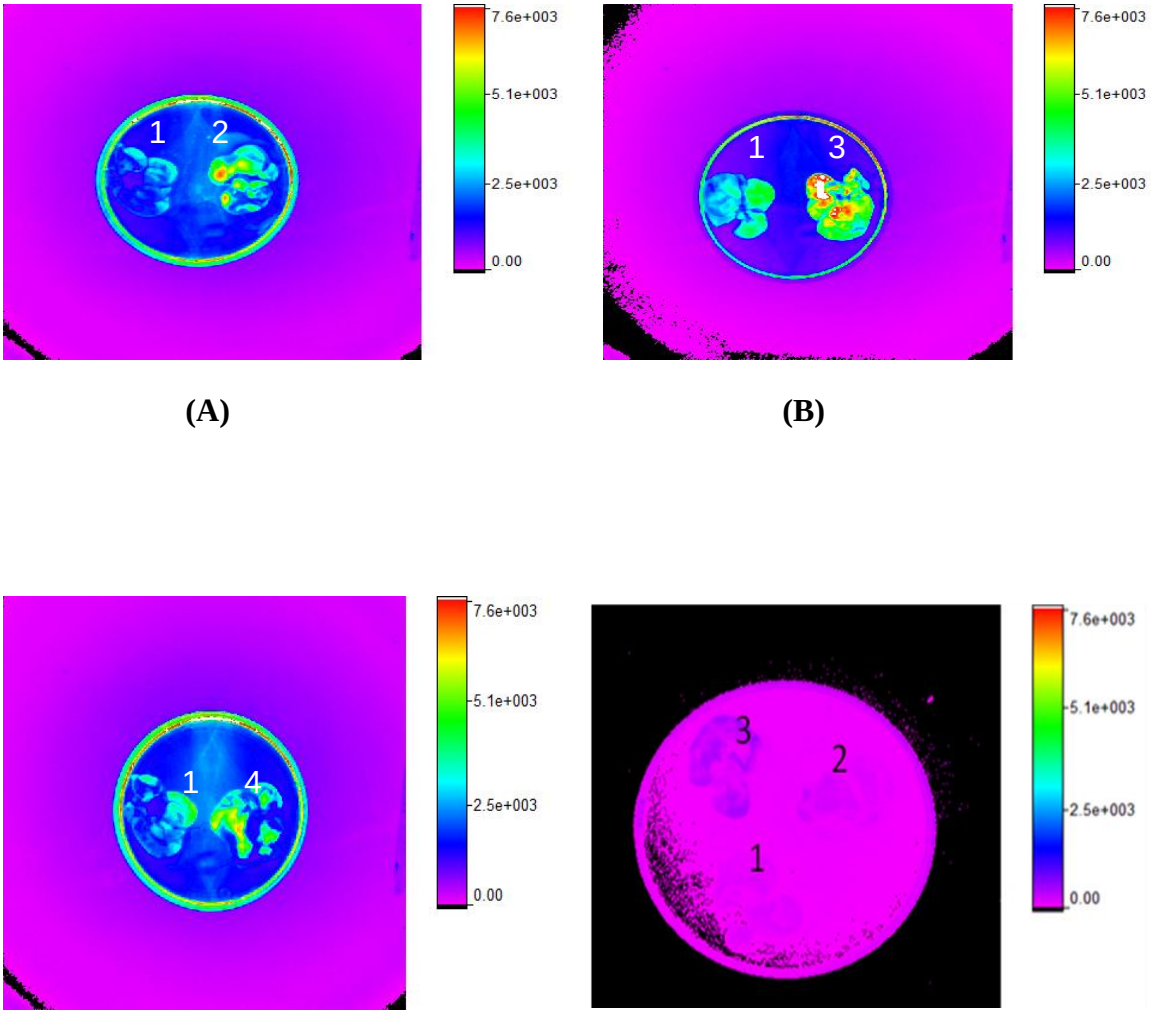

(A) **(B)**

(C) **(D)**

Figure 6.14: *Ex-vivo* imaging of liver from rats administered Rho-BSA coated NP (A-C), or bare NP (D).
A: 1. Rho-BSA conjugate, 2. Rho-BSA GNP;
B. 1. Rho-BSA conjugate, 3. Rho-BSA SNP;
C. 1. Rho-BSA conjugate, 4. Rho-BSA CuNP;
D: 1. GNP, 2. SNP, 3. CuNP

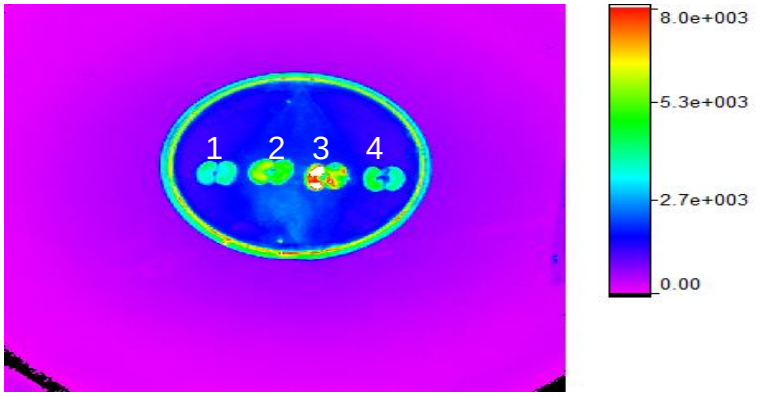

(A)

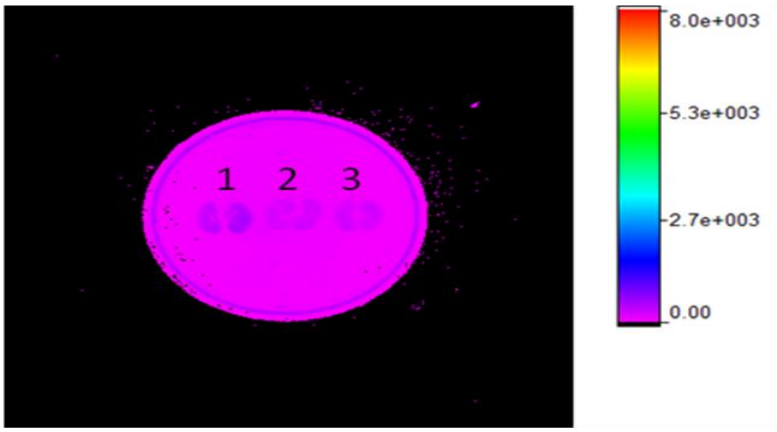

(B)

Figure 6.15: *Ex-vivo* imaging of kidneys from rats administered Rho-BSA coated NP (A), or bare NP (B).
A: 1. Rho- BSA conjugate; 2. Rho-BSA GNP; 3. Rho-BSA SNP; 4. Rho-BSA CuNP
B: 1. GNP; 2. SNP; 3. CuNP

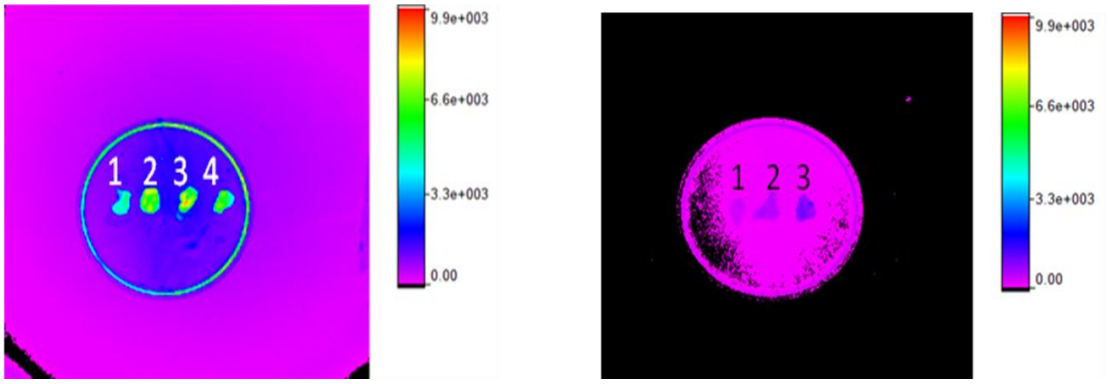

(A) **(B)**

Figure 6.16: *Ex-vivo* imaging of thymus from rats administered Rho-chitosan coated NP (A), or bare NP (B).
A: 1. Rho-chitosan conjugate; 2. Rho-chitosan GNP; 3. Rho-chitosan SNP; 4. Rho-chitosan CuNP. B: 1. GNP; 2. SNP; 3. CuNP

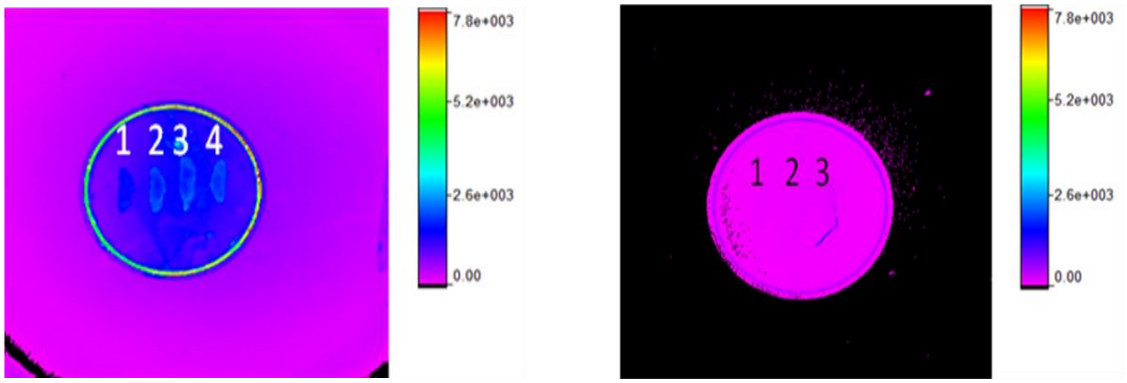

(A) **(B)**

Figure 6.17: *Ex-vivo* imaging of spleen from rats administered Rho-chitosan coated NP (A), or bare NP (B).
A: 1. Rho-chitosan conjugate; 2. Rho-chitosan GNP; 3. Rho-chitosan SNP; 4. Rho-chitosan CuNP. B: 1. GNP; 2. SNP; 3. CuNP

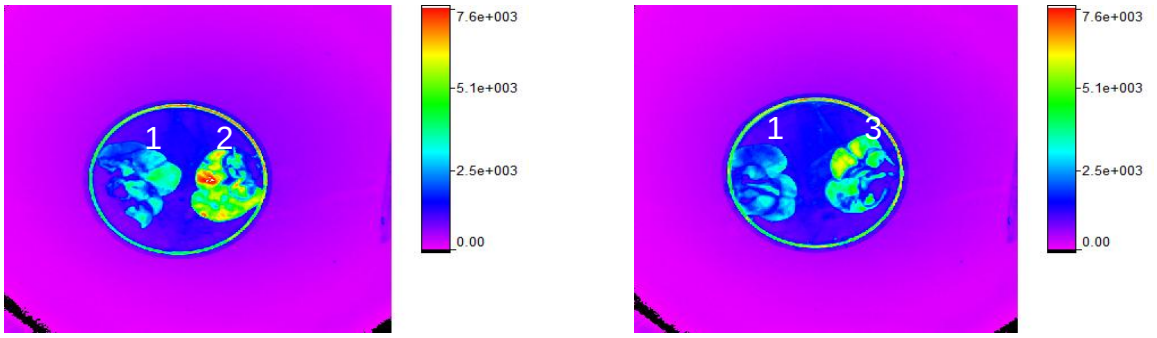

(A) **(B)**

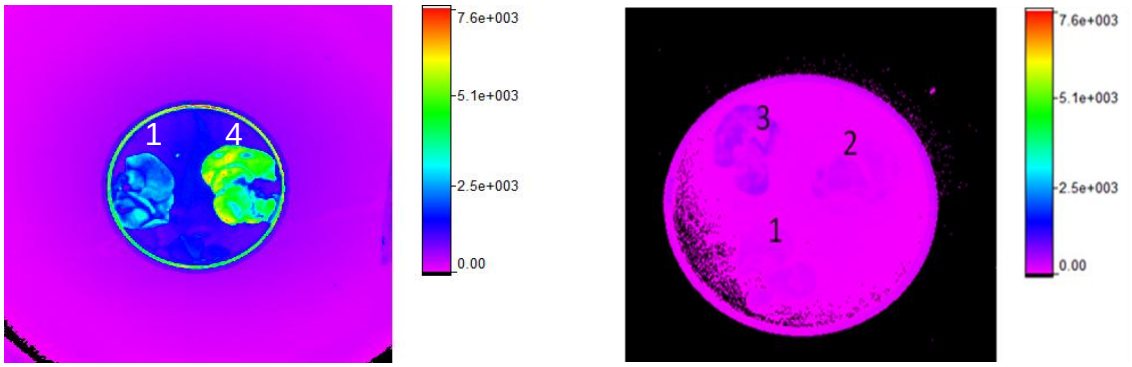

(C) **(D)**

Figure 6.18: *Ex-vivo* imaging of liver from rats administered Rho-chitosan coated NP (A-C), or bare NP (D).
A: 1. Rho-chitosan conjugate, 2. Rho-chitosan GNP;
B: 1 Rho-chitosan conjugate, 3. Rho-chitosan SNP;
C: 1 Rho-chitosan conjugate, 4. Rho-chitosan CuNP
D: 1. GNP, 2. SNP, 3. CuNP

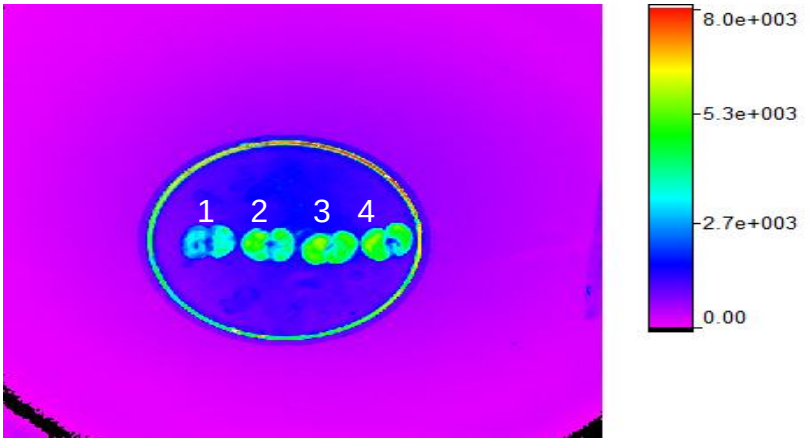

(A)

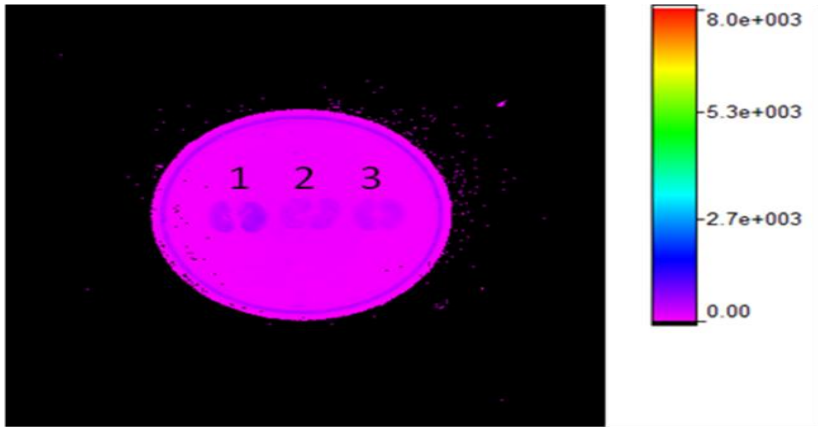

(B)

Figure 6.19: *Ex-vivo* imaging of kidneys from rats administered Rho-chitosan coated NP (A) or bare NP (B).
A: 1. Rho-chitosan conjugate; 2. Rho- chitosan GNP; 3. Rho- chitosan SNP; 4. Rho-chitosan - CuNP
B: 1.GNP, 2.SNP, 3. CuNP

Table 6.2: Fluorescence intensity of rhodamine in different organs from rats administered orally with Rho-BSA conjugate and Rho-BSA coated NP. Computation was carried out using imaging software (Bruker MI). Counts are arbitrary units.

	Rho-BSA	Rho-BSA coated		
		GNP	SNP	CuNP
Organ	Mean Intensity (counts)			
Thymus	503	5165	5550	4878
Spleen	139	2138	2229	1668
Liver	268	3016	8500	2670
Kidney	302	4243	5528	3020

Table 6.3: Fluorescence intensity of rhodamine in different organs from rats administered orally with Rho-chitosan conjugate and Rho-chitosan coated NP. Computation was carried out using imaging software (Bruker MI). Counts are arbitrary units.

	Rho-chitosan	Rho-chitosan coated		
		GNP	SNP	CuNP
Organ	Mean Intensity (counts)			
Thymus	331	3398	3222	2928
Spleen	112	1797	1772	1465
Liver	136	4241	2920	3859
Kidney	78	3505	4023	3613

Discussion

NP based therapeutics are gaining importance in clinical medicine as vehicles for site-specific delivery of drugs. Manipulation of size, surface properties, chemical nature, dose, route of administration, etc., has been experimented to design effective and safe NP delivery systems (Harper et al., 2008). In addition to their therapeutic efficacy, there has been increasing concern about biosafety of NP. After *in vivo* delivery of NP, biodistribution and biopersistence are important factors which determine biocompatibility or toxicity (De Jong and Borm, 2008). NP as drug delivery vehicles have been administered via several routes – intravenous, subcutaneous, oral, intra-peritoneal, intra-tracheal, etc., (Kang et al., 2015). Each one of routes mentioned has its advantages and disadvantages. But, oral route for drug delivery has been preferred for non-invasive and ease of administration (Yun et al., 2013). The major disadvantages for oral delivery are – absorption, size limitation and stability of NP in the gastro-intestinal tract (Bakhru et al., 2013). Majority of the studies reported have been carried out using intravenous route of administration of NP (Lin et al., 2015). A few studies have been conducted using oral route (Fröhlich and Roblegg, 2016).

Different techniques have been used for the localization of metallic NP in tissues, cells and sub-cellular compartments. TEM has been used for quantification of the biodistribution of silica and titanium dioxide NP (Tsutsumi et al., 2011). But, ICP-MS provides quantitative measurement of elements released as a result of dissolution of NP (Alger et al., 2014). Among various techniques, one which is cost-effective and allows visualization of NP ex-*vivo* is preferred (Ostrowski et al., 2015). Due to high sensitivity and resolution, fluorescence imaging has become a powerful technique when compared to other imaging modalities. Small organic fluorescent probes have been used to study *in vivo* and *ex-vivo* distribution of nanocolloids in small laboratory animals (Milankovic, 2012). Rhodamine derivatives have been evaluated as fluorescent probes for *in vivo* imaging applications (Terai and Nagano et al., 2008). In the present experiments, biodistribution of Rho- BSA and Rho-chitosan coated metallic NP was attempted 24 hours following oral administration.

In the present study, Rho-BSA/chitosan conjugated GNP/SNP/CuNP showed localization in thymus, spleen, liver and kidney following oral administration. Fluorescence intensity was higher (10 fold or more) with conjugates coated NP compared

to that observed with soluble conjugate. Highest fluorescence intensity was observed in thymus followed by kidney, liver and spleen with Rho-BSA or Rho-chitosan coated NP.

PEG-coated GNP have been shown to be localized in liver, spleen, kidney etc., following oral administration of a single dose of GNP (Hinkley et al., 2015). Identification of NP has been carried out using TEM as well as ICP-MS. Uncoated GNP showed significant agglomeration resulting in poor uptake compared to PEG-coated GNP (Hinkley et al., 2015). Hence, it is important to note that coating of NP is essential to prevent aggregation in the gastro-intestinal tract. Persorption and tissue distribution of GNP has been demonstrated using TEM and instrumental neutron activation analysis following oral administration (Hillier and Albrecht, 2001). Poor uptake of GNP and localization in tissues has been reported following oral dosage using dual radiolabelled particles (Rambanpasi et al., 2015). Various methods to evaluate the uptake of engineered nanomaterials by the alimentary tract has been reported (Alger et al., 2014). Accumulation of SNP in liver, kidney, spleen etc., has been demonstrated using ICP-MS in rats following oral treatment for 28 days (Van der Zande et al., 2012). Distribution of SNP in different organs following a 28 day oral exposure has been reported (Loeschner et al., 2011). SNP have been shown to be deposited in liver and kidney using laser ablation-ICP-MS imaging technique following oral exposure to rats (Jimenez-Lamana et al., 2014). Accumulation of CuNP in liver, kidney, spleen etc., has been shown following oral administration to mice (Chen et al., 2006). Presence of CuNP was carried out using TEM and atomic force microscopy. Comparative toxicity and biodistribution of CuNP and cupric ions given orally in a rat model has recently been reported (Lee et al., 2016).

All the studies mentioned above made use of techniques which involves elaborate sample preparation involving tissue disruption and expensive equipment. In this context, NIR imaging attempted in the present studies are a novel approach wherein the tissue is examined intact using no treatment. It offers a direct visualization of the fluorophore associated with the NP.

Milankovic (2012) has reported biodistribution of rhodamine conjugated covalently to solid polymer (polylactate-Polyglycolate) NP using confocal microscopy. In these studies, imaging was carried out *ex-vivo* after cryo-sectioning. In the present work, highly sensitive *in vivo* imaging system equipped with a CCD camera which has a very

low photon detection limit is used. The technique employed in the present experiments is simple with no requirement for sample processing. It allows for repeat image capturing on frozen specimens at a later date. The method adopted not only gives qualitative information in terms of images, but also permits computation of fluorescence intensity associated with the tissue for comparative analysis.

The results of the study strongly suggest that all three metallic NP localize to the lymphoid organs – thymus and spleen. This is the first report which demonstrates accumulation of NP in the primary lymphoid organ, thymus. Also, moderate localization has been observed in spleen. As reported in other studies using different methodology, NP localization was seen in liver and kidney.

The salient findings of the experiments presented in this chapter are:

1) Rho-BSA and Rho-chitosan coated GNP/SNP/CuNP were prepared and characterized for their suitability as fluorescent probes for *in vivo* use.

2) *Ex-vivo* imaging of liver, kidney, spleen and thymus showed significant localization of fluorescent NP compared to soluble conjugate (24 hours following oral administration at a dose of 1 mg / Kg body weight in a rat model)

3) Quantitative analysis revealed that the fluorescence intensity associated with coated NP distributed in all tissues studied was at least 10 fold higher than that with soluble conjugates.

4) Results show significant localization of metallic NP in lymphoid organs – thymus and spleen apart from other important organs- liver and kidney

Chapter 7

Effect of metallic NP on proliferative response and cytokine production of rat splenic and thymic lymphocytes: *in vivo* study

Introduction

Several *in vitro* cell culture systems have been employed to carry out preliminary evaluation of biological effects and putative toxicity of metallic NP. However, results obtained in such studies require verification using *in vivo* evaluation. Results of experiments presented in Chapter 4 strongly indicated that all three metallic NP inhibited mitogen-induced lymphocyte activation *in vitro*, whereas the three biological NP tested had no effect. Further, results of *ex-vivo* fluorescence imaging of tissues following oral administration of metallic NP showed localization of metallic NP in liver, kidney, spleen and thymus (Chapter 6). Based on these results, mitogen-induced proliferative responses of lymphocytes from spleen and thymus, secretion of certain cytokines by mitogen activated splenic lymphocytes has been carried out after oral administration of GNP/SNP/CuNP.

Studies on NP using *in vivo* systems would provide information on their biodistribution, pharmaco-kinetics, metabolism, biopersistence, biological effects. *In vivo* studies are also important to understand the relation between physico-chemical properties of NP and their toxicological effects on biological system (Fischer and Chan, 2007). Prior to use of NP based products in humans, detailed assessment of their toxicological properties and biological behavior is mandatory (Fadeel and Garcia-Bennett, 2010). Biodistribution and biological effects of NP depend not only on their physico-chemical properties but also on dose, duration of exposure and route of administration (Khlebtsov and Dykman, 2011). Majority of published studies using experimental animals have reported administration of NP via intravenous, intraperitoneal and respiratory routes (Abdelhalim, 2013; Vandebriel et al., 2014; Adamcakova-Dodd et al., 2015). A few studies have used oral route of administration (Hadrup et al., 2016). Non-invasive nature and ease of administration makes oral route a preferred method. Large surface area, presence of microfold cells (M cells) in Peyer's patches and sticky mucus lining of intestine are some important factors favorable for oral administration of NP (Gamboa and Leong, 2013).

After persorption from gastro-intestinal tract, NP will enter systemic circulation and are localized in different organs / tissues (Chapter 6). NP present in the lymphoid organs interacts with immune cells present in various tissues such as spleen and thymus. Interaction of the NP may lead to their clearance and /or modulation of the immune

system. Only a few studies reported the function of immune cells following *in vivo* administration of NP (Chen et al., 2010; Park et al., 2016).

In the present experiments, GNP/ SNP/CuNP were administered orally to rats for 14 days using selected dosage and immune function of splenic and thymic lymphocytes was assessed in terms of mitogen induced proliferative response and cytokine secretion.

Methods

Animals

Female wistar rats, 6 weeks of age were obtained from National Center for Laboratory Animal sciences, National Institute of Nutrition, Hyderabad. Rats were acclimatized for 3 days in Animal facility of University of Hyderabad.

Experimental groups and dosage

Rats were randomly distributed into one experimental group for each dose of metallic NP and one control group. Each group consisted of 4-5 animals. All rats were housed in individual cages and were fed standard pelleted diet and water *ad libitum* during the experimental period. Doses of metallic NP administered are given below:

GNP: 500 µg, 2 mg / Kg body weight
SNP: 500 µg, 2 mg, and 10 mg / Kg body weight
CuNP: 2 mg, 10 mg / Kg body weight

Oral administration of NP and experimental schedule

GNP, Rats were fasted over night prior to NP administration. Amount of NP to be administered was calculated based on body weight of each rat and was taken in a volume of 0.20 ml. Control rats received 0.20 ml of phosphate buffered saline, pH 7.40. NP were given orally, daily at 9 A.M. using a syringe fitted with an oral gavage needle. NP were administered daily for 14 days. Body weight of the rats was measured for every 3 days using an electronic weighing scale. Weight gain during the experimental period was calculated by deducting initial weight (day 1) from final weight (day 14).

Proliferative response of rat splenic and thymic lymphocytes

Rats were euthanized and spleen and thymus were collected aseptically. Single cell suspension of the lymphocytes was prepared following the method described in Chapter 2. Lymphocyte-rich preparations were incubated with B or T-cell specific mitogens and ^{3}H-thymidine incorporation into DNA was determined as described in Chapter 2. Results were expressed as stimulation index:

Stimulation index (SI) = Average cpm in presence of mitogen /Average cpm with cells only

Estimation of cytokines in culture supernatant of mitogen stimulated lymphocytes

Splenic lymphocytes were incubated with T-cell mitogen at the concentration of 5µg/ml for 72 hours. After 72 hours, the supernatants were collected and TNF-alpha, IFN-gamma, IL-2 and IL-4 levels were estimated by ELISA method as described in Chapter 2.

Statistical analysis

One-way analysis of variance followed by post-hoc Tukey test was done using Sigma plot software as described in Chapter 2.

Results

Effect of metallic NP on the body weight of rats

Body weight gain of rats that received GNP, SNP and CuNP orally is presented in Tables 7.1-7.3 respectively. Body weight gain of rats that received different doses of NP was similar to control group.

Proliferative response of splenic and thymic lymphocytes and cytokine concentrations from rats that received metallic NP orally

GNP

Proliferative response of splenic lymphocytes to LPS and Con A is presented in Figure 7.1(A&B). Response was significantly decreased with both the mitogens at 500 µg and 2 mg GNP per Kg body weight ($p < 0.05$). Proliferative response of thymic lymphocytes stimulated by Con A was also significantly diminished (Figure 7.1, C). Cytokine concentrations were determined using supernatants of Con A stimulated splenic

lymphocytes obtained from rats administered 2 mg GNP/ Kg body weight. TNF-alpha, IFN- gamma and IL-2 concentrations were significantly diminished compared to control group (Figure 7.2 A-C). However, IL-4 concentration was similar compared to controls (Figure 7.2, D).

SNP

Proliferative response of splenic and thymic lymphocytes from rats administered SNP at 500 µg, 2 mg and 10 mg / Kg body weight are presented in Figure 7.3. LPS and Con A stimulated responses were significantly inhibited in lymphocytes from all three SNP fed groups compared to controls (A & B). Con A stimulated thymocyte proliferation was also inhibited (Figure 7.3 – C). Cytokine concentrations were determined in supernatants of Con A stimulated splenic lymphocytes obtained from rats that were given 10 mg SNP / Kg body weight. TNF-alpha and IL-2 concentrations were significantly reduced compared to controls (Figure 7.4- A & C). Interferon-gamma and IL-4 levels were similar to those of controls (Figure 7.4- B & D).

CuNP

Splenic and thymic lymphocyte proliferative responses induced by LPS and Con A were significantly lower in CuNP administered groups (2 mg and 10 mg / Kg body weight) compared to control group (Figure 7.5- A-C). Concentration of TNF- alpha and IL-2 were significantly low in CuNP treated group compared to controls (Figure 7.6- A &C). IL-4 concentration was similar to that of controls (Figure 7.6- D). However, Interferon-gamma concentration was significantly elevated compared to controls (Figure 7.6- B).

Table 7.1: Oral administration of GNP to rats- effect on body weight

Treatment group	Initial (g)	Final (g)	Weight gain (g)
Control	128 ± 3	150 ± 3	21 ± 2
GNP- 500 µg / kg	131 ± 6	151 ± 7	20 ± 2
GNP - 2mg / kg	132 ± 2	152 ± 3	20 ± 3

Values presented are mean ±SEM of 5 rats

Table 7.2: Oral administration of SNP to rats- effect on body weight

Treatment group	Initial (g)	Final (g)	Weight gain (g)
Control	124 ± 3	144 ± 3	20 ± 2
SNP - 500µg / kg	118 ± 8	142 ± 11	24 ± 3
SNP - 2mg / kg	123 ± 6	143 ± 8	20 ± 3
SNP - 10mg / kg	107 ± 9	125 ± 9	18 ± 2

Values presented are mean ± SEM of 5 rats

Table 7.3: Oral administration of CuNP to rats- effect on body weight

Treatment group	Initial (g)	Final (g)	Weight gain (g)
Control	128 ± 3	147 ± 3	19 ± 2
CuNP - 2mg / kg	123 ± 3	143 ± 4	20 ± 3
CuNP - 10mg /kg	122 ± 2	140 ± 3	18 ± 2

Values presented are mean ± SEM of 5 rats.

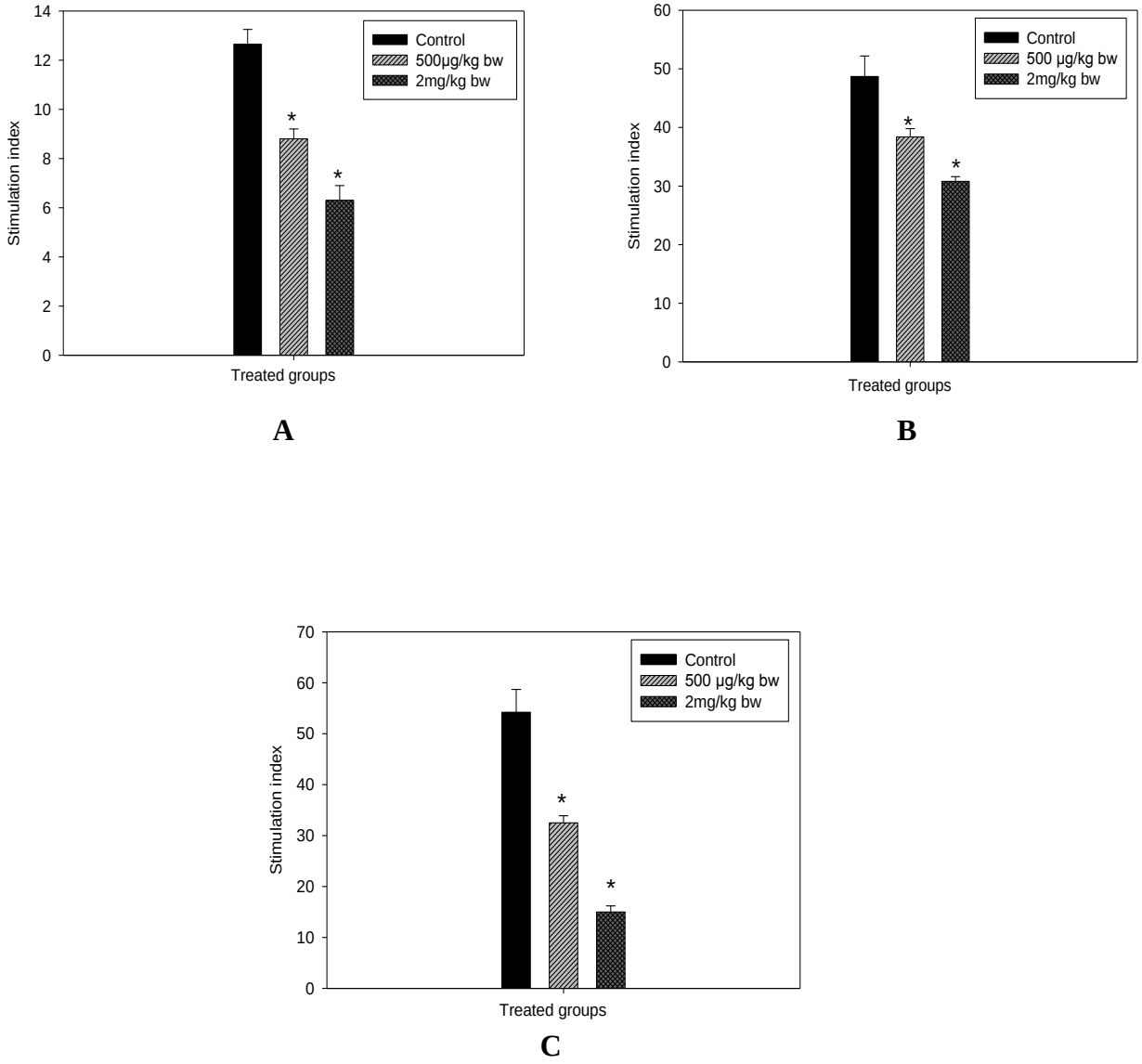

Figure 7.1: Mitogen stimulated proliferative response of splenic and thymic lymphocytes obtained from GNP administered rats: A) Splenic lymphocytes + LPS (50µg/ml); B) Splenic lymphocytes + Con A (5µg/ml); C) Thymic lymphocytes + Con A (5µg/ml). Data presented are mean ± SEM of 5 experiments. * p<0.05, treated vs. control.

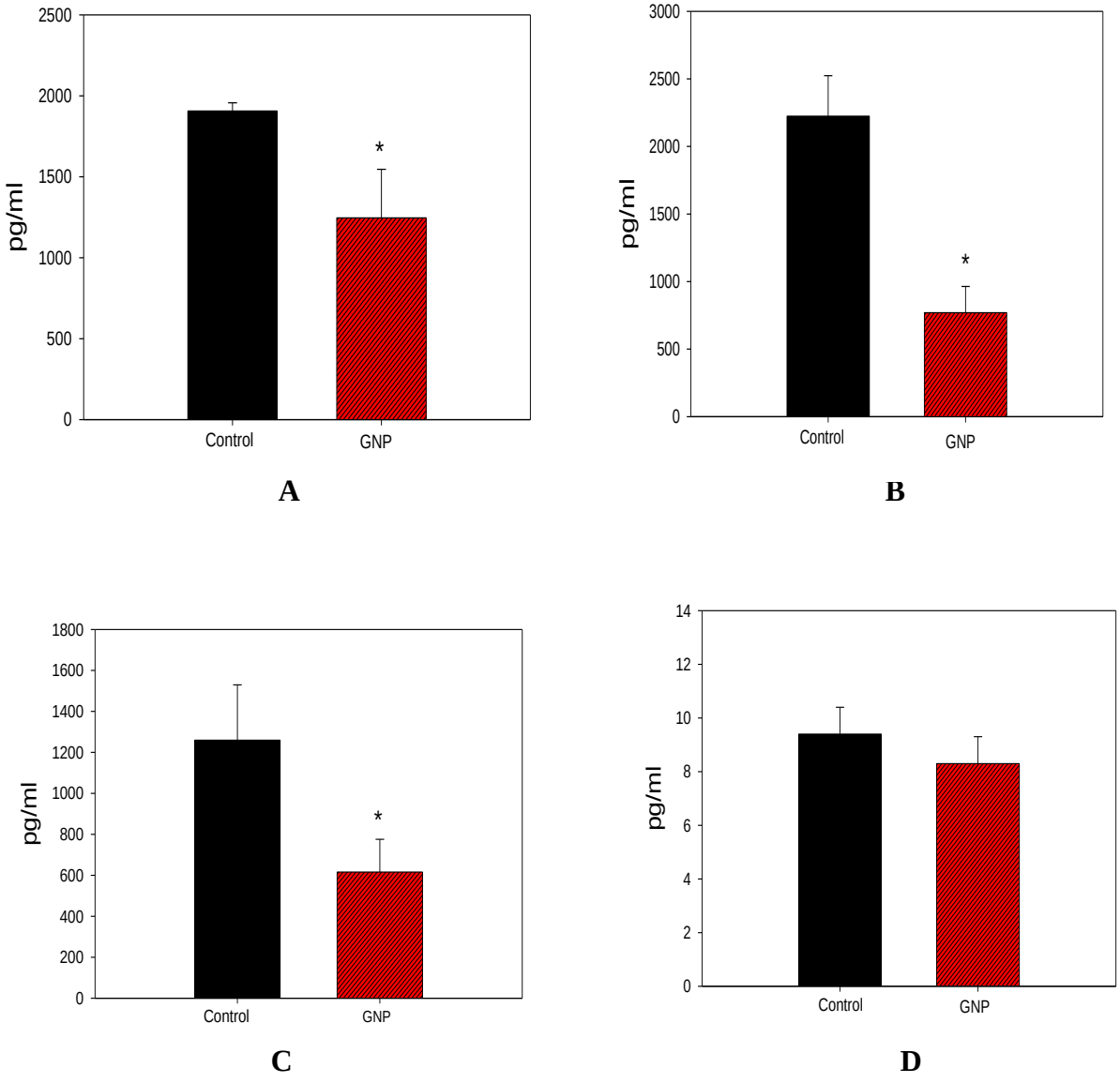

Figure 7.2: Cytokine concentration in culture supernatant of Con A stimulated splenic lymphocytes from GNP (2mg /Kg) administered rats: A) TNF – Alpha; B) IFN – gamma; C) IL-2; and D) IL-4. Data presented are mean ± SEM of 3 experiments. * p <0.05, treated vs. control.

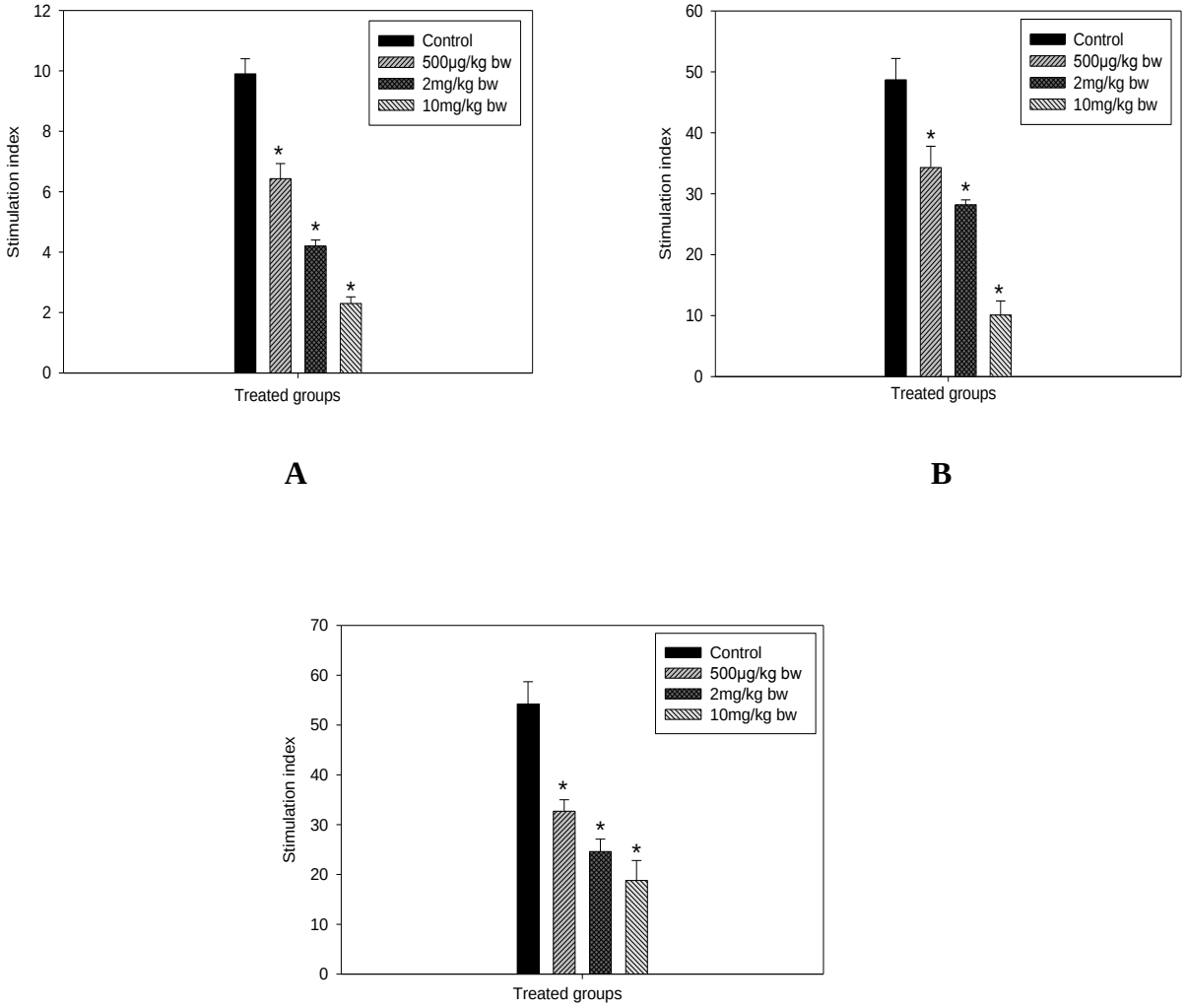

Figure 7.3: Mitogen stimulated proliferative response of splenic and thymic lymphocytes obtained from SNP administered rats: A) Splenic lymphocytes + LPS (50µg/ml); B) Splenic lymphocytes + Con A (5µg/ml); C) Thymic lymphocytes + Con A (5µg/ml). Data presented are mean ± SEM of 5 experiments. * p< 0.05, treated vs. control.

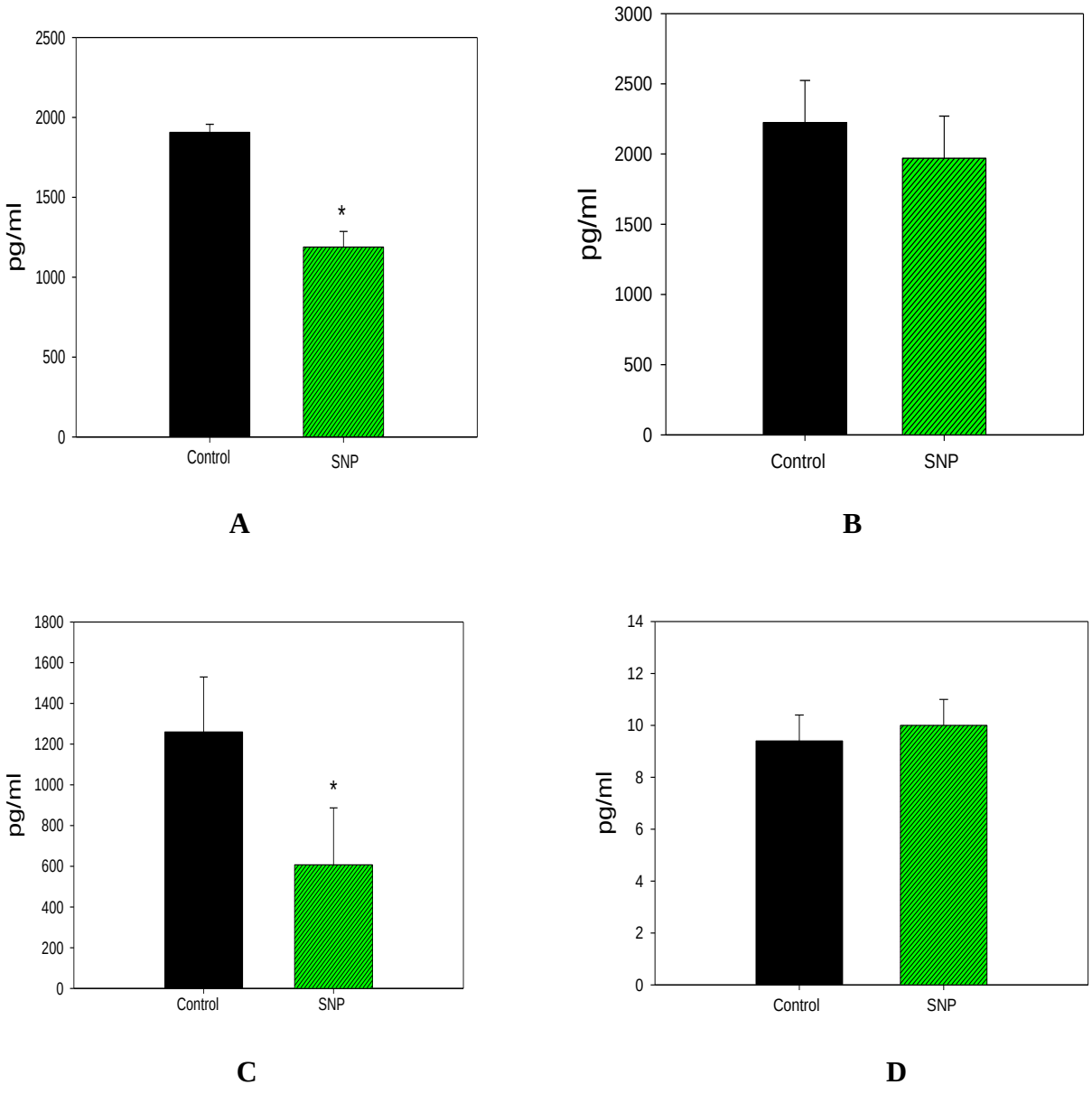

Figure 7.4: Cytokine concentration in culture supernatant of Con A stimulated splenic lymphocytes from SNP (10 mg/Kg) administered rats: A) TNF – Alpha; B) IFN – gamma; C) IL-2; and D) IL-4. Data presented are mean ± SEM of 3 experiments. * $p < 0.05$, treated vs. control.

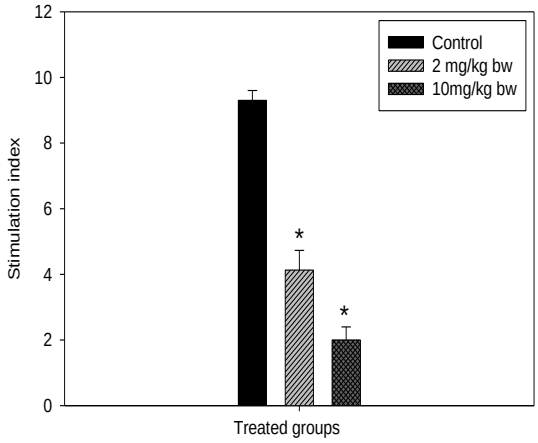

A

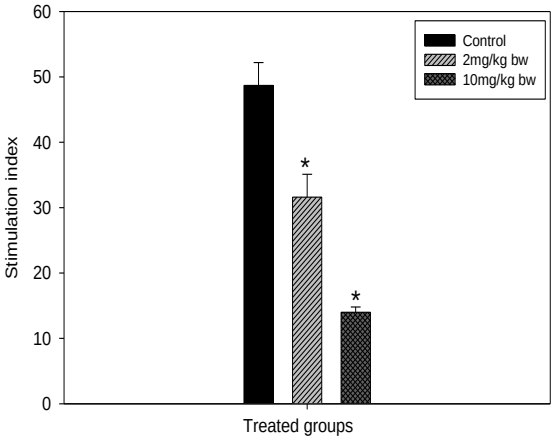

B

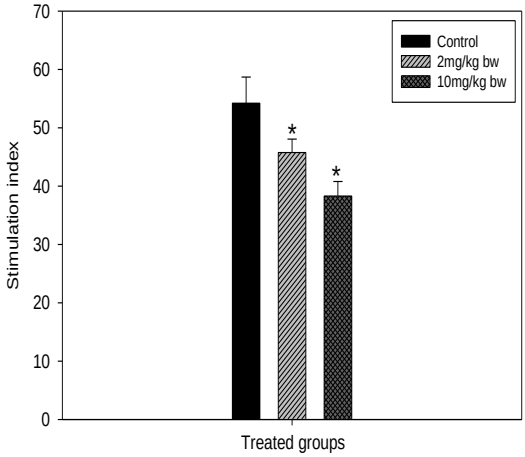

C

Figure 7.5: Mitogen stimulated proliferative response of splenic and thymic lymphocytes obtained from CuNP administered rats: A) Splenic lymphocytes + LPS (50µg/ml); B) Splenic lymphocytes + Con A (5µg/ml); C) Thymic lymphocytes + Con A (5µg/ml). Data presented are mean ± SEM of 5 experiments. * $p<0.05$, treated vs. control.

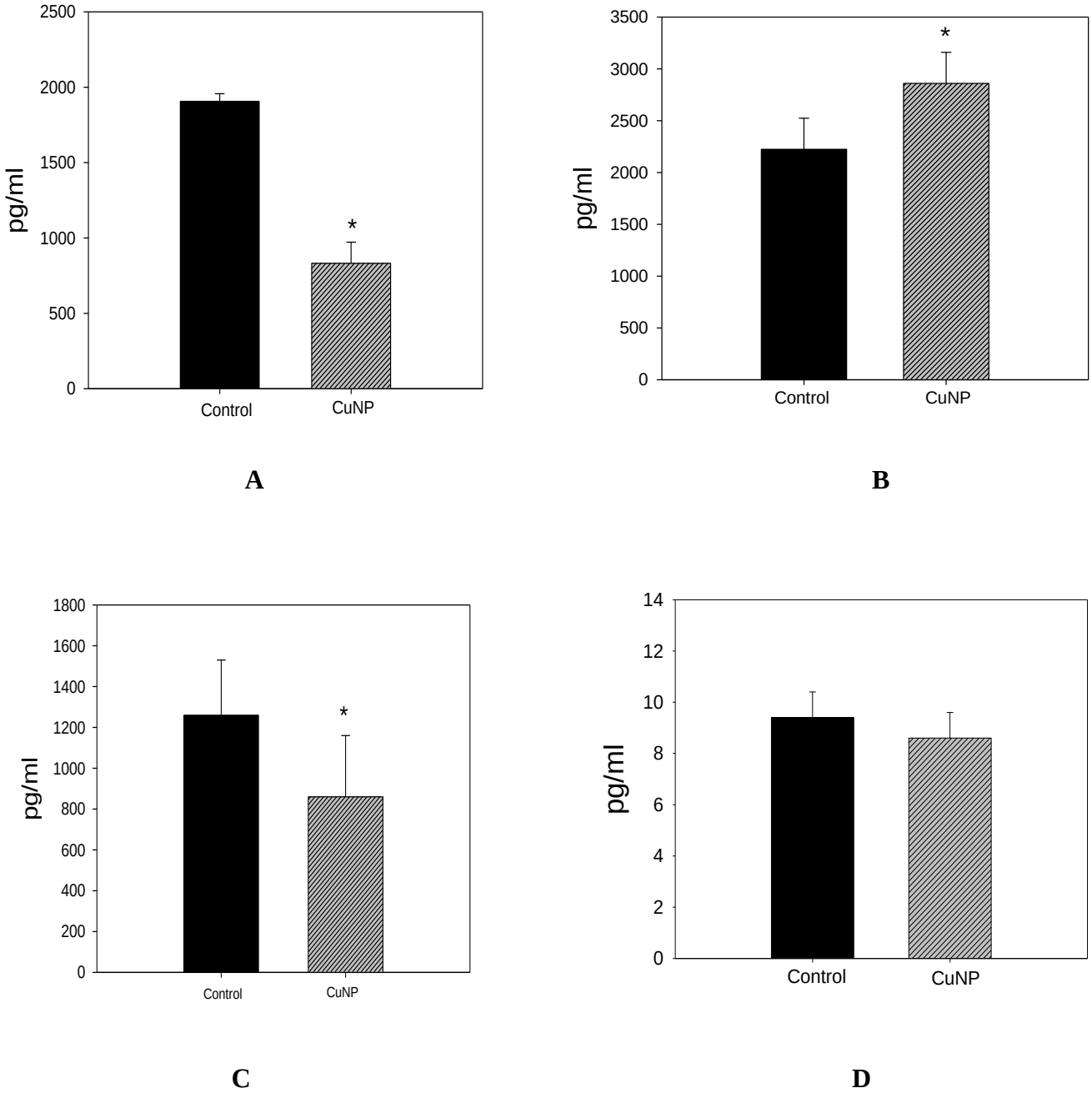

Figure 7.6: Cytokine concentration in culture supernatant of Con A stimulated splenic lymphocytes from CuNP (10mg / Kg) administered rats: A) TNF – Alpha; B) IFN – gamma; C) IL-2; and D) IL-4. Data presented are mean ± SEM of 3 experiments. * $p < 0.05$, treated vs. control.

Discussion

Following *in vivo* administration of NP, biodistribution and biopersistence will determine the biological effects or toxicity mediated by them. Route of administration, dosage, size, surface properties of NP etc., play an important role in the tissue localization and clearance. Due to non-degradability, persistence of metallic NP in tissues can be anticipated. Hence, assessment of functional changes that occur due to continued presence of metallic NP in lymphoid organs needs to be investigated.

The *in vitro* experiments presented in Chapter 4 revealed that metallic NP inhibited proliferative response of B and T lymphocytes. *Ex-vivo* imaging data presented in Chapter 6 also revealed that upon oral administration, metallic NP were probably absorbed / persorbed from gastrointestinal tract and were distributed to various organs such as thymus, spleen, liver and kidneys. Based on these observations, effect of metallic NP *in vivo* on lymphocyte activation has been investigated. Some of the studies reported earlier on *in vivo* effects of metallic NP on immune cells are described below.

Toxicological effects and biokinetics of GNP administered by different routes in a mouse model has been reported (Zhang et al., 2010). Results of this study showed that low dose of GNP was non-toxic, but high doses of GNP (2.2 mg/ Kg body wt) administered by oral and intraperitoneal routes caused moderate decrease in body weight, changes in hematocrit and spleen index compared with controls. In a study using a mouse model, 13 nm size GNP were administered intraperitoneally at doses of 40, 200 and 400 µg / Kg body wt / day. Accumulation of GNP was noted in tissues such as liver, kidney, spleen etc., but no toxicity was observed in terms of survival, effect on body weight, organ morphology, tissue histology, blood biochemistry etc. (Lasagna-Reeves et al., 2010). Biodistribution and toxicity of several types of engineered GNP administered via different routes has been reviewed in detail (Khlebtsov and Dykman, 2010). BSA and PEG capped GNP injected to mice via tail vein daily for 8 day period showed accumulation in liver as analyzed by TEM, but no toxicity was detected (Lien Nghiem et al., 2012). Size and charge dependent homing of radiolabeled GNP to liver, spleen and other tissues after intestinal absorption following oral exposure has been demonstrated (Schleh et al., 2012). Accumulation of GNP has been shown in lymphoid follicles of mesenteric lymph nodes of

rats that were given NP via oral route (Zlobina et al., 2013). Enhanced activity of phagocytes and increase in percentage of T and B lymphocytes in peripheral blood of mice following oral administration of commercial preparation of GNP (5 nm) has been reported (Malaczewska, 2015a). Comprehensive toxicological risk assessment of elemental gold has recently been reviewed (Hadrup et al., 2015).

Alterations in morphology of lymphoid organs following oral administration of 5, 15 and 50 nm size GNP at 190 µg / Kg body wt for 15 days in a rat model has been reported (Bucharskaya et al., 2016a). Results of this study suggested that GNP induces an immune activation in peripheral lymph nodes in terms of migration, proliferation and differentiation of immune cells based on histochemical analysis. Another recent study reported dystrophic and necrobiotic changes in liver, kidney and spleen with 50 nm size GNP, whereas 2 nm GNP were immunostimulatory (Bucharskaya et al., 2016b).

A few studies have been reported on *in vivo* effects of SNP on immune system by oral route. It has been demonstrated that ingestion of SNP at a dose of 2.5 mg for 3 days caused non-specific medullary congestion of spleen (Cha et al., 2008). Oral administration of SNP to mice for 28 days increased the levels of cytokines, IL-1, IL-6, IL-10, IL-12 and TGF-beta. In addition, B cell distribution and IgE levels were also increased (Park et al., 2010). No effect on the serum Ig levels, lymphocyte proliferation and cytokine production of mitogen stimulated B and T lymphocytes from spleen was observed in rats that were given SNP orally (Van Der Zande et al., 2012). In contrast, it has been reported that following intravenous administration of SNP for 28 days lowered natural killer cell activity and cytokine production by mitogen activated lymphocytes of spleen (De Jong et al., 2013). Intravenous administration SNP has been shown to suppress T-cell dependent antibody response to keyhole limpet hemocyanin (Vandebriel et al., 2014).

Oral administration of high doses of CuNP (1 g / Kg body wt) to mice has been shown to results in gross changes in cellular architecture of liver, spleen and kidney as assessed by tissue morphology and cell histology (Chen et al 2006). Further, it has also been demonstrated that cupric ions may be released from CuNP and are responsible for the toxicity via generation of reactive oxygen species (Chen et al., 2007; Meng et al., 2007). A recent study reported *in vivo* effects of CuNP administered orally to rats as a single dose

as well as repeated doses at concentration ranging from 312 mg to 2500 mg / kg body weight (Lee et al., 2016). Gross morphological and biochemical changes in liver, spleen, kidney etc., were observed in this study.

Intraperitoneal administration of GNP 785µg/ 100g body wt to mice has been shown to reduce the levels of TNFα and IL-6 in adipose tissue (Chen et al., 2013b). GNP at a dose of 2.5 ppm administered orally to mice for 1/2/4 week period resulted in significant reduction in synthesis of IL-1β, IL-6 and TNF-α, while at 0.25 and 25 ppm doses, a stimulatory response was observed (Malaczewska, 2015b). However, IL- 2 secretion was modulated at all doses. Apart from oxidative stress and DNA damage, cytokine induction was considered as one of the mechanism of SNP induced toxicity (Stensberg et al., 2011). Serum levels of IL-1β, IL-6 and TNF-α were increased, whereas IL-12 levels were decreased following oral SNP treatment of mice at doses of 0.25, 2.5 and 25 ppm to mice (Malaczewska, 2011). Elevated levels of IL-6, IL-12 and TNF-α were observed in lavage fluid obtained from mice exposed to CuNP compared to controls (Kim et al., 2011). All the above mentioned studies indicate modulation of cytokine secretion by immune cells of metallic NP treated experimental animals.

Results of present studies using two doses of GNP demonstrated that the mitogen induced proliferative response of thymocytes as well as splenic lymphocytes is reduced significantly. Further, the effect observed was dose-dependent. The cytokines (TNF-alpha, IFN-gamma and IL-2) secretions of stimulated splenic lymphocytes were decreased significantly in the GNP treated groups, when compared with controls, indicated the GNP anti-inflammatory activity. It can be surmised that GNP accumulated in the lymphoid tissues and has brought about the changes observed. In the present *in vivo* study, SNP was administered at three doses – 0.50, 2.0 and 10mg / kg body weight by oral route for 14 days. Body weight gain of SNP administered rats was similar to controls. A few other studies have also shown that body weight was unaffected upon oral administration of SNP (Kim et al., 2010; Hadrup et al., 2012b; Park et al., 2010). Splenic and thymic lymphocytes proliferative response in the presence of mitogens was significantly diminished in a dose- dependent manner. Further, TNF-alpha and IL-2 levels were significantly decreased compared to controls indicating an impairment of T cell function. In the present study, CuNP had shown no effect on the body weight of rats. Proliferative

response of the splenic and thymic lymphocytes was significantly decreased in the CuNP treated groups when compared with control group. Secretion of cytokines (TNF-alpha and IL-2) was decreased significantly in CuNP treated groups when compared with control group. However, in CuNP treated group, interferon-gamma was significantly elevated suggesting a pro-inflammatory response.

The mechanism by which metallic NP have inhibited lymphocyte activation *in vivo* is not clear. It is surmised that as the lymphocytes do not internalize the NP, they get accumulated in the extracellular matrix; this might lead to "intercellular stress". Induction of "intracellular stress" in the endoplasmic reticulum has been documented with respect to NP (Noel et al., 2012; Huo, et al, 2015). However, evidence for extracellular stress is scanty (Barua and Mitragotri, 2014; Durymanov et al., 2015). Hence, further experiments are required to address this issue.

The salient findings of the experiments reported in this chapter are:

1) Growth of rats (body weight gain) which received metallic NP orally was not affected at all doses administered
2) Mitogen stimulated splenic and thymic lymphocyte proliferative response was lowered significantly in metallic NP administered rats at all doses compared to controls.
3) Alterations in cytokine production by mitogen activated splenic lymphocytes from metallic NP administered rats suggest modulation of T cell differentiation.
4) The above observation suggests inhibition of lymphocyte activation by metallic NP due to their persistence in the extracellular matrix of spleen and thymus.

Chapter 8

Evaluation of biochemical markers for assessment of possible tissue toxicity following oral administration of metallic NP

Introduction

Exposure of human beings to NP can occur through environment, consumer food products and as a part of medical applications (Malysheva et al., 2015). After gaining entry into body, NP are carried to different body organs via the circulatory and lymphatic system. Although some NP are eliminated, remaining may persist in the body for a long time which may lead to disturbances in cell / tissue / organ function (Zhang et al., 2014). *In vivo* administration of NP for therapeutic use can sometimes result in off-target accumulation, there by not only lowering their diagnostic and therapeutic index, but also causes adverse effects such as inflammation, hepato-toxicity, nephron-toxicity, immunogenicity, altered protein and gene expression etc. (Kanasty et al., 2012; Yildirimer et al., 2011, De Jong and Borm, 2008).

Elevated levels of alanine aminotransferase (ALT) and aspartate aminotransferase (AST) have been reported in mice (fed on a methionine and choline deficient diet) administered intravenously with GNP (Hwang et al., 2012).Administration of GNP to Sprague-Dawley rats for 7 weeks followed by 14 day washout period, showed no significant change in serum markers of liver and kidney (Rambanapasi et al., 2016). Intra-peritoneal administration of GNP for 3 days to wistar- kyoto rats resulted in increase in serum AST and ALT with no significant change in urea and createnine (Abdelhalim and Abdelmottaleb Moussa, 2013). Oral administration of GNP and SNP to wistar rats for 21 days has been shown to cause increase in blood urea and serum transaminase activity (Rathore et al., 2014). Subcutaneous injection of albumin stabilized SNP to mice showed no significant changes in serum enzymes, urea and creatinine levels (Chakraborty et al., 2016). Oral administration of SNP to male Sprague-Dawley rats resulted no significant changes in ALT, AST and ALP activity in serum (Pourhamzeh et al., 2016). In a similar study, SNP given orally to Sprague-Dawley rats for two weeks did not bring about any significant change in the levels of ALP, AST and ALP (Kulthong et al., 2012).

Oral administration of CuNP to mice resulted in significant increase in levels of creatinine and ALP when compared to untreated controls (Chen et al., 2006). Significantly higher level of ALT and AST were observed in rats that received CuONP (Doudi and Setorki, 2015). All the studies mentioned indicate that oral administration of metallic NP may bring about changes in liver and kidney function. In majority of studies, only one NP

has been used. In the present experiments, effect of GNP, SNP and CuNP on liver and kidney function was evaluated using ALP, ALT, AST, creatinine and urea as biochemical markers.

Methods

ALP assay

Enzyme activity was determined using p- nitrophenyl phosphate (p-NPP) as substrate at alkaline pH (Bessey et al., 1946).

Principle

ALP catalyzes release of p-nitrophenol (p-NP) from p-NPP. Absorbance of p-NP at 405 nm was measured and a molar extinction coefficient of 18,000 $M^{-1}cm^{-1}$ was used to calculate the amount of p-NP. Formation of 1µmole p-NP/minute is taken as 1 International Unit (IU) of enzyme activity.

$$\text{p-nitrophenyl phosphate} + H_2O \xrightarrow[Mg^{2+}]{\text{ALP}} \text{p-nitrophenol} + \text{phosphate}$$

Reagents

1. 0.1 M bicarbonate buffer, pH9.8
2. p- NPP, 1 mg / ml in bicarbonate buffer
3. 1 M NaOH

Procedure

Plasma was prepared from whole blood containing citrate as an anticoagulant by centrifugation at 2000 x g for 10 minutes. A plasma volume of 40µl from control, GNP, SNP and CuNP groups was added to micro-titer plate wells in triplicate. 150µl of p-NPP (2mg/ml in 0.1M bicarbonate buffer, pH 9.8) was added to plasma and incubated for 30 minutes at 37ºC. 10µl of NaOH (1 N) was added to stop the reaction and absorbance was measured at 405nm using a microplate reader. Amount of p-NP was calculated from a standard graph.

ALT assay

Activity in plasma sample was assayed using a spectrophotometric assay (Moss and Henderson, 1994).

Principle

ALT catalyzes transamination of L-alanine to α-ketoglutarate to form pyruvate and L-glutamate. Lactate dehydrogenase (LDH) reduces pyruvate to lactate and oxidizes nicotinamide adenine dinucleotide-reduced form (NADH) to nicotinamide adenine dinucleotide (NAD). Rate of oxidation of NADH is measured kinetically by monitoring the decrease in absorbance at 340nm using a spectrophotometer.

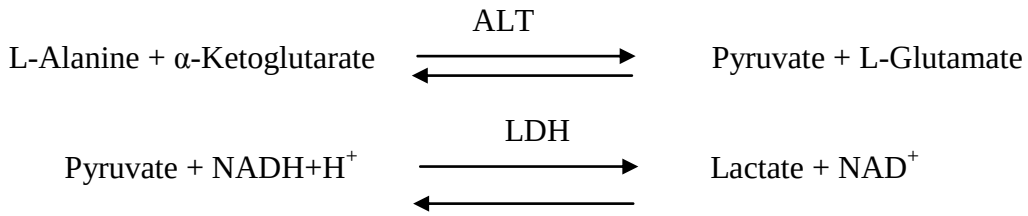

Reagents

1. Tris-HCl buffer, pH 7.5, 100 mM
2. L-alanine, 500 mM
3. α-Ketoglutarate, 15 mM
4. Lactate dehydrogenase, 1200 U / mg
5. NADH, 0.18 mM

Procedure

Substrate solution of 1.0 ml, containing 80 mM Tris-HCl buffer, 0.40 M alanine, 3 mM α-Ketoglutarate, 2.0 IU of LDH and 0.04 mM NADH was prepared and taken in to a quartz cuvette. To this, 0.10 ml of plasma sample was added and mixed. Absorbance was recorded at an interval of 1 minute for a period of 5 minutes. Mean absorbance change per minute (Δ) was determined and enzyme activity was calculated by using the following formula:

ALT activity (IU/L) = Δ absorbance / minute x 1768 (Kinetic factor)

AST assay

Activity in plasma sample was assayed using a spectrophotometric assay (Moss and Henderson, 1994).

Principle

AST catalyzes transamination of L-aspartate and α-ketoglutarate to form oxaloacetate and L-glutamate. Malate dehydrogenase (MDH) reduces oxaloacetate to malate and oxidizes NADH to NAD. Rate of oxidation of NADH is measured kinetically by monitoring the decrease in absorbance at 340 nm using a spectrophotometer.

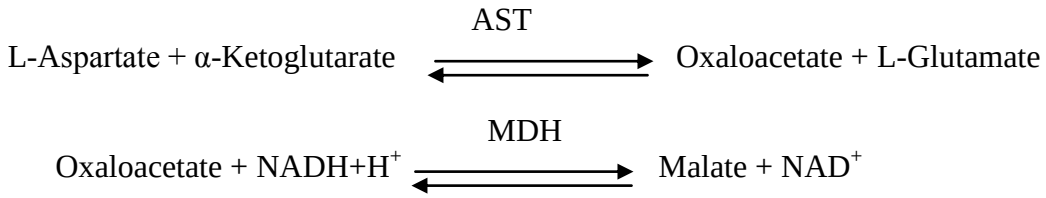

Reagents

1. Tris-HCl buffer, pH 7.8, 80 mM
2. L-aspartate, 240 mM
3. α-Ketoglutarate, 15 mM
4. Malate dehydrogenase, 600 U / L
5. NADH, 0.18 mM

Procedure

Substrate solution of 1.0 ml, containing 60 mM Tris-HCl buffer, 0.20 M alanine, 3 mM α-Ketoglutarate, 2.0 IU of MDH and 0.04 mM NADH was prepared and taken into a quartz cuvette. To this, 0.10 ml of plasma sample was added and mixed. Absorbance was recorded at an interval of 1 minute for a period of 5 minutes. Mean absorbance change per minute (Δ) was determined and enzyme activity was calculated by using the following formula:

$$\text{AST activity (IU/L)} = \Delta \text{ absorbance / minute} \times 1768 \text{ (Kinetic factor)}$$

Estimation of Urea

Urea is estimated using the method of Talka and Schubert, 1965.

Principle

Urea is converted to glutamate in a two step reaction with the help of enzymes, urease and glutamate dehydrogenase (GLDH). Ammonia is formed by the action of urease on urea. Amino group from ammonia is donated to α-Ketoglutarate in presence of NADH which is oxidized to NAD+. Rate of oxidation of NADH is measured kinetically by monitoring the decrease in absorbance at 340nm using a spectrophotometer.

$$\text{Urea} + H_2O \xrightarrow{\text{Urease}} 2NH_3 + CO_2$$

$$NH_3 + \alpha\text{-Ketoglutarate} + \text{NADH} \xrightarrow{\text{GLDH}} \text{Glutamate} + NAD^+$$

Reagents

1. Tris-HCl buffer, pH 7.9, 0.50 M
2. α-Ketoglutarate, 75 mM
3. Glutamate dehydrogenase
4. Urease
5. NADH, 5.0 mM
6. ADP, 10 mM
7. Urea standard, 50 mg / 100 ml

Procedure

Working reagent containing α-Ketoglutarate, 7.5 mM, malate dehydrogenase, 8 mIU, urease, 1 mIU, NADH, 0.32 mM, ADP, 1.2 mM and Tris-HCl buffer, 0.10 M was prepared. To 1.0 ml of working reagent, 20 µl of plasma sample or 20 µl of standard urea solution was added and mixed. Absorbance was recorded at an interval of 1 minute for a period of 5 minutes. Mean absorbance change per minute (Δ) was determined and enzyme activity was calculated by using the following formula:

$$\text{Urea (mg/dl)} = \frac{\Delta A \text{ of test}}{\Delta A \text{ of standard}} \times \text{concentration of standard (mg/dl)}$$

Estimation of creatinine

Plasma creatinine is estimated using Jaffe's reaction (Slot, 1965).

Principle

Creatinine reacts with alkaline picrate to produce an orange-yellow colored product. Absorbance of the product is measured photometrically at 500-520 nm and is directly proportional to creatinine concentration.

Reagents

1. Picric acid, 26 mM
2. NaOH, 0.10 M
3. Creatinine standard , 0.166 mM(0.02 mg /ml)

Procedure

Working reagent was prepared by mixing equal volumes of picric acid and sodium hydroxide and was kept for 15 minutes before use. 1.0 ml of working reagent was added to 0.10 ml of standard or 0.10 of plasma sample. Increasing concentrations of standard were taken along with blanks in triplicate were used. After mixing absorbance was measured immediately and after one minute at 520 nm. Creatinine was calculated using the following formula:

$$\text{Creatinine (mg/dl)} = \frac{\Delta A \text{ of test}}{\Delta A \text{ of standard}} \times \text{concentration of standard (mg/dl)}$$

Results

ALP, ALT and AST activity in plasma

ALP activity in plasma from rats that received metallic NP orally is presented in Figure 8.1. Activity in GNP and SNP administered rats was similar to the controls. A significant increase in ALP activity was observed in CuNP treated group ($p < 0.05$). Plasma ALT and AST activities of control and metallic NP treated groups are presented in Figure 8.2 and Figure 8.3 respectively. Both transaminase activities are similar in GNP and SNP administered rats compared to controls. However, both ALT and ASP activities are elevated in plasma of rats that received CuNP.

Plasma urea and creatinine

Concentrations of urea and creatinine determined in plasma of control and NP treated rats and presented in Figure 8.4 and Figure 8.5 respectively. No significant change in the concentration of urea and creatinine were observed in NP treated groups compared to controls.

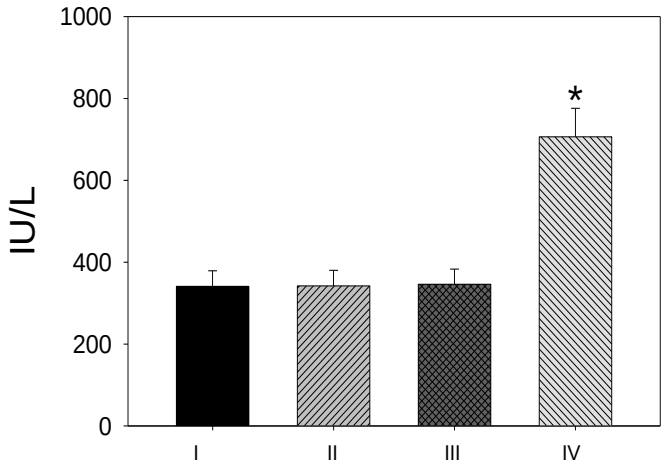

Figure 8.1: ALP activity in plasma of rats administered metallic NP. Data presented are Mean ± SEM of 5 experiments. I. Control, II. GNP , III. SNP , IV. CuNP. *p <0.05, control vs. treated

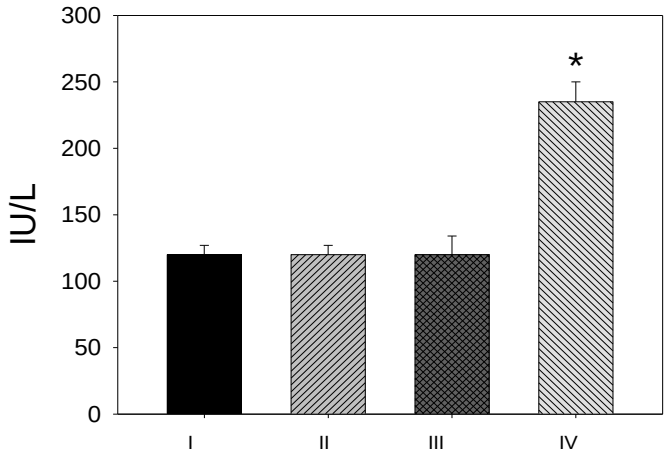

Figure 8.2: ALT activity in plasma of rats administered metallic NP. Data presented are Mean ± SEM of 5 experiments. I. Control, II. GNP , III. SNP , IV. CuNP. *p <0.05, control vs. treated

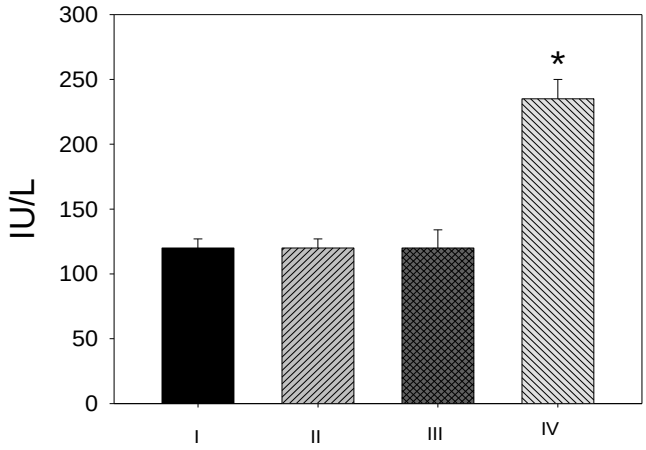

Figure 8.3: AST activity in plasma of rats administered metallic NP. Data presented are Mean ± SEM of 5 experiments. I. Control, II. GNP , III. SNP , IV. CuNP. *p <0.05, control vs. treated

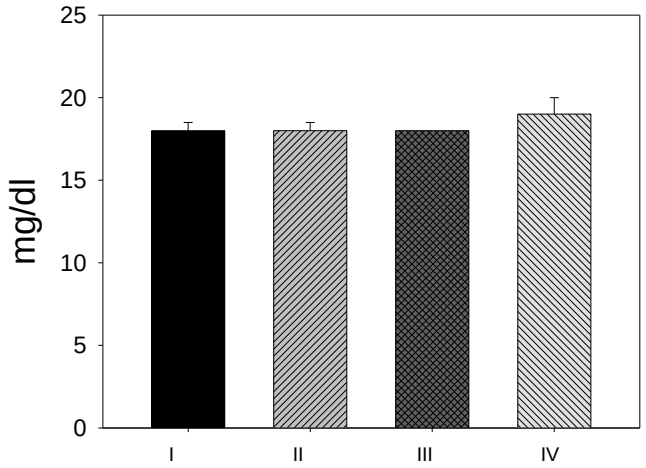

Figure 8.4: Concentration of urea in plasma of rats administered metallic NP. Data presented are Mean ± SEM of 5 experiments. I. Control, II. GNP , III. SNP , IV. CuNP.

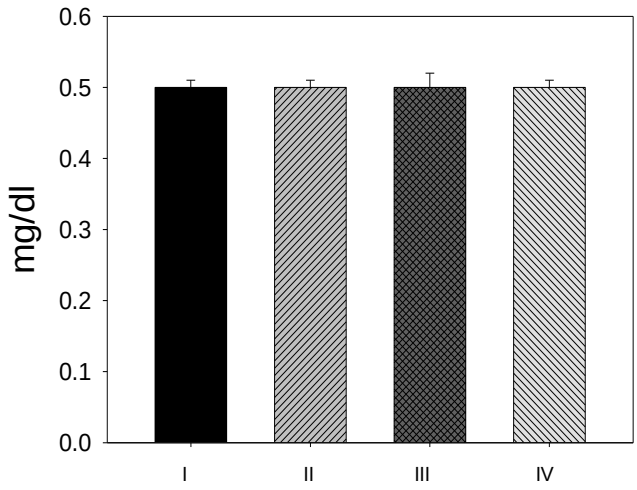

Figure 8.5: Concentration of creatinine in plasma of rats administered metallic NP. Data presented are Mean ± SEM of 5 experiments. I. Control, II. GNP , III. SNP , IV. CuNP.

Discussion

Following oral administration, NP that are translocated from gastrointestinal tract are localized to different organs via systemic circulation. Liver being the major constituent of reticuloendothelial system, NP are actively taken up hepatocytes and kupffer cells (Cheng et al., 2012). Although liver has anti-oxidant mechanisms and other metabolizing enzymes, retention and persistence of NP may pose a risk for hepatotoxicity (Yang et al., 2008). In addition to liver, NP also accumulates in kidneys, which are the important for their elimination (Hou et al., 2010). NP having less than 8nm diameter have been shown to be filtered by the kidneys, where as large sized NP with more than 80nm diameter are trapped by liver and spleen and have been demonstrated to be excreted via the hepatobiliary pathway (Longmire et al., 2008). As kidney is involved excretion of NP, accumulation due to non-excretion may lead to possible tissue injury/ toxicity (Yamagishi et al., 2013). Understanding the mechanisms of NP induced nephrotoxicity may help in designing strategies to make them non-toxic and therapeutically compatible (Kim and Moon, 2012).

Biochemical markers are evaluated for monitoring the possible toxic effects of xenobiotics (Adeyemi and Adewumi, 2014). Serum enzymes such as ALP, ALT and AST have been used as markers for hepatotoxicity. These enzymes are contained in normal liver tissue and are present in low levels in plasma. But, high amounts of enzymes enter the blood circulation following liver injury (Patlolla et al., 2015). Nephrotoxicity occurs when the detoxification or secretory / excretory function(s) are impaired due to damage of renal tissue (Kim and Moon, 2012). Renal function is evaluated by estimating blood urea and creatinine levels and biochemical markers (Fuchs and Hewitt, 2011).

Earlier studies have shown that orally administered GNP crossed gastrointestinal tract and were distributed to organs such as liver and kidney (Hillyer and Albrecht, 2001). Size and surface charge influenced the absorption of GNP through intestinal barrier and their accumulation in target organs (Schleh et al., 2012). Effects of GNP on serum markers of liver and renal tissue injury have been ambiguous. Some studies have reported no change in serum enzymes, urea and createnine (Rambanapasi et al., 2016; Abdelhalim and Abdelmottaleb Moussa, 2013). In contrast others have shown elevated levels (Hwang et al., 2012; Rathore et al., 2014). In the present study, oral

administration of GNP for 14 days at a concentration of 2mg / Kg body weight showed no significant change in all the parameters measured, in agreement with some studies reported earlier (Rambanapasi et al., 2016; Abdelhalim and Abdelmottaleb Moussa, 2013). This suggests that GNP of 28 nm hydrodynamic size and at the concentration mentioned above do not affect hepatic and renal function despite their localization in these tissues (as shown by the *ex-vivo* imaging data). However, it is to be noted that further studies are needed to address the effect of varying size, concentration, duration of study etc. in comprehensive pre-clinical evaluation.

In a few studies reported earlier, no significant change has been observed in ALP, AST, ALT, urea and createnine rats upon oral administration of SNP (van der Zande et al., 2012; Kulthong et al., 2012; Park et al., 2010; Chakraborty et al., 2016; Pourhamzeh et al., 2016). But, elevated levels in liver and kidney injury have been reported by few studies (Kim et al., 2008; Adeyemi and Adewumi, 2014). In the present study, SNP (of size range of 40-80 nm and mean hydrodynamic size of 65 nm) administered orally at a concentration of 10mg / Kg body weight for 2 weeks showed no significant change in the levels of hepatic enzymes in plasma as well as urea and creatinine. This observation is in agreement with those reported earlier in majority of studies (van der Zande et al., 2012; Kulthong et al., 2012; Park et al., 2010; Chakraborty et al., 2016; Pourhamzeh et al., 2016). Hence, similar to GNP, SNP does not seem to affect liver and kidney function at the size and dose employed. Results obtained in the present experiments are preliminary in nature and extensive work is required for comprehensive evaluation of hepatic and nephro-toxicity of SNP *in vivo*.

Available evidence in literature on the effect of orally administered CuNP on biomarkers of livery and kidney inury is based on dose effect, one study showed dose-dependent increase in the ALP and createnine levels (Chen et al., 2006), whereas other study showed elevated levels of ALT and AST at lower dose (10mg/kgbw than 300mg/kgbw) (Doudi and Setorki, 2015).

In the present study, results of present work showed that oral administration of CuNP at a concentration of 10mg / kg body weight causes significant increase in ALP, AST and ALT activity in plasma compared to controls. But, no change in plasma urea and creatinine concentration was observed. These results are in agreement

with studies which reported elevated levels of plasma ALP, ALT and AST in CuNP treated animals (Chen et al., 2006; Doudi and Setorki, 2015). It has been proposed that release of free copper ions from CuNP cause damage to hepatic tissue resulting in lipodystrophy, steatosis and increase in ALP activity (Chen et al., 2006). Similar mechanism may be operational in the present experiments, though no direct evidence exists to substantiate such a proposal. Preliminary evidence has been reported with regard to increased MDA formation (as a marker of oxidative stress) in supernatant of lymphocytes treated with CuNP (Chapter 4). Proposed mechanisms for CuNP induced toxicity include - induction of oxidative stress, decrease in levels of catalase and glutathione reductase, increase of glutathione peroxidase, and also increase in the ratio of oxidized glutathione to total glutathione (Doudi and Setorki, 2015; Fahmy and Cormier, 2009). Thus, preliminary evidence obtained in the present work suggests that CuNP affects liver function and probably without affecting kidney function.

The salient findings of the studies reported in this chapter are:

1) Oral administration of CuNP increased plasma ALP, ALT and AST activity compared to untreated controls suggesting an impairment of liver function. However, no change in plasma enzyme activity was observed in GNP and SNP administration, indicating that hepatic function is unaffected.

2) Urea and creatinine concentration in plasma of rats administered metallic NP (GNP, SNP and CuNP) were similar to untreated controls suggesting that kidney function is unaffected.

Summary and conclusions

The salient results and conclusions of the present thesis work are summarized below:

1) Gold and silver NP could be prepared reproducibly using citrate reduction method. Absorption spectra in visible range of gold, silver and copper NP revealed characteristic surface plasmon absorption maximum at 520 nm (GNP), 420 nm (SNP) and 505 nm (CuNP) respectively. Transmission electron microscopic analysis revealed a spherical morphology for all the three metallic NP. Average diameter was 13 nm (GNP), 40-60nm (SNP) and 23-33 nm (CuNP). Hydrodynamic diameter of NP was determined using NTA and was found to be higher than that obtained with the transmission microscopic analysis. NP number in the suspension could also be determined reproducibly by NTA. Mean diameter of the particles was 28 nm (GNP), 65 nm (SNP) and 134 nm (CuNP) respectively using NTA. Characterization using NTA provided valuable information on the hydrodynamic size and number of particles which are of great relevance to study NP and cell (lymphocyte) interactions, especially *in vitro*.

2) NP of apo-transferrin, bovine serum albumin and chitosan showed a spherical morphology and mean diameter of 40-50 nm, 80-120 nm, 120-150 nm respectively using scanning electron microscopy. NTA analysis revealed an average diameter of 104, 114 and 180 nm for apo-transferrin, bovine serum albumin and chitosan NP respectively. Number of particles was also determined using NTA.

3) Proliferative response of mouse splenic lymphocytes induced by mitogens, Con A (T cell specific) and LPS (B cell specific) was significantly inhibited in presence of GNP (25-200 µg/ml), SNP (12.5-50 µg/ml) and CuNP (2.5- 10 µg/ml) in cell culture. Viability of lymphocytes decreased significantly at higher concentrations of NP, the effect being CuNP > SNP > GNP. Similarly, proliferative response of human PBL induced by mitogens, PHA (T cell specific) and PWM (T and B cell specific) was also significantly inhibited in presence of metallic NP. However, viability of human PBL was decreased significantly only at higher concentration of NP, the effect being less compared to that observed with mouse splenic lymphocytes. The results strongly suggested that all three metallic NP inhibit mitogen induced activation *in vitro*.

Further experiments indicated that the inhibitory effect of gold and silver NP on lymphocyte activation may not due to free metal ions released from the respective particles. However, in case of CuNP, release of free copper ions may be responsible for the inhibitory effect observed. Malondialdehyde levels were increased in CuNP treated lymphocyte culture supernatant compared to controls, but not in GNP and SNP treated cultures. Hence, reactive oxygen species generation may be involved in the cytotoxic effect observed with CuNP.

4) All three metallic NP exerted a significant inhibitory effect on proliferative response of mitogen stimulated rat splenic and thymic lymphocytes in a dose dependent manner. Results were similar to those obtained with mouse splenic lymphocytes.

5) Mitogen stimulated proliferative response of primary murine splenic and human peripheral blood lymphocytes was not affected by apo-transferrin and BSA NP. But, the proliferative response was significantly inhibited in presence of chitosan NP. Inhibition observed could be due to the interaction of chitosan with mitogens per se. Results indicated that the biological NP are immune compatible.

6) Proliferation of U266B1 and SUPT-1 cell lines decreased significantly in a dose-dependent manner in presence of metallic NP in culture.

7) Rho- BSA and Rho-chitosan conjugates coated on metallic NP were stable and were administered orally to fasted rats. Localization of Rho fluorescence in different tissues / organs was monitored *ex-vivo* using small animal *in vivo* imaging system. Significant fluorescence was detected in liver, kidney and in the lymphoid organs-spleen and thymus indicating tissue distribution of NP following absorption/persorption from the gastro-intestinal tract.

8) GNP were given orally to Wistar rats at two doses, 500 µg / kg and 2 mg / kg body weight, daily for 14 days. Proliferative response of splenic lymphocytes stimulated with Con A and LPS was significantly inhibited compared with controls at both the doses. Con A stimulated proliferative response of thymic lymphocytes was also reduced compared to controls. Concentrations of TNF-alpha, IL-2 and IFN-

gamma were significantly decreased in mitogen stimulated lymphocyte culture supernatants of GNP administered rats (2 mg / kg body weight) compared to controls. Results suggested that GNP inhibits lymphocyte activation *in vivo*.

9) SNP were administered orally at three doses, 500 µg / kg and 2 mg / kg and 10 mg / kg body weight, daily for 14 days. Mitogen stimulated proliferative response of splenic and thymic lymphocytes was significantly reduced in a dose-dependent manner compared to controls. A significant decrease in the concentrations of IL-2 and TNF-alpha was observed in the culture supernatants of lymphocytes in rats administered 10 mg/ kg body weight of SNP compared to control rats. Results indicated that SNP *in vivo* probably inhibits activation of T and B cells in the lymphoid tissues.

10) Proliferative response of splenic and thymic lymphocytes in presence of mitogens was significantly decreased in CuNP administered rats (2 and 10 mg / kg body weight) compared to controls. Concentrations of IL-2 and TNF- alpha were also significantly decreased in the CuNP administered rats, whereas IFN-gamma showed a significant increase compared to control rats. These results suggested an inhibition of lymphocyte activation with a concomitant induction of pro-inflammatory response following *in vivo* CuNP treatment.

11) In order to assess possible organ / tissue toxicity of NP administered *in vivo*, a few biochemical markers of liver and kidney function were estimated in plasma of rats which received the three metallic NP as mentioned above. No significant changes were observed in serum protein, creatinine, urea, alkaline phosphatase and aminotransferases in GNP and SNP administered rats. In the CuNP administered rats, specific activity of all three enzyme markers of liver function was elevated as compared to controls. However, in CuNP treated group, the concentration of serum creatinine and urea was unaltered compared to controls. The results suggested that CuNP may mediate hepatotoxicity which needs to be evaluated detail.

References

Abbas, AK, Murphy KM, Sher A. 1996. Functional diversity of helper T lymphocytes. Nature. 383(6603): 787–793.

Abdelhalim MA, Abdelmottaleb Moussa SA. 2013. The gold nanoparticle size and exposure duration effect on the liver and kidney function of rats: *in vivo*.Saudi J Biol Sci. 20(2):177-81.

Abdelhalim MA. 2013. Uptake of gold nanoparticles in several rat organs after intraperitoneal administration *in vivo*: a fluorescence study. Biomed Res Int. 2013:353695.

Adamcakova-Dodd A, Monick MM, Powers LS, Gibson-Corley KN, Thorne PS. 2015. Effects of prenatal inhalation exposure to copper nanoparticles on murine dams and offspring. Part Fibre Toxicol.12:30.

Adeyemi OS, Adewumi I. 2014. Biochemical evaluation of silver nanoparticles in wistar rats.International Scholarly Research Notices. dx.doi.org/10.1155/2014/196091.

Albanese A, Chan WC. 2011. Effect of gold nanoparticle aggregation on cell uptake and toxicity. ACS Nano. 5(7):5478-89.

Albanese A, Tang PS, Chan WC. 2012. The effect of nanoparticle size, shape, and surface chemistry on biological systems. Annu Rev Biomed Eng. 14:1-16.

Alger H, Momcilovic D, Carlander D, Duncan TV. 2014. Methods to evaluate uptake of engineered nanomaterials by the alimentary tract. Compr Rev Food Sci Food Saf. 13(4):705-729.

Almeida JP, Chen AL, Foster A, Drezek R. 2011. *In vivo* biodistribution of nanoparticles.Nanomedicine (Lond). 6(5):815-35.

Almeida JP, Figueroa ER, Drezek RA. 2014. Gold nanoparticle mediated cancer immunotherapy. Nanomedicine. 10:503-514.

Anderson J, Sjoberg O, Moller G. 1972. Induction of immunoglobulin and antibody synthesis *in vitro* by lipopolysaccharides. Eur J Immunol. 2(4): 349-53.

Arvizo RR, Bhattacharyya S, Kudgus RA, Giri K, Bhattacharya R, Mukherjee P. 2012. Intrinsic therapeutic applications of noble metal nanoparticles: past, present and future. Chem Soc Rev. 41(7):2943-70.

Aseichev AV, Azizova OA, Beckman EM, Skotnikova OI, Dudnik LB, Shcheglovitova ON, Sergienko VI. 2014. Effects of gold nanoparticles on erythrocyte hemolysis. Bull Exp Biol Med. 156(4): 495-8.

Asharani PV, Hande MP, Valiyaveettil S. 2009. Anti-proliferative activity of silver nanoparticles. BMC Cell Biol. 10:65.

Auffan M, Rose J, Bottero JY, Lowry GV, Jolivet JP, Wiesner MR. 2009. Towards a definition of inorganic nanoparticles from an environmental, health and safety perspective. Nat Nanotechnol. 4 (10): 634-641.

Austin LA, Mackey MA, Dreaden EC, El-Sayed MA. 2014. The optical, photothermal, and facile surface chemical properties of gold and silver nanoparticles in biodiagnostics, therapy, and drug delivery. Arch Toxicol. 88(7):1391-417.

Avvakumova S, Colombo M, Tortora P, Prosperi D. 2014. Biotechnological approaches toward nanoparticle biofunctionalization. Trends Biotechnol. 32 (1): 11-20.

Bakhru SH, Furtado S, Morello AP, Mathiowitz E.2013.Oral delivery of proteins by biodegradable nanoparticles. Adv Drug Deliv Rev. 65(6):811-21.

Barkalina N, Charalambous C, Jones C, Coward K. 2014. Nanotechnology in reproductive medicine: Emerging applications of nanomaterials. Nanomedicine. 10(5): 921–938.

Barreto JA, OMalley W, Kubeil M, Graham B, Stephan H, Spiccia L. 2011. Nanomaterials: applications in cancer imaging and therapy. Adv Mater. 23 (12): H18–H40.

Bartneck M, Keul HA, Zwadlo-Klarwasser G, Groll J. 2010. Phagocytosis independent extracellular nanoparticle clearance by human immune cells. Nano Lett. 10(1): 59-63.

Barua S, Mitragotri S. 2014. Challenges associated with penetration of nanoparticles across cell and tissue barriers: a review of current status and future prospects. Nano today. 9(2):223-243.

Benyettou F, Rezgui R, Ravaux F, Jaber T, Blumer K, Jouiad M, Motte L, Olsen J-C, Platas-Iglesias C, Magzoub M, Trabolsi A. 2015.Synthesis of silver nanoparticles for the dual delivery of doxorubicin and alendronate to cancer cells. J Mater Chem. B. 3: 7237.

Bertrand N, Wu J, Xu X, Kamaly N, Farokhzad OC. 2014. Cancer nanotechnology: the impact of passive and active targeting in the era of of modern cancer biology. Adv Drug Deliv Rev. 66:2-25.

Bessey OA, Lowry OH, Brock MJ. 1946. A method for the rapid determination of alkaline phosphates with five cubic millimeters of serum. J Biol Chem. 164:321-9.

Bhabra G, Sood A, Fisher B, Cartwright L, Saunders M, Evans WH, Surprenant A, Lopez-Castejon G, Mann S, Davis SA, Hails LA, Ingham E, Verkade P, Lane J, Heesom K, Newson R, Case CP. 2009. Nanoparticles can cause DNA damage across a cellular barrier. Nat Nanotechnol. 4 (12): 876–883.

Bhattacharya R, Patra CR,Verma R, Kumar S, Greipp PR, Mukherjee P. 2007. Gold nanoparticles inhibit the proliferation of multiple myeloma cells. Adv Mater. 19(5):711–716.

Blakey I, Merican Z, Thurecht KJ. 2013. A method for controlling the aggregation of gold nanoparticles: tuning of optical and spectroscopic properties. Langmuir. 29(26):8266-74.

Boyum A. 1964. Separation of white blood cells. Nature. 204:793-794.

Braakhuis HM, Gosens I, Krystek P, Boere JA, Cassee FR, Fokkens PH, Post JA, van Loveren H, Park MV. 2014. Particle size dependent deposition and

pulmonary inflammation after short-term inhalation of silver nanoparticles. Part Fibre Toxicol. 11:49.

Braden B C, Goldbaum FA, Chen BX, Kirschner AN, Wilson SR, Erlange BF. 2000. X-ray crystal structure of an anti Buckminsterfullerene antibody fab fragment:biomolecular recognition of C(60). Proc Natl Acad Sci U S A. 97(22): 12193–12197.

Bucharskayaa AB, Pakhomya SS, Zlobinaa OV, Maslyakovaa GN, Matveevaa OV, Bugaevaa IO, Navolokina NA, Khlebtsovb BN, Bogatyrevb VA , Khlebtsov NG, Tuchin VV. 2016a. The morphological changes in lymphoid organs and peripheral blood indicators in rats after peroral administration of gold nanoparticles.Proc SPIE 9709, Biophotonics and immune responses XI, 97090V.

Bucharskayaa AB, Pakhomya SS, Zlobinaa OV, Maslyakovaa GN, Matveevaa OV, Bugaevaa IO, Navolokina NA, Khlebtsovb BN, Bogatyrevb VA , Khlebtsov NG, Tuchin VV. 2016b. The morphological changes in lymphoid organs and peripheral blood indicators in rats after prolonged oral administration of gold nanoparticles.J Innove Opt Health Sci.9 (4):1642004

Burke T, Pollok K, Cushley W, Snow EC. 1989. Phosphorylation of class I but not class II MHC molecules by membrane-localized protein kinase C. Mol Immunol. 26(12): 1095-104.

Butler KS, Peeler DJ, Casey BJ, Dair BJ, Elespuru RK. 2015. Silver nanoparticles: correlating nanoparticlesize and cellular uptake with genotoxicity. Mutagenesis. 30(4):577-91.

Buzea C, Pacheco II, Robbie K. 2007. Nanomaterials and nanoparticles: Sources and toxicity. Biointerphases. 2 (4): MR17-MR71.

Calvo P, Remunan-Lopez C, Vila-Jato JL, Alonso MJ. 1997b. Novel hydrophilic chitosan-polyethylene oxide nanoparticles as protein carrier. J Appl Poly Sci. 63(1): 125-132.

Campbell KS, Cambier JC. 1990. B lymphocyte antigen receptors (mIg) are non covalently associated with a disulfide linked, inducibly phosphorylated glycoprotein complex. EMBO J. 9(2): 441-8.

Carter RH, Park DJ, Rhee SG, Fearon DT. 1991. Tyrosine phosphorylation of phospholipase C induced by membrane immunoglobulin in B lymphocytes**.** Proc Natl Acad Sci U S A. 88(7): 2745–2749.

Cha K, Hong HW, Choi YG, Lee MJ, Park JH, Chae HK, Ryu G, Myung H. 2008. Comparison of acute responses of mice livers to short-term exposure to nano-sized or micro-sized silver particles. Biotechnol Lett. 30(11):1893-9.

Chakraborty B, Pal R, Ali M, Singh LM, Rahman DS, Ghosh SK, Sengupta M. 2016. Immunomodulatory properties of silver nanoparticles contribute to anticancer strategy for murine fibrosarcoma.Cell Mol Immunol. 13(2): 191–205.

Chen BA, Jin N, Wang J, Ding J, Gao C, Cheng J, Xia G, Gao F, Zhou Y, Chen Y, Zhou G, Li X, Zhang Y, Tang M, Wang X. 2010. The effect of magnetic nanoparticles of Fe(3)O(4) on immune function in normal ICR mice. Int J Nanomedicine. 5:593-9.

Chen H, Dorrigan A, Saad S, Hare DJ, Cortie MB, Valenzuela SM. 2013b.In vivo study of spherical gold nanoparticles: inflammatory effects and distribution in mice. PLoS One. 8(2):e58208.

Chen J, Huang L, Lai H, Lu C, Fang M, Zhang Q, Luo X.2014. Methotrexate-loaded PEGylated chitosan nanoparticles: synthesis, characterization, and *in vitro* and *in vivo* antitumoral activity. Mol Pharmaceutics. 11: 2213−2223.

Chen JZ, Stall AM, Herzenberg LA, Herzenberg LA. 1990. Differences in glycoprotein complexes associated with IgM and IgD on normal murine B cells potentially enable transduction of different signal. EMBO J. 9(7): 2117-24.

Chen LQ, Fang L, Ling J, Ding CZ, Kang B, Huang CZ. 2015. Nanotoxicity of silver nanoparticles to red blood cells: size dependent adsorption, uptake, and hemolytic activity. Chem Res Toxicol. 28(3): 501–509.

Chen MC, Mi FL , Liao ZX , Hsiao CW , Sonaje K , Chung MF, Hsu LW , Sung HW. 2013a. Recent advances in chitosan-based nanoparticles for oral delivery of macromolecules. Adv Drug Deliv Rev. 65: 865–879.

Chen Z, Meng H, Xing G, Chen C, Zhao Y, Jia G, Wang T, Yuan H, Ye C, Zhao F, Chai Z, Zhu C, Fang X, Ma B, Wan L. 2006. Acute toxicological effects of copper nanoparticles *in vivo*.Toxicol Lett. 163(2):109-20.

Cheng SH, Li FC, Souris JS, Yang CS, Tseng FG, Lee HS, Chen CT, Dong CY, Lo LW. 2012. Visualizing dynamics of sub-hepatic distribution of nanoparticles using intravital multiphoton fluorescence microscopy. ACS Nano. 6: 4122–4131.

Choi J, Reipa V, Hitchins VM, Goering PL, Malinauskas RA. 2011. Physicochemical characterization and *in vitro* hemolysis evaluation of silver nanoparticles. Toxicol Sci. 123(1):133-43.

Choi SY, Jeong S, Jang SH, Park J, Park JH, Ock KS, Lee SY, Joo SW. 2012. In vitrotoxicity of serum protein-adsorbed citrate-reduced gold nanoparticles in human lung adenocarcinoma cells. Toxicol In Vitro. 26:229–237.

Connor EE, Mwamuka J, Gole A, Murphy CJ, Wyatt MD. 2005. Gold nanoparticles are taken up by human cells but do not cause acute cytotoxicity. Small. 1(3):325–327.

Cuña M, Alonso-Sandel M, Remuñán-López C, Pivel JP, Alonso-Lebrero JL, Alonso MJ. 2006. Development of phosphorylated glucomannan-coated chitosan nanoparticles as nanocarriers for protein delivery. J Nanosci and Nanotechnol. 6 (9-10): 2887-95.

Dang TMD, Le TTT, Fribourg-Blanc E, Dang MC. 2011. The influence of solvents and surfactants on the preparation of copper nanoparticles by a chemical reduction method. Adv Nat Sci Nanosci Nanotechnol. 2: 025004-025011.

Davydova VN, Bratskaya SY, Gorbach VI, Solov'eva TF, Kaca W, Yermak IM. 2008. Comparative study of electrokinetic potentials and binding affinity of lipopolysaccharides-chitosan complexes. Biophys Chem. 136(1): 1–6.

Dawidczyk CM, Kim C, Park JH, Russell LM, Lee KH, Pomper MG, Searson PC.2014. State-of-the-art in design rules for drug delivery platforms: lessons learned from FDA-approved nanomedicines. J Control Release. 10; 187.

De Franco AL. 1987. Molecular aspects of B-Lymphocyte activation. Ann Rev Cell Biol. 3: 143-78.

De Jong WH, Borm PJ. 2008. Drug delivery and nanoparticles: applications and hazards. Int J Nanomedicine. 3(2):133-49.

De Jong WH, Van Der Ven LT, Sleijffers A, Park MV, Jansen EH, Van Loveren H, Vandebriel RJ. 2013. Systemic and immunotoxicity of silver nanoparticles in an intravenous 28 days repeated dose toxicity study in rats. Biomaterials. 34(33):8333-43.

Deng ZJ, Liang M, Toth I, Monteiro M, Minchin RF. 2013. Plasma protein binding of positively and negatively charged polymer-coated gold nanoparticles elicits different biological responses. Nanotoxicology. 7(3): 314-22.

Di Gioacchino M, Petrarca C, Lazzarin F, Di Giampaolo L, Sabbioni E, Boscolo P, Mariani-Costantini R, Bernardini G. 2011. Immunotoxicity of nanoparticles. Int J Immunopathol Pharmacol. 24 (1 Suppl): 65S-71S.

Dobrovolskaia MA, Aggarwal P, Hall JB, McNeil SE. 2008. Preclinical studies to understand nanoparticle interaction with the immune system and its potential effects on nanoparticle biodistribution. Mol Pharm. 5(4):487-95

Donaldson K, Poland CA. 2013. Nanotoxicity: challenging the myth of nanospecific toxicity. Curr Opin Biotechnol. 24 (4):724–734.

Doudi M, Setorki M. 2015. Acute effect of nano-copper on liver tissue and function in rat. Nanomed J. 1(5): 331-338.

Dreaden EC, Mwakwari SC, Sodji QH, Oyelere AK, El-Sayed MA. 2009. Tamoxifen-poly (ethylene glycol)-thiol gold nanoparticle conjugates: Enhanced potency and selective delivery for breast cancer treatment. Bioconj Chem. 20(12):2247–2253.

Drelich J, Li B, Bowen P, Hwang JY, Mills O, Hoffman D. 2011.Vermiculite decorated with copper nanoparticles: Novel antibacterial hybrid material. Applied Surface Science. 257(22): 9435– 9443.

Duan X, Li Y. 2013. Physicochemical characteristics of nanoparticles affect circulation, biodistribution, cellular internalization, and trafficking. Small. 9(9-10):1521-32.

Durymanov MO, Rosenkranz AA, Sobolev AS. 2015. Current approaches for improving intratumoral accumulation and distribution of nanomedicines.Theranostics. 5(9):1007-20.

Dykman L, Khlebtsov N. 2012.Gold nanoparticles in biomedical applications: recent advances and perspectives. Chem Soc Rev. 41(6): 2256–2282.

Dykman LA, Sumaroka MV, Staroverov SA, Zaitseva IS, Bogatyrev VA. 2004. Immunogenic properties of colloidal gold. Izv Akad Nauk Ser Biol. 1: 86–91.

Elsabahy M, Wooley KL.2013. Cytokines as biomarkers of nanoparticle immunotoxicity. Chem Soc Rev. 42(12): 5552—5576. 2013.

Elsaesser A, Howard CV. 2012. Toxicology of nanoparticles. Adv Drug Deliv Rev. 64 (2): 129–137.

Elzoghby AO, Samy WM, Elgindy NA. 2012. Albumin-based nanoparticles as potential controlled release drug delivery systems. J Controlled Release. 157: 168–182.

Eom HJ, Choi J. 2010. p38 MAPK Activation, DNA damage, cell cycle arrest and apoptosis as mechanisms of toxicity of silver nanoparticles in Jurkat T Cells. Environ Sci Technol. 44(21):8337-42.

Fadeel B, Feliu N, Vogt C, Abdelmonem AM, Parak WJ. 2013. Bridge over troubled waters: understanding the synthetic and biological identities of engineered nanomaterials. Wiley Interdiscip Rev Nanomed and Nanobiotechnol. 5(2): 111–129.

Fadeel B, Garcia-Bennett AE. 2010. Better safe than sorry: Understanding the toxicological properties of inorganic nanoparticles manufactured for biomedical applications. Adv Drug Deliv Rev. 62(3):362-74.

Fadeel B. 2012. Clear and present danger? Engineered nanoparticles and the immune system, Swiss Med Wkly. 142: w13609.

Faedmaleki F, H Shirazi F, Salarian AA, Ahmadi Ashtiani H, Rastegar H. 2014. Toxicity effect of silver nanoparticles on mice liver primary cell culture and HepG2 cell line. Iran J Pharm Res. 13(1):235-42.

Fahmy B, Cormier SA. 2009. Copper oxide nanoparticles induce oxidative stress and cytotoxicity in airway epithelial cells. Toxicol In Vitro. 23(7): 1365-1371.

Farmarzi MA, Sidiqhi A. 2013. Insights into biogenic and chemical production of inorganic nanomaterials and nanostructures. Adv Colloid Interface Sci. 189-190:1-20.

Filipe V, Hawe A, Jiskoot W. 2010. Critical evaluation of nanoparticle tracking analysis (NTA) by nanosight for the measurement of nanoparticles and protein aggregates. Pharm Res. 27 (5): 796–810.

Fischer HC, Chan WC. 2007. Nanotoxicity: the growing need for in vivo study. Curr Opin Biotechnol. 18(6):565-71.

Flaswinkel H, Reth M. 1994. Dual role of the tyrosine activation motif of the Ig-alpha protein during signal transduction via the B cell antigen receptor. EMBO J. 13(1): 83-9.

Florento L, Matias R, Tuaño E, Santiago K, dela Cruz F, Tuazon A. 2012. Comparison of cytotoxic activity of anticancer drugs against various human tumor cell lines using *in vitro* cell-based approach. Int J Biomed Sci. 8(1): 76–80.

Fraga S, Faria H, Soares ME, Duarte JA, Soares L, Pereira E, Costa-Pereira C, Teixeira JP, de Lourdes Bastos M, Carmo H. 2013. Influence of the surface coating on the cytotoxicity, genotoxicity and uptake of gold nanoparticles in human HepG2 cells. J Appl Toxicol. 33(10):1111-9.

Frens G. 1973. Controlled nucleation for the regulation of the particle size in monodisperse gold suspensions. Nature physical science. 241: 20-22.

Friedrich RJ, Campbell KS, Cambier JC. 1993. The gamma subunit of the B cell antigen-receptor complex is a C- terminally truncated product of the B29 gene. J Immunol. 150(7): 2814-22.

Fröhlich E, Roblegg E. 2016. Oral uptake of nanoparticles: human relevance and the role of *in vitro* systems. Arch Toxicol. 90(10):2297-2314.

Fu PP, Xia Q, Hwang HM, Ray PC,Yu H. 2014. Mechanisms of nanotoxicity: generation of reactive oxygen species. J Food Drug Anal. 22(1): 64-75.

Fuchs TC, Hewitt P. 2011. Biomarkers for drug-induced renal damage and nephrotoxicity—an overview for applied toxicology.AAPS J. 13(4): 615–631.

Gamboa JM, Leong KW. 2013. *In vitro and in vivo* models for the study of oral delivery of nanoparticles. Adv Drug Deliv Rev. 65(6):800-10.

Gandapu U, Chaitanya RK, Kishore G, Reddy RC, Kondapi AK. 2011. Curcumin-loaded apotransferrin nanoparticles provide efficient cellular uptake and effectively inhibit HIV-1 replication *in vitro*. PLoS One. 6(8): e23388.

Getts DR, Shea LD, Miller SD, King NJ. Harnessing nanoparticles for immune modulation. Trends Immunol. 36(7): 419-27.

Goding JW. 1976. Conjugation of antibodies with fluorochromes: modifications to the standard methods. J Immunol Methods.13(3-4): 215-26.

Gojova A, Guo B, Kota RS, Rutledge JC, Kennedy IM, Barakat AI. 2007. Induction of inflammation in vascular endothelial cells by metal oxide nanoparticles: effect of particle composition. Environ Health Perspect. 115(3): 403-9.

Golla K, Reddy PS, Bhaskar C, Kondapi AK. 2013. Biocompatibility, absorption and safety of protein nanoparticle-based delivery of doxorubicin through oral administration in rats. Drug Deliv. 20(3–4): 156–167.

Greulich C, Diendorf J, Simon T, Eggeler G, Epple M, Köller M. 2011. Uptake and intracellular distribution of silver nanoparticles in human mesenchymal stem cells. Acta Biomater. 7 (1): 347-354.

Guével X, Palomares F, Torres MJ, Blanca M, Fernandez TD and Mayorga C. 2015. Nanoparticle size influences the proliferative responses of lymphocyte subpopulations. RSC Adv. 5(104): 85305-85309.

Hadrup N, Loeschner K, Bergström A, Wilcks A, Gao X, Vogel U, Frandsen HL, Larsen EH, Lam HR, Mortensen A. 2012. Subacute oral toxicity investigation of nanoparticulate and ionic silver in rats. Arch Toxicol. 86(4):543-51.

Hadrup N, Sharma AK, Poulsen M, Nielsen E. 2016. Toxicological risk assessment of elemental gold following oral exposure to sheets and nanoparticles – A review. Regul Toxicol Pharmacol. 72(2):216-21.

Hall JB, Dobrovolskaia MA, Patri AK, McNeil SE. 2007. Characterization of nanoparticles for therapeutics. Nanomedicine (London). 2(6):789–803.

Hanini A, Schmitt A, Kacem K, Chau F, Ammar S, Gavard J. 2011. Evaluation of iron oxide nanoparticle biocompatibility. Int J Nanomedicine. 6:787-94.

Harper S, Usenko C, Hutchison JE, Maddux BLS, Tanguay RL. 2008. *In vivo* biodistribution and toxicity depends on nanomaterial composition, size, surface functionalisation and route of exposure. J. Exp. Nanosci.3:195-206.

Herrera GM, Padilla AC and Hernandez-Rivera SP. 2013. Surface enhanced raman scattering (SERS) studies of gold and silver nanoparticles prepared by laser ablation. Nanomaterials. 3(1), 158-172.

Hilderbrand SA, Weissleder R. 2010. Near-infrared fluorescence: application to *in vivo* molecular imaging. Curr Opin Chem Biol. 14 (1):71-79.

Hillyer JF, Albrecht RM. 2001. Gastrointestinal persorption and tissue distribution of differently sized colloidal gold nanoparticles.J Pharm Sci. 90(12):1927-36.

Hinkley GK, Carpinone P, Munson JW, Powers KW, Roberts SM. 2015. Oral absorption of PEG-coated versus uncoated gold nanospheres: does agglomeration matter?. Part Fibre Toxicol. 12:9.

Hirano T, Yasukawa K, Harada H, Taga T, Watanabe Y, Matsuda T, Kashiwamura S, Nakajima K, Koyama K, Iwamatsu A. 1986. Complementary DNA for a novel human interleukin (BSF-2) that induces B lymphocytes to produce immunoglobulin. Nature. 324(6092): 73-6.

Horie M, Kato H, Fujita K, Endoh S, Iwahashi H. 2012. *In vitro* evaluation of cellular response induced by manufactured nanoparticles. Chem Res Toxicol. 25(3):605-19.

Hou Y, Liu Y, Chen Z, Gu N, Wang J. 2010. Manufacture of IRDye800CW-coupled Fe_3O_4 nanoparticles and their applications in cell labeling and *in vivo* imaging. J. Nanobiotechnol. 8: 25.

Huang H, Lai W, Cui M, Liang L, Lin Y, Fang Q, Liu Y, Xie L. 2016. An evaluation of blood compatibility of silver nanoparticles. Sci Rep. 6:25518.

Huo, L, Chen, R, Zhao, L, Shi, X, Bai, R, Long, D, Chen, F, Zhao Y, Chang Y, Chen C. 2015. Silver nanoparticles activate endoplasmic reticulum stress signaling pathway in cell and mouse models: The role in toxicity evaluation.Biomaterials. 61(8): 307-315.

Hussain S, Boland S, Baeza-Squiban A, Hamel R, Thomassen LC, Martens JA, Billon-Galland MA, Fleury-Feith J, Moisan F, Pairon JC, Marano F. 2009. Oxidative stress and proinflammatory effects of carbon black and titanium dioxide nanoparticles: role of particle surface area and internalized amount. Toxicology. 260(1-3):142–149.

Hwang JH, Kim SJ, Kim YH, Noh JR, Gang GT, Chung BH, Song NW, Lee CH. 2012. Susceptibility to gold nanoparticle-induced hepatotoxicity is enhanced in a mouse model of nonalcoholic steatohepatitis. Toxicology. 294(1): 27-35.

Ibrahim MA, Khalaf AA, Galal MK, Ogaly HA, H M Hassan A. 2015. Ameliorative influence of green tea extract on copper nanoparticle-induced hepatotoxicity in rats. Nanoscale Res Lett. 10(1):363.

Iravani S, Korbekandi H, Mirmohammadi SV, Zolfaghari B. 2014.Synthesis of silver nanoparticles: chemical, physical and biological methods. Res Pharm Sci. 9(6): 385–406.

Ishida T, Kiwada H. 2008. Accelerated blood clearance (ABC) phenomenon upon repeated injection of PEGylated liposomes. Int J Pharm. 354 (1-2): 56-62.

Jain PK, Huang X, El-sayed IH, El-sayed MA. 2008. Noble metals on the nanoscale: optical and photothermal properties and some applications in imaging, sensing, biology, and medicine. Acc Chem Res. 41(12): 1578-1586.

Janossy G, Greaves MF. 1971. Lymphocyte activation. 1. Response of T and B lymphocytes to phytomitogens. Clin Exp Immunol. 9(4): 483-498.

Jelinek DF, Splawski JB, Lipsky PE. 1986. The roles of interleukin 2 and interferon-gamma in human B cell activation, growth and differentiation. Eur J Immunol. 16(8): 925-32.

Jeon YH, Kim YH, Choi K, Piao JY, Quan B, Lee YS, Jeong JM, Chung JK, Lee DS, Lee MC, Lee J, Chung DS, Kang KW. 2010. *In vivo* imaging of sentinel nodes using fluorescent silica nanoparticles in living mice. Mol. Imaging Biol. 12(2):155–162.

Jeong EH, Jung G, Hong CA, Lee H. 2014. Gold nanoparticle (AuNP)-based drug delivery and molecular imaging for biomedical applications. Arch Pharm Res. 37(1):53-9.

Jiao Q, Li L, Mu Q, Zhang Q.2014. Immunomodulation of nanoparticles in nanomedicine applications. Biomed Res Int. 2014:426028.

Jiménez-Lamana J, Laborda F,Bolea E,Abad-Álvaro I,Castillo JR,Bianga J,He M,Bierla K,Mounicou S,Ouerdane L,Gaillet S,Rouanet JM,Szpunar J. 2014. An insight into silver nanoparticles bioavailability in rats. Metallomics. 6: 2242-2249.

Jo MR, Bae SH, Go MR, Kim HJ, Hwang YG, Choi SJ. 2015. Toxicity and biokinetics of colloidal gold nanoparticles. Nanomaterials. 5(2): 835-850.

Johnston H, Brown D, Kermanizadeh A, Gubbins E, Stone V.2012. Investigating the relationship between nanomaterial hazard and physicochemical properties: Informing the exploitation of nanomaterials within therapeutic and diagnostic applications. J Controlled Release.164 (3): 307–313.

Johnston HJ, Hutchison G, Christensen FM, Peters S, Hankin S, Stone V. 2010. A review of the *in vivo and in vitro* toxicity of silver and gold particulates: particle attributes and biological mechanisms responsible for the observed toxicity. Crit Rev Toxicol. 40(4):328-46.

Josan JS, Handl HL, Sankaranarayanan R, Xu L, Lynch RM, Vagner J, Mash EA, Hruby VJ, Gillies R J. 2011. Cell-specific targeting by heterobivalent ligands. Bioconjug Chem. 22 (7): 1270–1278.

Jose GP, Santra S, Mandal SK, Sengupta TK. 2011. Singlet oxygen mediated DNA degradation by copper nanoparticles: potential towards cytotoxic effect on cancer cells. J Nanobiotechnology. 9:9.

Kagan VE, Kapralov AA, St. Croix CM, Watkins SC, Kisin ER, Kotchey GP, Balasubramanian K, Vlasova II, Yu J, Kim K, Seo W, Mallampalli RK, Star A, Shvedova AA. 2014. Lung macrophages ‘‘digest’’ carbon nanotubes using a superoxide/peroxynitrite oxidative pathway. ACS Nano. 8(6): 5610–5621.

Kanasty RL, Whitehead KA, Vegas AJ , Anderson DG. 2012. Action and reaction: The biological response to siRNA and its delivery vehicles. Mol Ther. 20(3): 513–524.

Kang H, Mintri S, Menon AV, Lee HY, Choi HS, Kim J. 2015. Pharmacokinetics, pharmacodynamics and toxicology of theranostic nanoparticles. Nanoscale. 7(45): 18848–18862.

Kapralov AA, Feng WH, Amoscato AA, Yanamala N, Balasubramanian K, Winnica DE, Kisin ER, Kotchey GP, Gou P, Sparvero LJ, Ray P, Mallampalli RK,Klein-Seetharaman J, Fadeel B, Star A, Shvedova AA, Kagan VE. 2012. Adsorption of surfactant lipids by single walled carbon nanotubes in mouse lung upon pharyngeal aspiration. ACS Nano. 6(5): 4147-56.

Kapsenberg ML. 2003. Dendritic cell control of pathogen driven T-cell polarization. Nature Rev Immunol. 3(12): 984–993.

Karimi M, Bahrami S, Ravari SB, Zangabad PS, Mirshekari H, Bozorgomid M, Shahreza S, Sori M, Hamblin MR. 2016. Albumin nanostructures as advanced drug delivery systems. Expert Opin Drug Deliv. 3:1-15.

Karuppaiya P, Satheeshkumar E, Chao WT, Kao LY, Chen EC, Tsay HS. 2013. Anti-metastatic activity of biologically synthesized gold nanoparticles on human fibrosarcoma cell line HT-1080. Colloids Surf B Biointerfaces. 110:163-70.

Kasyapa CS, Ramanadham M. 1995. Positive regulatory role of cAMP on alkaline phosphatase activity and proliferation of mitogen stimulated B lymphocytes. Biochem Mol Biol Int. 35(3): 535-40.

Kaur H, Pujari G, Sarma A, Mishra YK, Kyung Jin MK, Nirala BK, Gohil NK, Adelung R, Avasthi DK. 2013. Study of *in vitro* toxicity of glucose capped gold nanoparticles in malignant and normal cell lines. Adv Mat Lett. 4(12): 888-894.

Kawai T, Akira S. 2010. The role of pattern-recognition receptors in innate immunity: update on Toll-like receptors. Nat Immunol. 11 (5): 373-384.

Khan AA, Steiner JP, Klein MG, Schneider MF, Snyder SH. 1992. IP3 receptor: localization to plasma membrane of T cells and co-capping with the T cell receptor. Science. 257(5071): 815-8.

Khlebtsov N, Dykman L. 2011. Biodistribution and toxicity of engineered gold nanoparticles: a review of *in vitro and in vivo* studies. Chem Soc Rev. 40(3):1647-71.

Kim AS, Chae CH, Kim J, Choi JY, Kim SG, Băciut G. 2012b. Silver nanoparticles induce apoptosis through the toll-like receptor 2 pathway. Oral Surg Oral Med Oral Pathol Oral Radiol. 113 (6):789-98.

Kim JA, Åberg C, Salvati A, Dawson KA. 2012a. Role of cell cycle on the cellular uptake and dilution of nanoparticles in a cell population. Nat Nanotechnol. 7 (1): 62-68.

Kim JS, Adamcakova-Dodd A,O'Shaughnessy PT,Grassian VH, Thorne PS. 2011. Effects of copper nanoparticle exposure on host defense in a murine pulmonary infection model . Part Fibre Toxicol. 8:29.

Kim S, Choi JE, Choi J, Chung KH, Park K, Yi J, Ryu DY. 2009. Oxidative stress-dependent toxicity of silver nanoparticles in human hepatoma cells. Toxicol In Vitro. 23(6):1076-84.

Kim SY,Moon A. 2012. Drug-induced nephrotoxicity and its biomarkers. Biomol Ther (Seoul). 20(3): 268–272.

Kim TH, Jin H, Kim HW, Cho MH, Cho CS. 2006. Mannosylated chitosan nanoparticle-based cytokine gene therapy suppressed cancer growth in BALB/c mice bearing CT-26 carcinoma cells. Mol Cancer Ther. 5 (7): 1723-32.

Kim YS, Song MY, Park JD, Song KS, Ryu HR, Chung YH, Chang HK, Lee JH, Oh KH, Kelman BJ, Hwang IK, Yu IJ. 2010. Subchronic oral toxicity of silver nanoparticles. Part Fibre Toxicol. 7:20.

Kim YS, Kim JS, Cho HS, Rha DS, Kim JM, Park JD, Choi BS, Lim R, Chang HK, Chung YH, Kwon IH, Jeong J, Han BS, Yu IJ. 2008. Twenty-eight-day oral toxicity, genotoxicity, and gender-related tissue distribution of silver nanoparticles in Sprague-Dawley rats.Inhal Toxicol. 20(6):575-83.

Kittler S, Greulich C, Diendorf J, Köller M , Epple M. 2010.Toxicity of silver nanoparticles increase during storage because of slow dissolution under release of silver ions. Chem Mater. 22 (16): 4548–4554.

Knight T, Chada VGR, Wise SS, Mason MD, Thompson WD, Wise Sr JP, Ng AK. 2007. Cell-based assays for cytotoxic and pro-inflammatory effects of gold nanoparticles. NSTI-Nanotech. 2:674-677.

Krishna ADS, Mandraju RK, Kishore G, Kondapi AK. 2009. An efficient targeted drug delivery through apotransferrin loaded nanoparticles. PLoS One. 4 (10): e7240.

Kruse PF, Patterson MK, Jr., Eds. 1973. Tissue culture: Methods and Applications. Academic Press, New York.

Kuhn DA, Vanhecke D, Michen B, Blank F, Gehr P, Petri-Fink A, Rothen-Rutishauser B. 2014. Different endocytotic uptake mechanisms for nanoparticles in epithelial cells and macrophages. Beilstein J Nanotechnol. 5:1625-36.

Kulthong K, Maniratanachote R, Kobayashi Y, Fukami T, Yokoi T. 2012. Effects of silver nanoparticles on rat hepatic cytochrome P450enzyme activity. Xenobiotica. 42(9):854-62

Kumar CSSR, Hormes J, Leuschner C, Ryan Richards R, Bönnemann H. Nanofabrication towards biomedical applications: techniques, tools, applications, and impact. 2005 WILEY-VCH Verlag GmbH & Co. KGaA, Weinheim.

Kumari A, Yadav SK, Yadav SC. 2010. Biodegradable polymeric nanoparticles based drug delivery systems. Colloids Surf B Biointerfaces. 75(1):1-18.

Kwok PC, Chan HK. 2014. Nanotechnology versus other techniques in improving drug dissolution. Curr Pharm Des. 20(3):474-82.

Laha D, Pramanik A, Maity J, Mukherjee A, Pramanik P, Laskar A, Karmakar P. 2014. Interplay between autophagy and apoptosis mediated by copper oxide nanoparticles in human breast cancer cells MCF7. Biochim Biophys Acta.1840(1):1-9.

Landriscina A, Rosen J, Friedman AJ.2015. Biodegradable chitosan nanoparticles in drug delivery for infectious disease. Nanomedicine (Lond).10(10):1609-19.

Lara HH, Garza-Treviño EN, Ixtepan-Turrent L, Singh DK. 2011. Silver nanoparticles are broad-spectrum bactericidal and virucidal compounds. J Nanobiotechnol. 9:30.

Lasagna-Reeves C, Gonzalez-Romero D, Barria MA, Olmedo I, Clos A, Sadagopa Ramanujam VM, Urayama A, Vergara L, Kogan MJ, Soto C. 2010. Bioaccumulation and toxicity of gold nanoparticles after repeated administration in mice. Biochem Biophys Res Commun. 393(4):649-55.

Lee IC, Ko JW, Park SH, Lim JO, Shin IS, Moon C, Kim SH, Heo JD, Kim JC. 2016. Comparative toxicity and biodistribution of copper nanoparticles and cupric ions in rats. Int J Nanomedicine.11:2883-900.

Lee JH, Kim YS, Song KS, Ryu HR, Sung JH, Park JD, Park HM, Song NW, Shin BS, Marshak D, Ahn K, Lee JE, Yu IJ. 2013. Biopersistence of silver nanoparticles in tissues from Sprague-Dawley rats. Part Fibre Toxicol. 10:36.

Lee PC, Meisel D. 1982. Adsorption and surface-enhanced Raman of dyes on silver and gold sols. J Phys Chem. 86(17): 3391-3395.

Leroueil PR, Berry SA, Duthie K, Han G, Rotello VM, McNerny DQ, Baker JR,Orr BG, Holl MM. 2008.Wide varieties of cationic nanoparticles induce defects in supported lipid bilayers. Nano Lett. 8(2): 420–424.

Li F, Lei C, Shen Q, Li L, Wang M, Guo M, Huang Y, Nie Z, Yao S. 2013. Analysis of copper nanoparticles toxicity based on a stress-responsive bacterial biosensor array. Nanoscale. 5(2): 653-662.

Li L, Fernández-Cruz ML, Connolly M, Schuster M, Navas JM. 2015. Dissolution and aggregation of Cu nanoparticles in culture media: effects of incubation temperature and particles size. J. Nanopart. Res. 17:38.

Li SD, Huang L. 2008. Pharmacokinetics and biodistribution of nanoparticles. Mol Pharm. 5(4):496-504.

Lien Nghiem TH, Nguyen TT, Fort E, Nguyen TP, Hoang TMN, Nguyen T Q, Tran H N. 2012. Capping and *in vivo* toxicity studies of gold nanoparticles. Adv. Nat. Sci.: Nanosci. Nanotechnol.3:015002.

Lin PC, Lin S, Wang PC, Sridhar R. 2014. Techniques for physicochemical characterization of nanomaterials. Biotechnol Adv. 32 (4): 711–726.

Lin Z, Monteiro-Riviere NA, Riviere JE. 2015. Pharmacokinetics of metallic nanoparticles. Wiley Interdiscip Rev Nanomed Nanobiotechnol. 7(2):189-217.

Linse S, Cabaleiro-Lago C, Xue WF, Lynch I, Lindman S, Thulin E, Radford SE, Dawson KA. 2007. Nucleation of protein fibrillation by nanoparticles. Proc Natl Acad Sci U S A. 104(21):8691-8696.

Liptrott NJ, Kendall E, Nieves DJ, Farrell J, Rannard S, Fernig DG, Owen A.2014. Partial mitigation of gold nanoparticle interactions with human lymphocytes by surface functionalization with a 'mixed matrix'. Nanomedicine (Lond). 9(16):2467-79.

Liu Y, Tseng YC, Huang L. 2012. Biodistribution studies of nanoparticles using fluorescence imaging: A qualitative or quantitative method? Pharm Res. 29(12):3273–3277.

Loeschner K,Hadrup N,Qvortrup K,Larsen A,Gao X,Vogel U,Mortensen A,Lam HR,Larsen EH. 2011. Distribution of silver in rats following 28 days of repeated oral exposure to silver nanoparticles or silver acetate. Part Fibre Toxicol. 8:18.

Longmire M, Choyke PL, Kobayashi H. 2008. Clearance properties of nano-sized particles and molecules as imaging agents: considerations and caveats. Nanomedicine (Lond). 3(5):703-17.

Lopez-Serrano A, Olivas RM, Landaluze JS, Camara C. 2014. Nanoparticles: a global vision. characterization, separation, and quantification methods. Potential environmental and health impact. Anal Methods. 6 (1): 38-56.

Lowry OH, Rosebrough NJ, Farr AL, Randall RJ. 1951. Protein measurement with the folin phenol reagent. J Biol Chem. 193(1):265-75.

Loza K, Diendorf J, Sengstock C, Ruiz-Gonzalez L, Gonzalez-Calbet JM, Vallet-Regi M, Koller M, Epple M.2014. Dissolution and biological effects of silver nanoparticles in biological media. J Mater Chem. 2:1634-1643.

Luo S, Zhang E, Su Y, Cheng T, Shi C. 2011. A review of NIR dyes in cancer targeting and imaging. Biomaterials. 32(29):7127-38.

Luyts K, Napierska D, Nemery B, Hoet PHM. 2013. How physico-chemical characteristics of nanoparticles cause their toxicity: complex and unresolved interrelations. Environ. Sci Processes Impacts. 15(1): 23–38.

Ma O, Lavertu M, Sun J, Nguyen S, Buschmann MD,Winnik FM, Hoemann CD. 2008. Precise derivatization of structurally distinct chitosans with rhodamine B isothiocyanate. Carbohydr Polym. 72 (4): 616–624.

Mahapatro A, Singh DK.2011.Biodegradable nanoparticles are excellent vehicle for site directed *in vivo* delivery of drugs and vaccines. J Nanobiotechnology. 9:55.

Małaczewska J. 2011.The effect of silver nanoparticles on splenocyte activity and selected cytokine levels in the mouse serum at early stage of experimental endotoxemia. Pol J Vet Sci. 14 (4): 597-604.

Małaczewska J. 2015a. Effect of oral administration of commercial gold nanocolloid on peripheral blood leukocytes in mice. Pol J Vet Sci. 18(2):273-82.

Malaczewska J. 2015b. The splenocyte proliferative response and cytokine secretion in mice after oral administration of commercialgold nanocolloid. Pol J Vet Sci. 18(1):181-9.

Mallick A, More P, Syed MMK, Basu S. 2016. Nanoparticle-mediated mitochondrial damage induces apoptosis in cancer. ACS Appl Mater Interfaces. 8(21):13218–13231.

Malysheva A, Lombi E, Voelcker NH. 2015. Bridging the divide between human and environmental nanotoxicology. Nat Nanotechnol. 10(10): 835-44.

Mano SS, Kanehira K, Taniguchi A. 2013. Comparison of cellular uptake and inflammatory response via toll-like receptor 4 to lipopolysaccharide and titanium dioxide nanoparticles. Int J Mol Sci. 14 (7):13154-13170.

Martı´nez A, Iglesias I, Lozano R, Teijon, JM, Blanco MD. 2011. Synthesis and characterization of thiolated alginate albumin nanoparticles stabilized by disulfide bonds. Evaluation as drug delivery systems. Carbohydr Polym. 83(3): 1311–1321.

Maynard AD, Warheit DB, Philbert MA. 2011. The new toxicology of sophisticated materials: nanotoxicology and beyond. Toxicol Sci. 120 (Suppl 1): S109–S129.

McCauley J, Zivanovic A, Skropeta D. 2013. Bioassays for anticancer activities. Methods Mol Biol. 1055:191-205.

Meng H, Chen Z, Xing G, Yuan H, Chen C, Zhao F, Zhang C, Zhao Y. 2007. Ultrahigh reactivity provokes nanotoxicity: explanation of oral toxicity of nano-copper particles. Toxicol Lett. 175(1-3):102-10.

Milankovic SS. 2012. *In vivo* biodistribution of fluorescent nanocolloids intended for drug delivery. Evaluation of PEGylation state and fluorophore incorporation approach. Centre for Pharmacy, Department of Biomedicine, University of Bergen.

Mischak H, Kolch W, Goodnight J, Davidson WF, Rapp U, Rose-John S, Mushinski JF. 1991. Expression of protein kinase C genes in hemopoietic cells is cell-type- and B cell-differentiation stage specific. J Immunol.147(11): 3981-7.

Mishell BB, Shigii SM.1980. Selected methods in cellular immunology.W.H.Freeman & Co,San Fransisco,USA.

Mitchell LA, Lauer FT, Burchiel SW, McDonald JD. 2009. Mechanisms for how inhaled multiwalled carbon nanotubes suppress systemic immune function in mice. Nat Nanotechnol. 4(7): 451–456.

Miyajima A, Kitamura T, Harada N, Yokota T, Arai K. 1992. Cytokine receptors and signal transduction. Annu Rev Immunol.10: 295-331.

Mohanraj VJ, Chen Y. 2006. Nanoparticles – A Review. Trop J Pharm Res. 5 (1): 561-573.

Monroe JG, Cambier JC. 1983a. B cell activation. III. B cell plasma membrane depolarization and hyper-Ia antigen expression induced by receptor immunoglobulin cross-linking are coupled. J Exp Med. 158(5): 1589-99.

Mosmann T. 1983. Rapid colorimetric assay for cellular growth and survival: application to proliferation and cytotoxicity assays. J Immun methods. 65 (1-2):55-63.

Mosmann TR, Cherwinski H, Bond MW, Giedlin MA, Coffman RL. Two types of murine helper T cell clone. I. 1986. Definition according to profiles of lymphokine activities and secreted proteins. J Immunol. 136(7): 2348-57.

Moss DW, Henderson AK. 1994. Clinical enzymology, In Tietz Textbook of Clinical Chemistry, 3rd ed. Burtis CA, Ashwood ER, editors. Philadelphia: W.B Saunders Company. 617-721.

Moyano DF, Goldsmith M, Solfiell DJ, Landesman-Milo D, Miranda OR, Peer D, Rotello VM. 2012. Nanoparticle hydrophobicity dictates immune response. J Am Chem Soc. 134(9): 3965-7.

Mu Q, Jiang G, Chen L, Zhou H, Fourches D, Tropsha A, Yan B. 2015. Chemical basis of interactions between engineered nanoparticles and biological systems. Chem Rev.114(15):7740-81.

Myers CD. 1991. Role of B cell antigen processing and presentation in the humoral immune response. FASEB J. 5(11): 2547-53.

Nam J, Won N, Bang J, Jin H, Park J, Jung S, Jung S, Park Y, Kim S. 2013. Surface engineering of inorganic nanoparticles for imaging and therapy. Adv Drug Deliv Rev. 65(5):622-48.

Namvar F, Rahman HS, Mohamad R, Rasedee A, Yeap SK, Chartrand MS, Azizi S, Tahir P. 2015. Apoptosis induction in human leukemia cell lines by gold nanoparticles synthesized using the green biosynthetic approach. J Nanomater. http://dx.doi.org/10.1155/2015/642621.

Nemmar A, Yuvaraju P, Beegam S, Yasin J, Kazzam EE, Ali BH. 2016. Oxidative stress, inflammation, and DNA damage in multiple organs of mice acutely exposed to amorphous silica nanoparticles. Int J Nanomedicine. 11: 919-28.

Nie S. 2010. Understanding and overcoming major barriers in cancer nanomedicine. Nanomedicine (Lond). 5 (4): 523–528.

Nishizuka Y.1992. Intracellular signaling by hydrolysis of phospholipids and activation of protein kinase C. Science. 258(5082): 607-14.

Noël C, Simard JC, Girard D. 2016. Gold nanoparticles induce apoptosis, endoplasmic reticulam stress events and cleavage of cytoskeletal proteins in human neutrophils. Toxicol In Vitro. 31:12-22.

Norian R, Delirezh N, Azadmehr A. 2015. Evaluation of proliferation and cytokines production by mitogen-stimulated bovine peripheral blood mononuclear cells. Vet Res Forum. 6(4): 265–271.

Nune SK, Gunda P, Thallapally PK, Lin YY, Forrest ML, Berkland CJ. 2009. Nanoparticles for biomedical imaging. Expert Opin.Drug Deliv. 6:1175-1194.

Ohkawa H, Ohishi N, Yagi K. 1979. Assay for lipid peroxides in animal tissues by thiobarbituric acid reaction. Anal Biochem. 95(2): 35l-358.

Oostingh GJ,Casals E,Italiani P,Colognato R, Stritzinger R,Ponti J,Pfaller T,Kohl Y,Ooms D, Favilli F, Leppens H,Lucchesi D,Rossi F,Nelissen I, Thielecke H,Puntes VF,Duschl A,Boraschi D. 2011. Problems and challenges in the development and validation of human cell-based assays to determine nanoparticle-induced immunomodulatory effects. Part Fibre Toxicol. 8(1): 8

Ostrowski A, Nordmeyer D, Boreham A, Holzhausen C, Mundhenk L, Graf C, Meinke MC, Vogt A, Hadam S, Lademann J, Rühl E, Alexiev U,Gruber AD. 2015. Overview about the localization of nanoparticles in tissue and cellular context by different imaging techniques. Beilstein J Nanotechnol. 6:263-80.

Pante N, Kann M. 2002. Nuclear pore complex is able to transport macromolecules with diameters of 39 nm. Mol Biol Cell. 13 (2): 425–434.

Park EJ, Bae E, Yi J, Kim Y, Choi K, Lee SH, Yoon J, Lee BC, Park K. 2010. Repeated-dose toxicity and inflammatory responses in mice by oral administration of silver nanoparticles. Environ Toxicol Pharmacol. 30(2):162-8.

Park EJ, Kim SN, Kang MS, Lee BS, Yoon C, Jeong U, Kim Y, Lee GH, Kim DW, Kim JS. 2016. A higher aspect ratio enhanced bioaccumulation and altered immune responses due to intravenously-injected aluminum oxide nanoparticles. J Immunotoxicol. 13(4):439-48.

Parkhouse RM. 1990. Three B cell surface molecules associating with membrane immunoglobulin. Immunology. 69(2): 298-302.

Parnsamut C, Brimson S. 2015. Effects of silver nanoparticles and gold nanoparticles on IL-2, IL-6, and TNF-α production via MAPK pathway in leukemic cell lines. Genet Mol Res. 14(2):3650-68.

Patlolla AK, Hackett D,Tchounwou PB. 2015.Silver nanoparticle induced oxidative stress-dependent toxicity in sprague-dawley rats. Mol Cell Biochem. 399(1-2): 257–268.

Patra HK, Banerjee S, Chaudhuri U, Lahiri P, Dasgupta AK. 2007. Cell selective response to gold nanoparticles. Nanomedicine. 3(2):111-9.

Pleiman CM, D'Ambrosio D, Cambier JC. 1994. The B-cell antigen receptor complex: structure and signal transduction. Immunol Today. 15(9): 393-9.

Pourhamzeh M, Mahmoudian ZG, Saidijam M, Asari MJ, Alizadeh Z. 2016. The effect of silver nanoparticles on the biochemical parameters of liver function in serum, and the expression of caspase-3 in the liver tissues of male rats. Avicenna. J. Med. Biochem. DOI: 10.17795/ajmb-35557.

Powell JJ, Faria N, Thomas-McKay E, Pele LC. 2010. Origin and fate of dietary nanoparticles and microparticles in the gastrointestinal tract. J Autoimmun. 34 (3): J226–J233.

Prathna TC, Chandrasekaran N, Mukherjee A. 2011. Studies on aggregation behaviour of silver nanoparticles in aqueous matrices: Effect of surface functionalization and matrix composition. Colloids Surf A. 390(1-3):216-224.

Qi L, Xu Z, Jiang X, Li Y, Wang M. 2005.Cyotoxic activities of chitosan nanoparticles and copper-loaded nanoparticles.Bioorg Med Chem Lett. 15:1397-1399.

Radomski A, Jurasz P, Alonso-Escolano D, Drews M, Morandi M, Malinski T, Radomski MW. 2005. Nanoparticle-induced platelet aggregation and vascular thrombosis. Br J Pharmacol. 146(6):882–893.

Rambanapasi C, Barnard N,Grobler A,Buntting H,Sonopo M,Jansen D, Jordaan A,Steyn H,Zeevaart JR. 2015. Dual radiolabeling as a technique to track nanocarriers: the case of gold nanoparticles. Molecules. 20: 12863-12879

Rambanapasi C, Zeevaart JR,Buntting H,Bester C,Kotze D,Hayeshi R,Grobler A. 2016. Bioaccumulation and subchronic toxicity of 14 nm gold nanoparticles in rats. Molecules, 21: 763.

Rathore M, Ray Mohanty IR, Maheswari U, Dayal N, Suman R,Joshi DS. 2014. Comparative in vivo assessment of the subacute toxicityof gold and silver nanoparticles. J Nanopart Res. 16:2338

Rivera-Gil P, Jimenez de Aberasturi D, Wulf V, Pelaz B, del Pino P, Zhao Y, de la Fuente JM, Ruiz de Larramendi I, Rojo T, Liang XJ, Parak WJ. 2013. The challenge to relate the physicochemical properties of colloidal nanoparticles to their cytotoxicity. Acc Chem Res. 46(3):74

Rizzello L, Pompa PP. Nanosilver-based antibacterial drugs and devices: Mechanisms, methodological drawbacks, and guidelines. Chem Soc Rev. 43(5): 1501—1518.

Roduner E. 2006. Size matters: why nanomaterials are different. Chem Soc Rev. 35 (7): 583–592.

Ryan JJ, Bateman HR, Stover A, Gomez G, Norton SK, Zhao W, Schwartz LB, Lenk R, Kepley CL. Fullerene nanomaterials inhibit the allergic response. J Immunol. 179 (1): 665–672.

Sabella S, Carney RP, Brunetti V, Malvindi MA, Al-Juffali N, Vecchio G, Janes SM, Bakr OM, Cingolani R, Stellacci F, et al. 2014. A general mechanism for intracellular toxicity of metal-containing nanoparticles. Nanoscale. 6:7052-7061.

Salvati A, Pitek AS, Monopoli MP, Prapainop K, Bombelli FB, Hristov DR, Kelly PM, Åberg C, Mahon E, Dawson KA. 2013. Transferrin-functionalized nanoparticles lose their targeting capabilities when a biomolecule corona adsorbs on the surface. Nat Nanotechnol. 8 (2): 137-143.

Sapsford KE, Tyner KM, Dair BJ, Deschamps JR, Medintz IL. 2011. Analyzing nanomaterial bioconjugates: a review of current and emerging purification and characterization techniques. Anal Chem. 83(12): 4453–88.

Schleh C, Semmler-Behnke M, Lipka J, Wenk A, Hirn S, Schäffler M, Schmid G, Simon U, Kreyling WG. 2012. Size and surface charge of gold nanoparticles determine absorption across intestinal barriers and accumulation in secondary target organs after oral administration. Nanotoxicology. 6(1): 36–46.

Scott Jr., TA & Melvin EH. 1953. Determination of Dextran with Anthrone. Anal Chem. 25 (11):1656–1661.

Seigneuric R, Markey L, Nuyten DSA, Dubernet C, Evelo CTA, Finot E, Garrido C. 2010. From nanotechnology to nanomedicine: applications to cancer research. Curr Mol Med. 10(7):640-52.

Sekhon BS, Kamboj SR. 2010. Inorganic nanomedicine-Part 1. Nanomedicine. 6 (4): 516–522.

Sengupta S, Eavarone D, Capila I, Zhao G, Watson N, Kiziltepe T, Sasisekharan R.2005. Temporal targeting of tumour cells and neovasculature with a nanoscale delivery system. Nature. 436(7050):568-72.

Shafagh M, Rahmani F, Delirezh N. 2015.CuO nanoparticles induce cytotoxicity and apoptosis in human K562 cancer cell line via mitochondrial pathway, through reactive oxygen species and P53.Iran J Basic Med Sci. 18(10): 993–1000.

Shaffer AL, Rosenwald A, Staudt LM. 2002. Lymphoid malignancies: the dark side of B-cell differentiation. Nat Rev Immunol. 2(12):920-32.

Shang L, Nienhaus K, Nienhaus GU. 2014. Engineered nanoparticles interacting with cells: size matters. J. Nanobiotechnology. 12:5.

Sharma VK, Yngard RA, Lin Y. 2009. Silver nanoparticles: Green synthesis and their antimicrobial activities. Adv Colloid Interface Sci. 145(1-2): 83–96.

Shen CC, Wang CC, Liao MH, Jan TR. 2011. A single exposure to iron oxide nanoparticles attenuates antigen-specific antibody production and T-cell reactivity in ovalbumin-sensitized BALB/c mice. Int J Nanomedicine. 6: 1229–1235.

Shibata A, Furukawa K, Abe H, Tsuneda S, Ito Y. 2008. Rhodamine-based fluorogenic probe for imaging biological thiol. Bioorg Med Chem Lett. 18(7):2246-9.

Shukla R, Bansal V, Chaudhary M, Basu A, Bhonde RR, Sastry M. 2005. Biocompatibility of gold nanoparticles and their endocytotic fate inside the cellular compartment: a microscopic overview. Langmuir. 21(23): 10644–10654.

Siddiqui MA, Alhadlaq HA, Ahmad J, Al-Khedhairy AA, Musarrat J, Ahamed M. 2013.Copper oxide nanoparticles induced mitochondria mediated apoptosis in human hepatocarcinoma cells. PLoS One. 8(8):e69534.

Singh P, Kim YJ, Zhang D, Yang DC. 2016. Biological synthesis of nanoparticles from plants and microorganisms. Trends Biotechnol. 34(7):588-99.

Slot C. 1965. Plasma creatinine determination. A new and specific Jaffe reaction method. Scand J Clin Lab Invest. 17(4):381-7.

Smith DM, Simon JK, Baker JR Jr. 2013. Applications of nanotechnology for immunology. Nat Rev Immunol. 13(8): 592-605.

Stensberg MC, Wei Q, McLamore ES, Porterfield DM, Wei A, Sepúlveda MS. 2011. Toxicological studies on silver nanoparticles: challenges and opportunities in assessment, monitoring and imaging.Nanomedicine (Lond). 6(5): 879–898.

Szunerits S, Boukherroub R. 2012. Sensing using localised surface plasmon resonance sensors.Chem Commun (Camb). 48(72):8999-9010.

Takahashi H, Sawada S, Akiyoshi K. 2011. Amphiphilic polysaccharide nanoballs: a new building block for nanogel biomedical engineering and artificial chaperones. ACS Nano. 5 (1): 337–345.

Talka, H. Schubert, G.E. 1965. Enzymatic urea determination in the blood and serum in the warburg optical test. Klin. Wochschr. 43: 174-5.

Tan Y, Li S, Pitt BR, Huang L. 1999. The inhibitory role of CpG immunostimulatory motifs in cationic lipid vector-mediated transgene expression *in vivo*. Hum Gene Ther. 10(13): 2153-61.

Terai T, Nagano T. 2008. Fluorescent probes for bioimaging applications. Curr Opin Chem Biol. 12(5):515-21.

Thakkar KN, Mhatre SS, Parikh RY. 2010. Biological synthesis of metallic nanoparticles. Nanomedicine. 6 (2): 257–262.

Tiwari PM, Vig K, Dennis VA, Singh SR. 2011. Functionalized gold nanoparticles and their biomedical applications. Nanomaterials. 1(1): 31-63.

Tkach AV, Shurin GV, Shurin MR, Kisin ER, Murray AR, Young SH, Star A, Fadeel B, Kagan VE, Shvedova AA. 2011. Direct effects of carbon nanotubes on dendritic cells induce immune suppression upon pulmonary exposure. ACS Nano. 5(7): 5755–5762.

Tong R, Kohane DS. 2012. Shedding light on nanomedicine. Wiley Interdiscip Rev Nanomed Nanobiotechnol. 4(6): 638–662.

Tsai CY, Lu SL, Hu CW, Yeh CS, Lee GB, Lei HY. 2012. Size-dependent attenuation of TLR9 signaling by gold nanoparticles in macrophages. J Immunol. 188 (1): 68-76.

Tsutsumi Y, Yoshioka Y. 2011. Quantifying the biodistribution of nanoparticles. Nat Nanotechnol. 6(12):755.

Turabekova M, Rasulev B, Theodore M, Jackman J, Leszczynska D, Leszczynski J. 2014. Immunotoxicity of nanoparticles: a computational study suggests that CNTs and C60 fullerenes might be recognized as pathogens by Toll-like receptors. Nanoscale. 6 (7): 3488–3495.

Turkevich J, Stevenson PC, Hillier J. 1951. A Study of the nucleation and growth processes in the synthesis of colloidal gold. Discuss Faraday Soc. 11, 55–75.

Umer A, Naveed S, Ramzan N.2012. Selection of a suitable method for the synthesis of copper nanoparticles. Nano. 7(5):1230005.

Van der Zande M, Vandebriel RJ, Van Doren E, Kramer E, Herrera Rivera Z, Serrano-Rojero CS, Gremmer ER, Mast J, Peters RJ, Hollman PC, Hendriksen PJ, Marvin HJ, Peijnenburg AA, Bouwmeester H. 2012. Distribution, elimination, and toxicity of silver nanoparticles and silver ions in rats after 28-Day oral exposure. ACS Nano. 6(8):7427-42.

Vandebriel RJ, Tonk EC, de la Fonteyne-Blankestijn LJ, Gremmer ER, Verharen HW, van der Ven LT, van Loveren H, de Jong WH. 2014. Immunotoxicity of silver nanoparticles in an intravenous 28-day repeated-dose toxicity study in rats. Part Fibre Toxicol. 11:21.

Vardanyan Z, Gevorkyan V, Ananyan M,Vardapetyan H, Trchounian A. 2015. Effects of various heavy metal nanoparticles on *Enterococcus hirae* and *Escherichia coli* growth and proton-coupled membrane transport. J Nanobiotechnology. 13:69.

Vatsan RS, Bross PF, Liu K1, Theoret M, De Claro AR, Lu J, Helms W, Niland B, Husain SR, Puri RK. 2013. Regulation of immunotherapeutic products for cancer and FDA's role in product development and clinical evaluation. J Immunother Cancer. 1:5.

Vauthier C, Bouchemal K. 2009. Methods for the preparation and manufacture of polymeric nanoparticles. Pharm Res. 26 (5): 1025-1058.

Vijayakumar S, Ganesan S. 2012. *In vitro* cytotoxicity assay on gold nanoparticles with different stabilizing agents. J Nanomater. http://dx.doi.org/10.1155/2012/734398

Vonarbourg A, Passirani C, Saulnier P, Simard P, Leroux JC, Benoit JP. 2006. Evaluation of PEGylated lipid nanocapsules versus complement system activation and macrophage uptake. J Biomed Mater Res A. 78(3): 620-8.

Wagner SC, Roskamp M, Pallerla M, Araghi RR, Schlecht S, Koksch B. 2010. Nanoparticle-induced folding and fibril formation of coiled-coil-based model peptides. Small. 6(12): 1321–1328.

Walkey CD, Olsen JB, Guo H, Emili A, Chan WC. 2012. Nanoparticle size and surface chemistry determine serum protein adsorption and macrophage uptake. J Am Chem Soc. 134 (4): 2139–2147.

Wang F, Yu L, Monopoli MP, Sandin P, Mahon E, Salvati A, Dawson KA. 2013. The biomolecular corona is retained during nanoparticle uptake and protects the cells from the damage induced by cationic nanoparticles until degraded in the lysosomes. Nanomedicine. 9(8): 1159–1168.

Wang JJ, Zeng ZW, Xiao RZ, Xie T, Zhou GL, Zhan XR, Wang SL. 2011. Recent advances of chitosan nanoparticles as drug carriers. Int J Nanomedicine. 6: 765–774.

Wang L, Min Y, Xu D, Yu F, Zhou W, Cuschieri A. 2014. Membrane lipid peroxidation by the peroxidase-like activity of magnetite nanoparticles. Chem commun (Camb). 50 (76): 11147-11150.

Wen J, Xu Y, Li H, Lu A, Sun S. 2015. Recent applications of carbon nanomaterials in fluorescence biosensing and bioimaging. Chem. Commun (Camb). 51 (57):11346-58.

Yacobi NR, Malmstadt N, Fazlollahi F, DeMaio L, Marchelletta R, Hamm-Alvarez SF, Borok Z, Kim KJ, Crandall ED. 2010. Mechanisms of alveolar epithelial translocation of a defined population of nanoparticles. Am J Respir Cell Mol Biol. 42(5): 604–614.

Yamagishi Y,Watari A,Hayata Y, Li X,Kondoh M,Yoshioka Y,Tsutsumi Y,Yagi K. 2013. Acute and chronic nephrotoxicity of platinum nanoparticles in mice.Nanoscale Res Lett. 8(1): 395.

Yamashita K, Yoshioka Y, Higashisaka K, Mimura K, Morishita Y, Nozaki M, Yoshida T, Ogura T, Nabeshi H, Nagano K, Abe Y, Kamada H, Monobe Y, Imazawa T, Aoshima H, Shishido K, Kawai Y, Mayumi T, Tsunoda Si, Itoh N,Yoshikawa T, Yanagihara I, Saito S, Tsutsumi Y. 2011. Silica and titanium dioxide nanoparticles cause pregnancy complications in mice. Nat Nanotechnol. 6 (5): 321–328.

Yang EJ, Kim S, Kim JS, Choi IH. 2012. Inflammasome formation and IL-1beta release by human blood monocytes in response to silver nanoparticles. Biomaterials. 33 (28): 6858–6867.

Yang ST, Wang X, Jia G, Gu Y, Wang T, Nie H, Ge C, Wang H, Liu Y. 2008. Long-term accumulation and low toxicity of single-walled carbon nanotubes in intravenously exposed mice. Toxicol. Lett. 181: 182–189.

Yao Q, Liu W, Gou XJ, Guo XQ, Yan J, Song Q, Chen FZ, Zhao Q, Chen C, Chen T. 2013.Preparation, characterization, and cytotoxicity of various chitosan nanoparticles. J Nanomat. http://dx.doi.org/10.1155/2013/183871.

Yildirimer L, Thanh NTK, Loizidou M, Seifalian AM. 2011. Toxicology and clinical potential of nanoparticles. Nanotoday. 6(6): 585–607

Yu X, Di Y, Xie C, Song Y, He H, Li H, Pu X, Lu W, Fu D, Jin C.2015. An *in vitro* and *in vivo* study of gemcitabine-loaded albumin nanoparticles in a pancreatic cancer cell line. Int J Nanomedicine. 10: 6825–6834.

Yu Z, Yu M, Zhang Z, Hong G, Xiong Q. 2014. Bovine serum albumin nanoparticles as controlled release carrier for local drug delivery to the inner ear. Nanoscale Res Lett. 9:343.

Yue ZG, Wei W, Lv PP, Yue H, Wang LY, Su ZG, Ma GH. 2011. Surface charge affects cellular uptake and intracellular trafficking of chitosan-based nanoparticles. Biomacromolecules. 12: 2440–2446.

Yun Y, Cho YW, Park K. 2013.Nanoparticles for oral delivery: Targeted nanoparticles with peptidic ligands for oral protein delivery. Adv Drug Deliv Rev. 65(6): 822–832.

Zabetakis K, Ghann WE, Kumar S, Daniel M. 2012.Effect of high gold salt concentrations on the size and polydispersity of gold nanoparticles prepared by an ex-tended Turkevich-Frens method.Gold Bulletin. 45(4):203-211.

Zaman M, Ahmad E, Qadeer A, Rabbani G, Khan RH. 2014. Nanoparticles in relation to peptide and protein aggregation. Int J Nanomedicine. 9: 899–912.

Zazo H, Colino CI, Lanao JM. 2016. Current applications of nanoparticles in infectious diseases. J Control Release. 224:86-102.

Zhang J, Xia W, Liu P, Cheng Q, Tahirou T, Gu W, Li B.2010b. Chitosan modification and pharmaceutical/biomedical applications. Mar Drugs. 8:1962-87.

Zhang XD,Wu HY,Wu D,Wang YY,Chang JH,Zhai ZB,Meng AM,Liu PX,Zhang LA,Fan FY. 2010a. Toxicologic effects of gold nanoparticles *in vivo* by different administration routes. Int J Nanomedicine. 5: 771–781.

Zhang Y, Bai Y, Jia J, Gao N, Li Y, Zhang R, Jiang G, Yan B. 2014.Perturbation of physiological systems by nanoparticles. Chem Soc Rev. 43(10):376-3809.

Zhao D, Zhao X, Zu Y, Li J, Zhang Y, Jiang R, Zhang Z. 2010. Preparation, characterization, and *in vitro* targeted delivery of folate-decorated paclitaxel-loaded bovine serum albumin nanoparticles. Int J Nanomedicine. 5: 669–677.

Zhao Y, Wang B, Feng W, Bai C. 2014. Nanotoxicology: toxicological and biological properties of nanomaterials. Encyclopedia of life support systems. Available from: http://www.eolss.net.

Zimmerman DH, Kern M.1973. Differentiation of lymphoid cells: Effect of serum and other mitogenic agents on the selective induction of immunoglobulin M secreting lymph node cells in tissue culture. J Immunol. 111 (5):1326-1333.

Zlobina OV, Pakhomiy SS, Bucharskaya AB, Bugaeva IO, Maslyakova GN, Khlebtsov NG, Khlebtsov BN, Bogatyrev VA. 2013. Accumulation and biodistribution of gold nanoparticles in the mesenteric lymph nodes at oral administration. Russ Open Med J. 2: 0301.

JOURNAL OF IMMUNOTOXICOLOGY, 2016
http://dx.doi.org/10.1080/1547691X.2016.1234522

Taylor & Francis
Taylor & Francis Group

RESEARCH ARTICLE

Immunotoxic effects of gold and silver nanoparticles: inhibition of mitogen-induced proliferative responses and viability of human and murine lymphocytes in vitro

Mallaiah Devanabanda, Shaik Latheef and Ramanadham Madduri

Cellular Immunology Laboratory, Department of Biochemistry, School of Life Sciences, University of Hyderabad, Hyderabad, India

ABSTRACT

Understanding the effects of nanoparticles (NP) on immune cell functions is essential in designing safe and effective NP-based in vivo drug delivery systems. The immunomodulatory potential of gold nanoparticles (GNP) and silver nanoparticles (SNP) was investigated in vitro using murine splenic and human peripheral blood lymphocytes (PBL) in terms of effects on viability and mitogen-induced proliferation. Hydrodynamic size and number of NP were characterized using NP tracking analysis (NTA); modal diameters of GNP and SNP were 28 (±1.5) and 66 (±2.7) nm, respectively, with a unimodal distribution. Lymphocytes were incubated with GNP or SNP in the presence/absence of B- or T-cell mitogens and proliferative responses then determined using [^{3}H]-thymidine incorporation. Concanavalin A (T-cell-specific) and lipopolysaccharide- (B-cell-specific) stimulated responses of murine splenic lymphocytes, as well as phytohemagglutinin (T-cell-specific) and pokeweed mitogen- (B-and T-cell specific) induced responses of human lymphocytes, were significantly inhibited by GNP (25–200 μg/ml) and SNP (12.5–50 μg/ml). However, [^{3}H]-thymidine incorporation by unstimulated lymphocytes was unaffected in the presence of GNP or SNP. Viability of lymphocytes was determined using trypan blue dye exclusion and was significantly inhibited only at 200 GNP μg/ml and 25 or 50 μg SNP/ml. As mitogen responses are most useful to provide supportive mechanistic information on primary immunotoxicologic functional observations, and so far more comprehensive data (in vivo and in vitro) is still needed, the results nevertheless suggest to us that GNP and SNP might potentially be able to modulate immune responses by impacting on lymphocyte activation.

ARTICLE HISTORY
Received 17 August 2016
Accepted 6 September 2016
Published online 2 2 2

KEYWORDS
Gold; immunotoxic; lymphocytes; nanoparticles; proliferation; silver

Introduction

Nanoparticles (NP) have unique characteristics such as a small size, large surface area per unit mass, surface charge and an ability to exist in different stable geometric forms. These properties have been exploited for industrial and biomedical applications (Corot et al., 2006). Use of NP in consumer products has also been steadily growing; this has led to rising concern regarding their overall biosafety (Mironava et al., 2010; Vance et al., 2015).

Gold nanoparticles (GNP) have been used in many areas of medicine that include diagnostics, imaging, biosensing, drug delivery and cancer therapy. An amenability to functionalization with bioactive ligands, internalization by cells, a presence of a high electron density, size-dependent optical properties, thermal stability, etc. are some of the important features of GNP that have been exploited in biomedical applications (Mironava et al., 2010; Tomic et al., 2014). Silver nanoparticles (SNP) have been predominantly used in a variety of consumer and medical products primarily due to their apparent anti-bacterial properties (Rai et al., 2009; Vance et al., 2015; Vergallo et al., 2014).

Although there are potential beneficial uses of GNP and SNP, there are also untoward effects from exposure to these agents. Effects of GNP on dendritic cells and malignant B and T cells has been reported (Bhattacharya et al., 2007; Mukherjee et al., 2007; Villiers et al., 2010). Interestingly, GNP selectively inhibited the proliferation of myeloma cells, but had no effect on the proliferation of human peripheral blood lymphocytes (PBL) (Bhattacharya et al., 2007). Similarly, exposure of experimental animals to SNP has been shown to cause anemia, cardiac enlargement, growth retardation and degenerative changes in the liver (Butler et al., 2015). With regard to the immune system, the viability of human PBL was decreased in time- and dose-dependent manners upon exposure to SNP in vitro (Ghosh et al., 2012; Vergallo et al., 2014; Zhornik et al., 2014).

To better understand the adverse effects of NP in general, information on the response of different cell types—including immune cells—in terms of NP concentration, size, shape, surface composition and time is needed (Liu et al., 2013). Studies of the effects of NP on immune cells are generally scant (Becker et al., 2014; Hussain et al., 2012). Hence, there remains a pressing need to evaluate effects of various types of NP on immune cell function (Dobrovolskaia & McNeil, 2007; Dobrovolskaia et al., 2008; Elsabahy & Wooley, 2013; Zolnik et al., 2010). Accordingly, the present study was designed to evaluate effects of GNP and SNP on lymphocyte activation by mitogens in vitro to begin to provide some information (note: mitogen responses are most useful to provide supportive mechanistic information on primary immunotoxicologic functional observations) to better define potential immunotoxicities of these types of particles.

CONTACT Dr. Ramanadham Madduri mrnsl@uohyd.ernet.in Cellular Immunology Laboratory, Department of Biochemistry, School of Life Sciences, University of Hyderabad, Hyderabad 500046, India

Materials and methods

Chemicals

RPMI 1640, penicillin G, streptomycin, pokeweed mitogen (PWM), phytohemagglutinin (PHA), Concanavalin A (ConA), lipopolysaccharide (LPS, type 055:B5 from Escherichia coli), heparin and Histopaque (q ¼ 1.077 g/ml) were procured from Sigma (Hyderabad, India). [^{3}H]-Thymidine (specific activity ¼46.5 Ci/mmol) was purchased from BRIT (Mumbai, India). Fetal calf serum (FCS) was obtained from Biological Industries (Kibbutz Beit-Haemek, Israel). All other chemicals used were obtained from SRL Chemicals (Mumbai) and were analytical grade.

Preparation and characterization of GNP and SNP

Both GNP and SNP were synthesized using a chemical reduction method with trisodium citrate (Lee & Meisel, 1982; Basu et al., 2007). GNP and SNP formed in the suspension were sedimented by centrifugation (11 000g, 20 min) to remove excess citrate. Each NP pellet was then suspended in ultrapure water and stored at 4 C. Yields of each NP were calculated gravimetrically (typical yields of GNP and SNP were 73 and 60%, respectively). Characterizations (e.g. size, number and distribution) of each preparation were done using nanoparticle tracking analysis (NTA) (NanoSight, Malvern Instruments, Malvern, UK) as per protocols supplied by the manufacturer. For use in the assays outlined below, NP suspensions were sterile filtered using a 0.45-**1**m pore diameter membrane filter before use in cell culture.

Mouse splenic lymphocytes

Naïve C57BL/6J mice (female, 8–12-week-of-age) were obtained from the National Center for Laboratory Animal Sciences (National Institute of Nutrition, Hyderabad, India). All mice were housed under specific pathogen-free conditions in the University of Hyderabad Animal Facility maintained at 25 ± 2 C with a 50% relative humidity and 12 h light–dark cycle. Mice were provided ad libitum access to a standard rodent chow pellet diet and filtered water. The Institutional Animal Ethics Committee of the University of Hyderabad approved all of these studies.

As a source of splenic lymphocytes for these studies, each mouse was euthanized by ether anesthesia and their spleen aseptically removed at necropsy. The organ was placed in RPMI 1640 containing 5% FCS (complete medium) and single-cell suspensions of splenic lymphocytes then prepared as described in Zimmerman et al. (1977).

Human blood lymphocytes

Blood was drawn from consenting healthy volunteers at the University Health Center clinic. Lymphocytes from each heparinized sample were isolated by density gradient separation over Histopaque (Boyum, 1964). After isolation, enumeration of cell number and viability were carried out and the samples were used in the assays below. The Human Ethics Committee of the University of Hyderabad approved all of these protocols prior to any blood draw.

Lymphocyte proliferation assay

Lymphocytes (0.2 10^6 in 200 **1**l complete medium) from the mice or humans were placed into dedicated wells of 96-well flat-bottomedmicrotiter plates (Corning, NY). Triplicate wells then received different concentrations of each NP and also either medium or mitogen (ConA, LPS, PHA or PWM) at their optimal concentrations (Kasyapa & Ramanadham, 1992). After being cultured for 48 h at 37 C in a 5% CO_2 incubator, the cultures were pulsed with 0.5 **1**Ci [^{3}H]-thymidine and incubated a further 24 h. The cultures were then processed using an automatic cell harvester (Skatron, Oslo, Norway) and radioactivity in the harvested materials was measured in a scintillation counter (Beckman Coulter, Indianapolis, IN). The obtained cpm (counts per minute) for each sample was corrected for percentage of viable cells present. Proliferative responses were expressed in terms of stimulation index (SI) ¼ [average cpm in presence of mitogen (or mitogen þ NP)/average cpm with cells only]. Taking the SI of control cells stimulated with mitogen as 100%, proliferative responses for experimental samples treated with mitogen and NP were then calculated and expressed as % of control.

Determination of lymphocyte viability

Viability of the lymphocytes treated with different concentrations of each NP for 72 h (in absence of any mitogen) was determined using trypan blue dye exclusion. A minimum of 300 cells were evaluated/sample and data recorded for total cell number and dead cells (dye-stained). Viability was then expressed as % live of total cell number.

Statistical analysis

Data were expressed as means ± standard error of mean (SEM). Statistical analysis and significance were each evaluated using a one-way analysis of variance (ANOVA) followed by a post-hoc Tukey test. All analyzes were performed using Sigma Plot 11 software (Systat, San Jose, CA). Differences between control and treated samples were considered significant at $p < .05$.

Results

NP characterization

NTA data from a representative experiment are presented in Figure 1; pooled data from four individual NP preparations are presented (Table 1). The GNP showed a unimodal distribution (Figure 1A) with mean and modal diameters of 50 and 28 nm, respectively. The average number of particles in the GNP suspension was 0.59 10^9/**1**g (Table 1). The SNP also showed a unimodal distribution (Figure 1B) with mean and modal diameters of 76 and 66 nm, respectively. The average number of particles in the SNP suspension was 0.48 10^9/**1**g (Table 1).

Effect of GNP and SNP on murine splenic lymphocyte and human PBL viability

Murine splenic lymphocytes and human PBL were incubated with GNP or SNP for 72 h and their viability then determined. Viability of both populations was significantly reduced only by 200 **1**g GNP/ml (Figure 2A). In comparison, SNP inhibited viability of murine splenic lymphocytes at 25 and 50 **1**g/ml, whereas viability of human PBL was inhibited only at 50 **1**g/ml (Figure 2B).

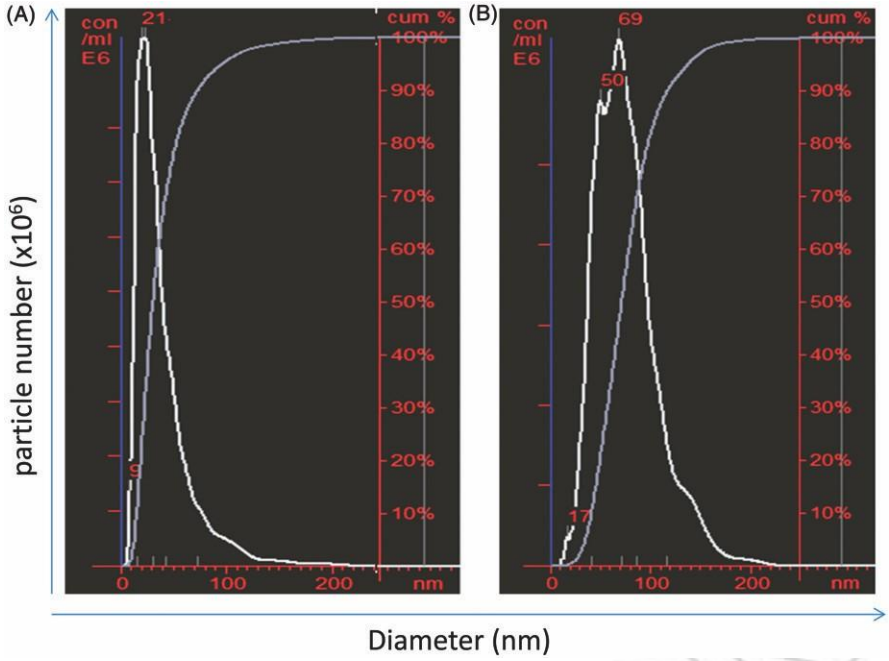

COLOR Online / B&W in Print

Figure 1. Size distribution and particle concentration. Measurements obtained using NTA. (A) GNP. (B) SNP. Graph presented is representative of four independent experiments. x-axis: diameter (nm); y-axis: particle number (10^6/ml).

Table 1. Distribution of size and number determined by NTA.

Sample	Preparation	Concentration (10^9/lg)	Diameter (nm): mean, mode
1	GNP	0.59 ± 0.06	50.0 ± 5.0, 28.0 ± 1.5
2	SNP	0.48 ± 0.03	76.0 ± 1.8, 66.0 ± 2.7

Values shown are means (±SEM) of four independent experiments.

Effect of GNP and SNP on [^{3}H]-thymidine incorporation by unstimulated murine splenic lymphocytes and human PBL

[^{3}H]-Thymidine incorporation by unstimulated lymphocytes in a presence of increasing levels of GNP and SNP is shown in Figure 3. Incorporation was unaffected by GNP at all the levels tested and remained near that of the control cultures (Figure 3A). Interestingly, SNP appeared to somewhat stimulate the mouse cells at most of the test doses, but these effects were not significant (Figure 3B). At 50 lg SNP/ml, the effect on mouse cells led to a value significantly lower level of thymidine incorporation than that of the control cells ($p < .05$). In comparison, the human cells were moreover unaffected by the SNP, albeit that there again was significantly inhibited incorporation at 50 lg SNP/ml ($p < .05$, Figure 3B).

Effect of GNP and SNP on mitogen-induced in vitro proliferative response of murine splenic lymphocytes and human PBL

[^{3}H]-Thymidine incorporation for each sample was corrected for corresponding cell viability and the SI then calculated. Thus, data presented in Figure 4 represents proliferative responses of equal numbers of viable lymphocytes in each sample.

When murine lymphocytes were incubated with GNP at 5–200 lg/ml (3.0–120 10^9 particles/ml; NP:cell ratios of 3 103–120 10^3) in the presence of LPS or ConA, the ConA-stimulated proliferation was significantly inhibited starting at 25 lg GNP/ml ($p < .05$, Figure 4A). The LPS-stimulated proliferation was inhibited starting at 50 lg GNP/ml ($p < .05$, Figure 4A). When the mouse lymphocytes were treated with SNP at 5–50 lg/ml (2.4–24 10^9 particles/ml; NP:cell ratios of 2.4 103–24 10^3) in the presence of LPS or ConA, responses induced by each were significantly inhibited starting at 12.5 lg SNP/ml ($p < .05$, Figure 4B). In both cases, the outcomes appeared dose-related but the effects as a function of specific mitogen did not differ.

With human cells, proliferative responses of PBL stimulated with PHA or PWM were significantly inhibited starting again at 25 lg GNP/ml ($p < .05$, Figure 5A) and at 12.5 lg SNP/ml ($p < 0.05$, Figure 5B). Again, in both cases, the outcomes appeared dose-related. However, in this set of studies, the effects as a function of specific mitogen did seem to differ, with the effects on induction by PHA being less impacted than that by PWM.

To evaluate whether free gold and silver ions released from NP could play a role in the observed effects, particle-free supernatants were collected from GNP and SNP incubated in culture medium. Specifically, GNP (50 and 200 lg/ml) and SNP (12.5 and 50 lg/ml) were incubated in RPMI 1640 containing 5% FCS for 72 h before NP-free supernatants were obtained by centrifugation under sterile conditions. Murine splenic lymphocytes and human PBL were then cultured in the above mentioned supernatants in the presence of mitogens (LPS, ConA, PHA and PWM) and proliferative responses assessed. Mitogen-induced proliferation was unaffected by a presence of GNP or SNP supernatants at the investigated concentrations (Figures 6A and B). Overall, mitogen-induced proliferation of murine splenic lymphocytes as well as human PBL was inhibited by GNP and SNP without any significant effect on cell viability.

Discussion

Metallic NP have been proposed for wide use in biomedical imaging, cancer therapy and as anti-microbial agents (Almeida et al., 2014; Lara et al., 2011; Nune et al., 2009). In order to use NP as carriers of drugs and other biologically active ligands in vivo, it is necessary to evaluate their biocompatibility

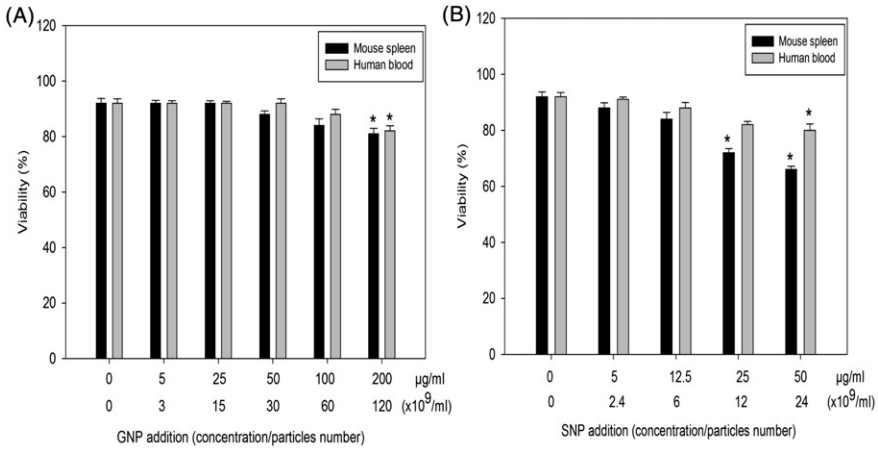

Figure 2. Effects of NP on mouse splenic lymphocyte and human PBL viability. (A) GNP. (B) SNP. Data shown are means (±SEM) of three experiments. $p < .05$, NP treated versus control.

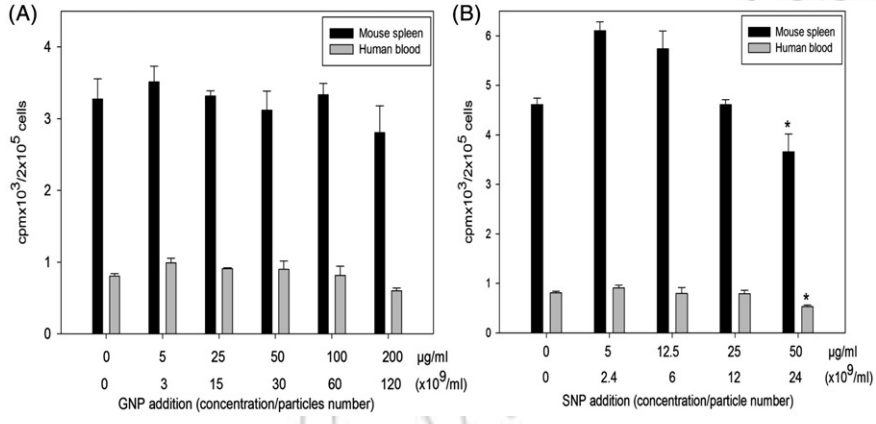

Figure 3. Effects of NP on unstimulated murine splenic lymphocytes and human PBL [^{3}H]-thymidine incorporation. (A) GNP. (B) SNP. Data shown are means (±SEM) of three experiments. $p < .05$, NP treated versus control.

(Hanini et al., 2011; Liu et al., 2011). Investigations of immunomodulatory effects are essential for designing safe NP for use in imaging and clinical applications (Jiao et al., 2014). In the present work, putative immunomodulatory effects of GNP and SNP on mitogen-induced proliferative response and viability were evaluated in vitro. Murine splenic lymphocytes and human PBL stimulated by T- and B-cell-specific mitogens were used as the models.

Significant inhibition of mitogen-stimulated proliferation of murine lymphocytes and human PBL was noted by treatment with GNP and SNP at a concentrations 25 and 5 µg/ml, respectively. GNP <200 µg/ml had no effect on viability of either population used but viabilities were decreased with 25–50 µg SNP/ml. Because the data for proliferative responses were corrected for viable cell numbers, any significant inhibition of these responses were not due to any marginal decreases in viability by the GNP and SNP (at lower doses tested). The other background analyzes here showed that GNP had no effect on [^{3}H]-thymidine incorporation by unstimulated human or mouse lymphocytes at all test concentrations. With SNP, significant inhibition in incorporation was only noted at 50 µg/ml. From all this we can surmise that any observed inhibition of mitogen-induced proliferative responses would not be due to any effects of the NP on [^{3}H]-thymidine entry into cells/incorporation into cell DNA per se.

Enhancement of PHA-induced proliferative responses by human PBL due to GNP has been reported before (Liptrott et al., 2014). In an in vivo study using mice, orally administered GNP were able to differentially affect ex vivo lymphocyte proliferative responses—stimulatory at low doses and inhibitory at high doses (Małaczewska, 2015). Dose-dependent increases in proliferative indices for CD3$^+$ and CD4$^+$ T-cells and no change in CD8$^+$ T-cells were seen in human PBL treated in vitro with GNP (12 nm diameter) at concentrations of 1–25 µg/ml (Guevel et al., 2015). A few studies have reported that SNP were cytotoxic and/or modulated immune responses (Greulich et al., 2011; van der Zande et al., 2012). Differential effects on PHA-stimulated lymphocyte proliferative responses were also seen using SNP coated with polyvinyl–pyrrolidone þ citrate; these SNP were stimulatory at 1 µg/ml but inhibitory at 10–40 µg/ml (Huang et al., 2016). In the present work, results suggested that SNP caused inhibitory (cytostatic) effects at low concentrations but cytotoxic effects at very high concentrations.

The findings reported here further indicate that metallic NP could potentially modulate lymphocyte function in situ in terms of inhibiting their activation by mitogens. The precise mechanisms by which NP bring about this inhibitory effect are not clear. As the NP are not internalized by lymphocytes, it is possible that the effects are mediated via their interactions with cell membranes or related components. It is also possible that

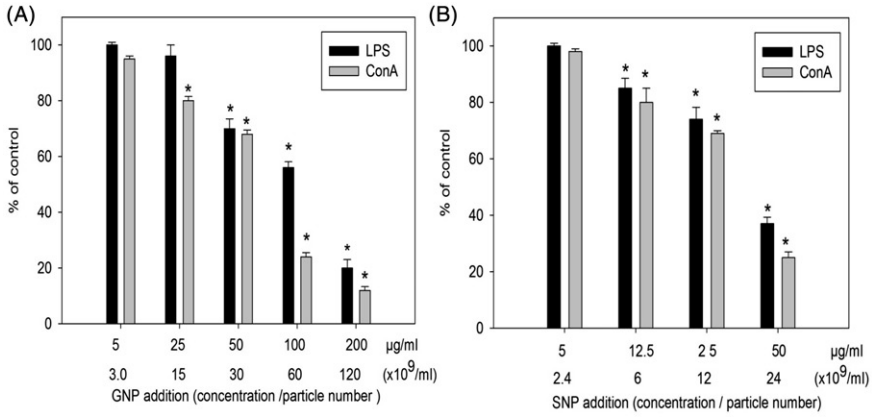

Figure 4. Effects of NP on mitogen-stimulated lymphocyte proliferative response of murine splenic lymphocytes. (A) GNP. (B) SNP. Mean stimulation indices with mitogens: LPS ¼23 (±1), ConA ¼25 (±1) are normalized to 100% value. Data shown are means (±SEM) of three experiments. $p < .05$, NP treated versus control.

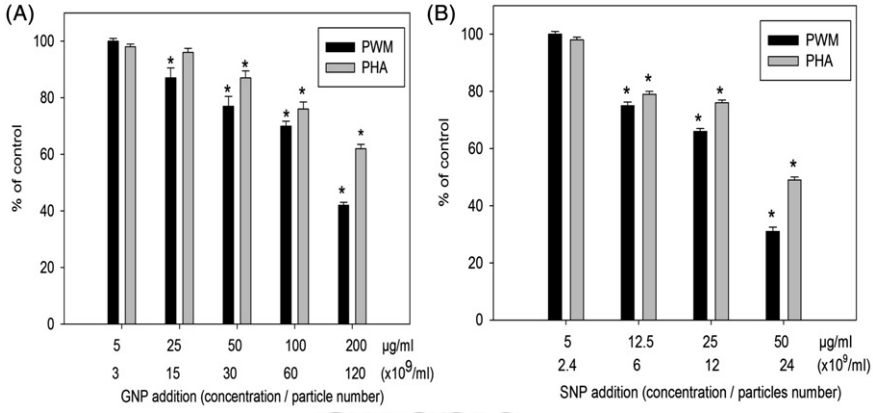

Figure 5. Effects of NP on mitogen-stimulated proliferative response of human PBL. (A) GNP. (B) SNP. Mean stimulation indices with mitogens: PHA ¼58 (±2) and PWM ¼24 (±1) are normalized to 100% value. Data shown are means (±SEM) of three experiments. $p < .05$, NP treated versus control.

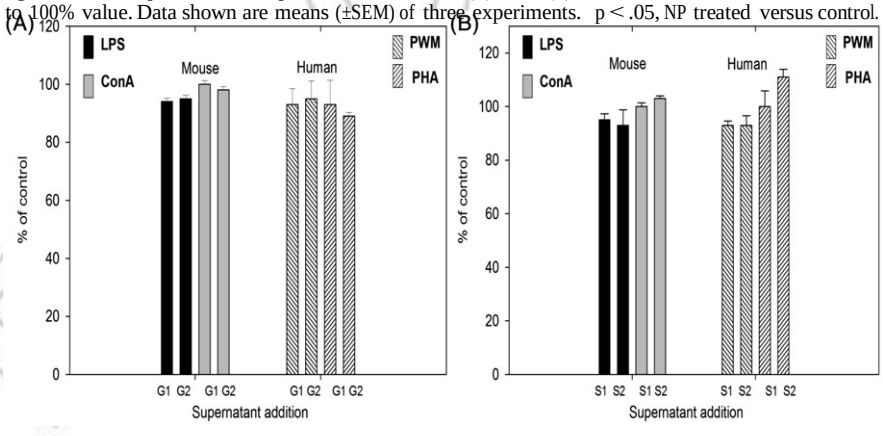

Figure 6. Mitogen-stimulated proliferative responses of lymphocytes cultured in NP-free supernatants obtained from GNP and SNP incubated in complete medium for 72 h. (A) GNP G1 ¼ 50 **l**g/ml, G2 ¼ 200 **l**g/ml. (B) SNP: S1 ¼ 12.5 **l**g/ml, S2 ¼ 50 **l**g/ml. Mean stimulation indices with mitogens: LPS ¼22 (±1), ConA ¼17 (±2), PHA ¼21 (±1) and PWM ¼54 (±3) are normalized to 100% value. Data shown are means (±SEM) of three experiments. $p < .05$, NP treated versus control.

cytostatic and cytotoxic effects observed could be due to release of respective metal ionic species from each NP. It has been proposed that ions released from metallic NP can bring about cellular and molecular toxicities, including cell death (Zhao et al., 2014).

In order to evaluate whether free gold and silver ions released from NP play a role in the inhibition of proliferative responses, particle-free supernatants were collected from GNP and SNP that had been incubated in culture medium. Mitogen-induced proliferative responses of splenic lymphocytes and human PBL cultured in these supernatants were identical to those of cells cultured in fresh medium. It has been shown by others that SNP release ions at negligible concentrations into culture medium containing serum (Loza et al., 2014). GNP have been shown to be stable in terms of release of ions into culture medium at pH 7.0 (Sabella et al., 2014). Thus, the effects on mitogen-induced proliferation by the GNP and SNP were not likely due to the release of ions from the parent particles. On the other hand, one

cannot rule out that the particles/liberated ions were being bound up by the serum proteins during this particular 72-h incubation period. If that were the case, this does not rule out the potential for liberated ions to have acted on the cells in the initial 48-h incubation period before the tritiated thymidine was added. Clearly, further studies are needed to ascertain how these GNP/SNP are acting to inhibit responses to the mitogens.

Conclusions

The results of the present work indicate that GNP and SNP impact on lymphocyte stimulation in vitro and therefore could potentially compromise immune function in situ. Based on these initial sets of findings, future studies are needed to even better characterize any immunomodulatory potentials for GNP and SNP. The outcomes of such studies will clearly help to guide the design and evaluation of metallic NP for use in biomedical applications.

Disclosure statement

The authors report no conflicts of interest. The authors alone are responsible for the content of this article.

Funding

Financial support from the Department of Science and Technology, Government of India, under the Nanotechnology Mission to the University of Hyderabad is gratefully acknowledged.

References

Almeida J, Figueroa E, Drezek R. 2014. Gold nanoparticle mediated cancer immunotherapy. Nanomedicine 10:503–514.

Basu S, Ghosh S, Kundu S, Panigrahi S, Praharaj S, Pande S, Jana S, Pal T. 2007. Biomolecule induced nanoparticle aggregation: effect of particle size on inter-particle coupling. J Colloid Interface Sci 313:724–734.

Becker K, Schroecksnadel S, Geisler S, Carriere M, Gostner J, Schennach H, Herlin N, Fuchs D. 2014. TiO(2) nanoparticles and bulk material stimulate human peripheral blood mononuclear cells. Food Chem Toxicol 65:63–69.

Bhattacharya R, Patra C, Verma R, Kumar S, Greipp P, Mukherjee P. 2007. Gold nanoparticles inhibit the proliferation of multiple myeloma cells. Adv Mater 19:711–716.

Boyum A. 1964. Separation of white blood cells. Nature 204:793–794.

Butler K, Peeler D, Casey B, Dair B, Elespuru R. 2015. Silver nanoparticles: correlating nanoparticle size and cellular uptake with genotoxicity. Mutagenesis 30:577–591.

Corot C, Robert P, Idee J, Port M. 2006. Recent advances in iron oxide nanocrystal technology for medical imaging. Adv Drug Deliv Rev 58:1471–1504.

Dobrovolskaia M, Aggarwal P, Hall J, McNeil SE. 2008. Preclinical studies to understand nanoparticle interaction with the immune system and its potential effects on nanoparticle biodistribution. Mol Pharm 5:487–495.

Dobrovolskaia M, McNeil S. 2007. Immunological properties of engineered nanomaterials. Nat Nanotechnol 2:469–478.

Elsabahy M, Wooley K. 2013. Cytokines as biomarkers of nanoparticle immunotoxicity. Chem Soc Rev 21:5552–5576.

Ghosh M, Manivannan J, Sinha S, Chakraborty A, Mallick S, Bandyopadhyay M, Mukherjee A. 2012. In vitro and in vivo genotoxicity of silver nanoparticles. Mutat Res 749:60–69.

Greulich C, Diendorf J, Gessmann J, Simon T, Habijan T, Eggeler G, Schildhauer T, Epple M, Köller M. 2011. Cell type-specific responses of peripheral blood mononuclear cells to silver nanoparticles. Acta Biomater 7:3505–3514.

Guevel X, Palomares F, Torresb M, Blancab M, Fernandez T, Mayorgab C. 2015. Nanoparticle size influences proliferative responses of lymphocyte sub-populations. RSC Adv 5:85305–85309.

Hanini A, Schmitt A, Kacem K, Chau F, Ammar S, Gavard J. 2011. Evaluation of iron oxide nanoparticle biocompatibility. Int J Nanomed 6:787–794.

Huang H, Lai W, Cui M, Liang L, Lin Y, Fang Q, Liu Y, Xie L. 2016. An evaluation of blood compatibility of silver nanoparticles. Sci Rep 6:25518.

Hussain S, Vanoirbeek J, Hoet P. 2012. Interactions of nanomaterials with the immune system. Wiley Interdiscip Rev Nanomed Nanobiotechnol 4:169–183.

Jiao Q, Li L, Mu Q, Zhang Q. 2014. Immunomodulation of nanoparticles in nanomedicine applications. Biomed Res Intl 2014:426028.

Kasyapa C, Ramanadham M. 1992. Alkaline phosphatase activity is expressed only in B lymphocytes committed to proliferation. Immunol Lett 31:111–116.

Lara H, Garza-Treviño E, Ixtepan-Turrent L, Singh D. 2011. Silver nanoparticles are broad-spectrum bactericidal and virucidal compounds. J Nanobiotechnology 9:30.

Lee P, Meisel D. 1982. Adsorption and surface-enhanced Raman dyes on silver and gold sols. J Phys Chem 86:3391–3395.

Liptrott N, Kendall E, Nieves D, Farrell J, Rannard S, Fernig D, Owen A. 2014. Partial mitigation of gold nanoparticle interactions with human lymphocytes by surface functionalization with a 'mixed matrix'. Nanomedicine 9:2467–2479.

Liu Y, Chen Z, Wang J. 2011. Systematic evaluation of biocompatibility of magnetic Fe_3O_4 nanoparticles with six different mammalian cell lines. J Nanopart Res 13:199–212.

Liu X, Huang N, Li H, Jin Q, Ji J. 2013. Surface and size effects on cell interaction of gold nanoparticles with both phagocytic and nonphagocytic cells. Langmuir 29:9138–9148.

Loza K, Diendorf J, Sengstock C, Ruiz-Gonzalez L, Gonzalez-Calbet J, Vallet-Regi M, Koller M, Epple M. 2014. Dissolution and biological effects of silver nanoparticles in biological media. J Mater Chem 2:1634–1643.

Małaczewska J. 2015. The splenocyte proliferative response and cytokine secretion in mice after oral administration of commercial gold nano-colloid. Pol J Vet Sci 18:181–189.

Mironava T, Hadjiargyrou M, Simon M, Jurukovski V, Rafailovich M. 2010. Gold nanoparticles cellular toxicity and recovery: effect of size, concentration and exposure time. Nanotoxicology 4:120–137.

Mukherjee P, Bhattacharya R, Bone N, Lee Y, Patra C, Wang S, Lu L, Secreto C, Banerjee P, Yaszemski M, et al. 2007. Potential therapeutic application of gold nanoparticles in B-chronic lymphocytic leukemia (BCLL): enhancing apoptosis. J Nanobiotechnol 5:4.

Nune S, Gunda P, Thallapally P, Lin Y, Forrest M, Berkland C. 2009. Nanoparticles for biomedical imaging. Expert Opin Drug Deliv 6:1175–1194.

Rai M, Yadav A, Aniket G. 2009. Silver nanoparticles as a new generation of antimicrobials. Biotechnol Adv 27:76–83.

Sabella S, Carney R, Brunetti V, Malvindi M, Al-Juffali N, Vecchio G, Janes S, Bakr O, Cingolani R, Stellacci F, et al. 2014. A general mechanism for intracellular toxicity of metal-containing nanoparticles. Nanoscale 6:7052–7061.

Tomic S, Dokic J, Vasilijic S, Ogrinc N, Rudolf R, Pelicon P, Vucevic D, Milosavljevic P, Jankovic S, Anzel I, et al. 2014. Size-dependent effects of gold nanoparticles uptake on maturation and antitumor functions of human dendritic cells in vitro. PLoS One 9:e96584.

van der Zande M, Vandebriel R, van Doren E, Kramer E, Rivera Z, Serrano-Rojero C, Gremmer E, Mast J, Peters R, Hollman P, et al. 2012. Distribution, elimination, and toxicity of silver nanoparticles and silver ions in rats after 28-day oral exposure. ACS Nano 6:7427–7442.

Vance M, Kuiken T, Vejerano E, McGinnis S, Hochella M, Rejeski D, Hull M. 2015. Nanotechnology in the real world: redeveloping the nanomaterial consumer products inventory. Beilstein J Nanotechnol 6:1769–1780.

Vergallo C, Panzarini E, Izzo D, Carata E, Mariano S, Buccolieri A, Serra A, Manno D, Dini L. 2014. Cytotoxicity of b-D-glucose coated silver nanoparticles on human lymphocytes. AIP Conf Proc 1603:78–86.

Villiers C, Freitas H, Couderc R, Villiers M, Marche P. 2010. Analysis of the toxicity of gold nano particles on the immune system: effect on dendritic cell functions. J Nanopart Res 12:55–60.

Zimmerman D, Gregory S, Kern M. 1977. Differentiation of lymphoid cells: the preferential binding of the lipid A moiety of lipopolysaccharide to B lymphocyte populations. J Immunol 119:1018–1023.

Zhao Y, Wang B, Feng W, Bai C. 2014. Nanotoxicology: toxicological and biological properties of nanomaterials. Encyclopedia of Life Support Systems. Available from: http://www.eolss.net.

Zhornik E, Baranova L, Drozd E, Sudas M, Chau N, Buu N, Dung T, Chizhik S, Volotovski I. 2014. Silver nanoparticles induce lipid peroxidation and morphological changes in human lymphocytes surface. Biophysics 59:380–386.

Zolnik B, Gonzalez-Fernandez A, Sadrieh N, Dobrovolskaia M. 2010. Nanoparticles and the immune system. Endocrinology 151:458–465.

Q1

EFFECT OF NANOPARTICLES ON B AND T - LYMPHOCYTE ACTIVATION: IN VITRO AND IN VIVO STUDIES

by D Mallaiah

EFFECT OF NANOPARTICLES ON B AND T - LYMPHOCYTE ACTIVATION: IN VITRO AND IN VIVO STUDIES

ORIGINALITY REPORT

%13	%7	%10	%3
SIMILARITY INDEX	INTERNET SOURCES	PUBLICATIONS	STUDENT PAPERS

PRIMARY SOURCES

1	Alekseenko, A.V.. "Ferritin, a protein containing iron nanoparticles, induces reactive oxygen species formation and inhibits glutamate uptake in rat brain synaptosomes", Brain Research, 20081119 Publication	%1
2	www.jci.org Internet Source	<%1
3	Farrera, Consol, and Bengt Fadeel. "It takes two to tango: Understanding the interactions between engineered nanomaterials and the immune system", European Journal of Pharmaceutics and Biopharmaceutics, 2015. Publication	<%1
4	Latheef, S.A.A., Mallaiah Devanabanda, Swetha Sankati, and Ramanadham Madduri. "Differential expression of alkaline phosphatase gene in proliferating primary lymphocytes and malignant lymphoid cell lines", Immunology Letters, 2016. Publication	<%1